

# **MITSUBISHI HEAVY INDUSTRIES Vol.35 No.2 1998** **TECHNICAL REVIEW**



PB99-153173



REPRODUCED BY: **NTIS**  
 U.S. Department of Commerce  
 National Technical Information Service  
 Springfield, Virginia 22161

**Front cover:**

**Non-stop Toll Collection System**

On April 1, 1998, the Electric Road Pricing (ERP) system for Singapore's Land Transport Authority (LTA) was put into service for the first time. This is the world's first non-stop system for charging automatically from vehicles running at high speed on multi lines through communication between In-vehicle Unit and roadside antennas.

The system is composed of 1 060 000 units of In-vehicle Unit, roadside Radio Frequency (RF) communication equipment, Vehicle Presence Detectors, Enforcement Camera System (cameras for capturing images of invalid vehicles), and Central Computer System. On April 1, operations were started at two toll points, and full operation at 34 toll points will begin on coming September 1.

The system is attracting attention as a means of bringing relief to urban traffic congestion, and its installation is being studied in major European cities, Hong Kong, and elsewhere. The basic technologies such as RF communication are the same as those used in Electric Toll Collection (ETC) system on tollways, and the system is expected to be applied in Japan's ETC, which is scheduled to start operation by the end of 1999.

Mitsubishi Heavy Industries Technical Review is published every four months (February, June, October) by Mitsubishi Heavy Industries, Ltd., 5-1, Marunouchi 2-chome, Chiyoda-ku, Tokyo, Japan.

Domestic distributor:

The Ohm-sha, Ltd., 1, 3-chome, Kanda-Nishikicho, Chiyoda-ku, Tokyo, Japan

The price in Japan is 1500 yen per copy, 4500 yen per annum. (postage not included)

For overseas subscription orders, payments or inquiries should be made to:

Japan Publications Trading Co. Ltd., P. O. Box 5030 Tokyo International, Tokyo, Japan

# TECHNICAL REVIEW

VOL.35 NO.2 SER. NO.102  
JUNE 1998

---

## Technical Papers and Articles

Development of the High-Speed Mono-Hull Type Passenger and Car Ferry "Unicorn" .....	47
Realization of CIM Based on Systematization of Production Department .....	52
Technical Feasibility of Ocean Sequestration of CO <sub>2</sub> .....	57
Construction of EDSA LRT Turnkey System in Manila City .....	62
Automated People Mover for Airports .....	67
Development of Non-Stop Toll Collection System .....	72
Development of Double Medium Corrugated Fiberboard Production Machine .....	77
Superplastic Forming of Titanium Matrix Composite (TMC) .....	82

---

## New Products

Low-Noise, Low-Vibration Spiral Compressor .....	87
Three Dimensional Inspection System of Road .....	88
ECU for Automobile (Front ECU) .....	89
Tunnel Inspection System .....	90
Automatic Guided Vehicle for Hot Stainless Coil and Slab .....	91
Air Conditioner of Hong Kong APM .....	92

---

## Introducing Mitsubishi Juko Giho .....

---

Published by Technical Administration Section, Technical Administration Department, Technical Headquarters, MITSUBISHI HEAVY INDUSTRIES, LTD., 3-1, Minatomirai 3-chome, Nishi-ku Yokohama, Japan,  
© 1998 (Editorial Inquiries: Phone: 045-224-9050, Telefax: 045-224-9906)

### **Contents of Next Issue**

—Volume 35 Number 3, October 1998—

#### **Technical Papers and Articles**

- Features and Operation Results of Tohoku Electric Power Co. Haramachi No.1 1 000 MW Boiler
- Development and Operating Status of “1 500°C Class” Gas Turbine
- Design and Operating Experience of 1 000 MW High-Temperature Turbine Electric Power Development Co. Ltd. Matuura No.2 Unit
- Numerical Analysis Method for Can Seaming Process
- Development of Generator of Liquid Air Storage Energy System
- Development of Large Capacity Ice Storage System
- Development of HCFC-22 Alternative Refrigerant Air Conditioners
- Development of Compact Air Condition for Vehicle Using CFD

#### **New Products**

- Driving Device for High Speed Balancing Machine of Large Capacity Rotor
- Compact Hot Strip Mill for TRICO STEEL CO., L. L. C., USA
- Continuous Galvanizing and Shearing Combination Line of PANZHIHUA Iron & Steel Co. of China
- Direct Driven Type Refrigeration Units for Truck TD 60 D Model
- Small Bus Air Conditioner
- Construction Report of Thermal Power Plant in Chile

# Development of the High-Speed Mono-Hull Type Passenger and Car Ferry "Unicorn"

Yushu Washio\*<sup>1</sup>  
Tsutomu Takimoto\*<sup>1</sup>

Chikafusa Hamada\*<sup>1</sup>  
Naoji Toki\*<sup>2</sup>  
Naoki Ueda\*<sup>3</sup>

*The fastest passenger and car ferry in Japan, which can carry 423 passengers and 106 cars, has been completed. The Ship can be operated at a speed of more than 42 knots which is about twice that of a conventional car ferry and now in commercial service on the Tsugaru Channel between the Honshu Island and Hokkaido Islands. The technical features are as follows. (1) Newly developed slender deep-V form mono-hull. (2) A tough light weight construction using high tensile steel in the main hull and aluminium alloy in the superstructure. (3) A reliable high-power propulsion system consisting of 4 high-speed diesel engines and 4 individually steerable water jet pumps.*

## 1. Introduction

Recently, ship speeds have been increasing, and in particular, there is strong demand for higher speed passenger and car ferries. "Unicorn" is the first high-speed mono-hull type passenger and car ferry in Japan. Developed to accommodate a loading capacity of more than 100 cars, the ship is capable of speeds of about twice that of conventional passenger and car ferries, and is designed to be competitive with other means of transport such as railways and tunnels.

Construction of the ship, "Unicorn" was started in May 1996, and business operation was started in June 1997 by East Nihon Ferry Co. The ship entered service on the route between Aomori and Hakodate winning a good reputation all around. (Fig. 1)

## 2. Present Status of High-speed Passenger and Car Ferries

Domestic passenger and car ferries engaged on long range routes in Japan shoulder the domestic physical distribution of trucks and trailers as the main means of transport. They operate at speeds as high as 20–27 knots, which falls into the high-speed range for general merchant ships. Such speeds are located at the upper limit of the speed range for conventional

displacement type ships.

Still, there is ever greater demand for fast passenger transportation on the sea. Recently, many small fast boats for commuters have appeared mainly ply the routes to and from isolated islands<sup>(1)</sup>.

Fig. 2 shows the relationship between the speed of existing ships and deadweight. High-speed passenger and car ferries are increasingly expected to have operating speeds of 30–40 knots in the high-speed range and a deadweight ranging from several hundred to one thousand tons. These factors are in the extrapolation range for conventional displacement type ships and fast passenger ferries, indicating that the undeveloped performance as the ship is required<sup>(2)</sup>.

Though high-speed passenger and car ferries have already appeared mainly in Europe 4–5 years ago, it will be necessary for fast ferry service in Japan to meet the present conditions of passenger and car ferry operations.

In particular, the following two matters are most important.

- (1) Such vessels must be highly reliable in keeping low rates of voyage cancellations close to those of conventional

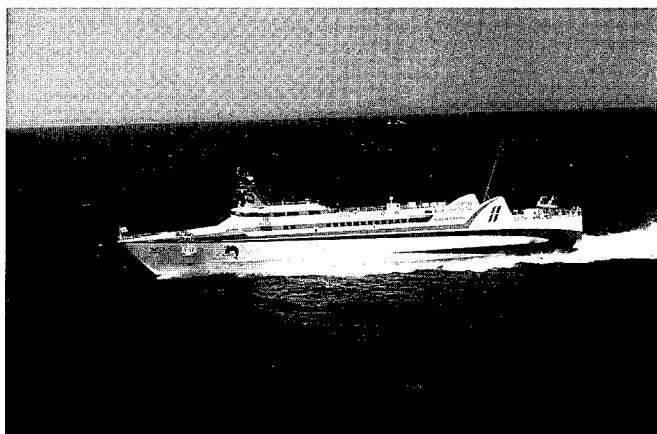


Fig. 1 Photograph of Unicorn

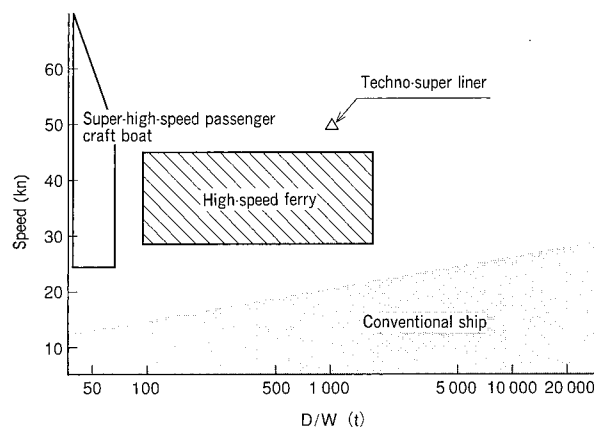


Fig. 2 Deadweight and speed range of high-speed passenger and car ferries

The figure indicates that the high-speed passenger and car ferry is an undeveloped region in terms of the deadweight and speed.

\*1 Shimonoseki Shipyard & Machinery Works

\*2 Nagasaki Research & Development Center, Technical Headquarters

\*3 Ship & Ocean Engineering Department, Shipbuilding & Ocean Development Headquarters

passenger and car ferries all year round even under the severe sea conditions common around Japan.

- (2) Such vessels must also be capable of loading cargo trucks in such fashion as not to ruin high-speed operations because the existing routes are commonly used for cargo transport.

Taking these two requirements into consideration, Mitsubishi Heavy Industries, Ltd. (MHI) developed a novel passenger and car ferry utilizing the specific technology the company evolved and applied taking advantage of its experiences with numerous high-speed boats, and the basic technology fostered in the development of the Techno-Super Liner.

### 3. Outline of Design

The hull form is a newly developed slender deep-V form mono-hull, which is excellent in sea kindliness.

Principal particulars of the ship are shown in **Table 1**, and its general arrangements are shown in **Fig. 3**, respectively.

Cars are loaded on the car deck which is the first deck. The mezzanine deck is made of aluminium alloy provided at the height of 2.65 m above the car deck, and two central lanes are used for large cars. A maximum of five large buses and trucks up to twenty tons can be loaded. Smaller size trucks can be loaded on the rear part of the car deck. One set of 5.2 m wide ramps is equipped at the stern in an arrangement where the direction of the cars can be reversed in the turning space located at the bow part. The movable ramp intended for the mezzanine deck is also made of aluminium alloy.

The most important matter to achieve the target speed in the case of high-speed ships is to reduce the light weight which comprises 70—80% of the total ship weight. For this purpose, the main hull below the upper deck is made of steel with extensive application of high-tensile steel, while the upper structures, including the passenger rooms, are made of aluminium alloy, taking into consideration the safety in collision,

**Table 1 Principal particulars**

Overall length	100.56 m	Maximum number of passengers	423 persons
Breadth	14.90 m	Number of cars	106 passenger cars
Depth	10.30 m		78 passenger cars, 5 large cars
Draught	2.70 m	Main engine	MTU 20 V 1163 TB 73 L × 4 sets
Gross tonnage	1 498 t	Maximum continuous output	8 840 PS × 1 275 rpm
Maximum speed at sea trial	42.39 kn	Propeller	KaMeWa W/J 112 SII × 4 sets

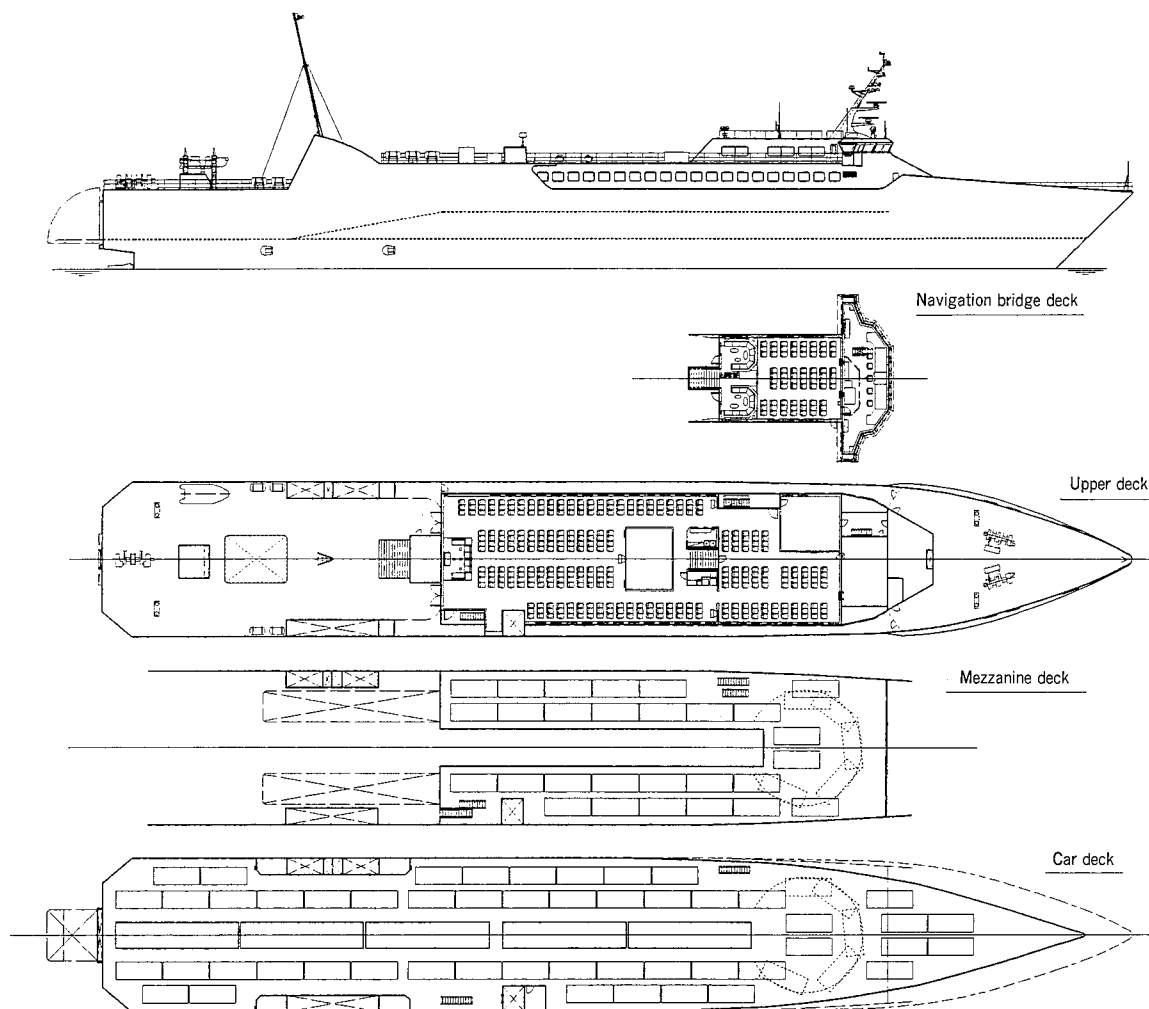


**Fig. 3 General arrangements**

measures for fire protection of the car deck space, repair work in dock, and the construction cost, etc. A system was adopted in which the aluminium upper structures are welded to the main hull through aluminium clad steel plate.

Complicated structure and design are eliminated in the propulsion plant as much as possible from the viewpoint of reliability. In order to realize uniformity of the parts, four independent engine-shaft systems were adopted in which the main engines, gears, and water jets of the same type are combined. The water jets for four shafts are independently steerable, operated by joystick controllers which are arranged on both bridge wings, enabling versatile maneuvering motion through interlocking operation with the bow thruster.

### 3.1 Propulsive performance

#### (1) Resistance by appendages

It is necessary to gain a quantitative grasp of the resistance caused by appendages such as fin-stabilizers and bow thruster which is small in ratio to the whole hull resistance from the viewpoint of improving propulsive performance through the minimization of hull resistance.

In one example, flow simulations by using CFD (Computational Fluid Dynamics) were performed on the bow thruster opening. The shape of the opening for the bow thruster was changed so as not to disturb the streamline near the opening, and the angle of the grid was examined by observing the flow using tafts. These results were incorporated in the basic hull form, and the optimum hull form was selected so that total hull resistance is minimized.

#### (2) Mutual interference of water jet intakes

Four sets of large output water jets are brought very close to each other due to restriction of the arrangement. It was feared that such an arrangement might result in deterioration of the thrust due to mutual interference of the fluid between water jet intakes.

To cope with this phenomenon, observations were made of the flow using a self-propulsion model having a small water jet. Measurements of the flow velocity distribution in the boundary layer were performed, after which the flow with the actual ship scale was estimated by CFD. In so doing the technology to estimate the self-propulsion factors and the quantity of mutual interference at the flush type intake was established.

#### (3) Propulsive performance in waves

When air suction is generated from the water jet intake while the ship is in waves, the load on the impeller instantaneously becomes close to zero, and the fuel injection is automatically cut off so that the main engine does not enter an over-speed condition. When this phenomenon is frequently generated, a drop in speed and adverse effects on the main engine are feared.

It was observed that the air sucked by the fin-stabilizers exposed above the water surface can be led into the outside water jet intakes from the result of the self-propulsion model test in the beam sea. The position of the fin-stabilizers was adjusted to be in a range in which motion damping is not adversely affected.

### 3.2 Hull Structure and fittings

In the hull structural design, emphasis was placed on the lively weight reduction design taking into consideration the

degree of importance of the various members and the possible effects thereof in a damaged condition.

Since the ship is of a character which falls between the conventional ship and the high-speed small craft, there are as yet no structural design standards that applicable directly to it at the present stage. Consequently, domestic standards for high-speed mono-hull type crafts up to 50 m in length which are recently established were applied with necessary modifications. In determining the final dimensions of each member, the design load was verified using ship motions and wave loads measured in tank tests and estimated by simulation calculations. After the arrangement of the main structures and the scantlings of the members were determined, various FEM (Finite Element Method) analyses were performed to review the detailed design. At the same time, fatigue strength was also evaluated to check the structural reliability of the vessel design.

One example of the FEM analysis model is illustrated in Fig. 4.

In the area where the ship is engaged in a certain season, whales are frequently seen, and the damage that would be generated in collision with a whale were estimated. The calculation results, shown in Fig. 5, indicate that the hull is strong enough not to be damaged in a collision with a whale. Further, collision acceleration is also very small thus verifying that there are no problems in terms of safety.

The manufacturers' standard of each fitting were reviewed taking into consideration the service conditions in which the ship is expected to operate, thereby greatly reducing the weight of the vessel. In particular, Danfoth type anchors and wire ropes of the anchoring equipment, armorless type electric cables, aluminium honeycomb internal wall materials, and the like made of light materials or weight-saving specifications were adopted.

In the construction stage, every block and piece of equipment was weighed in order to control weight. The difference in the light weight when completed from the weight in the design plans was only 0.5%.

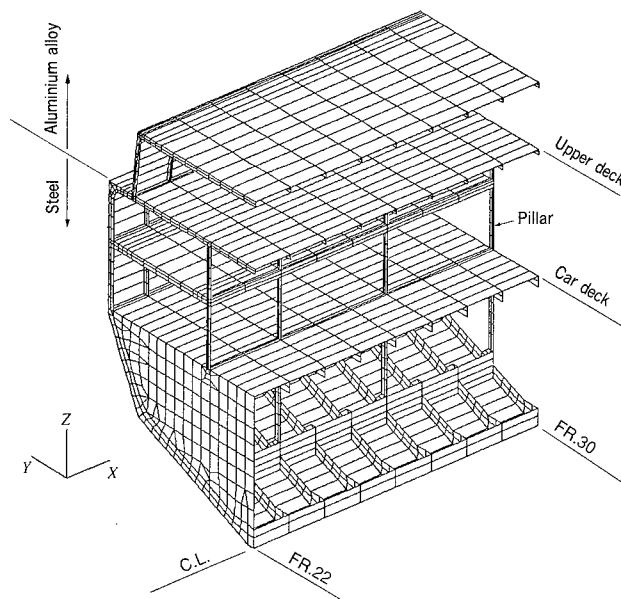
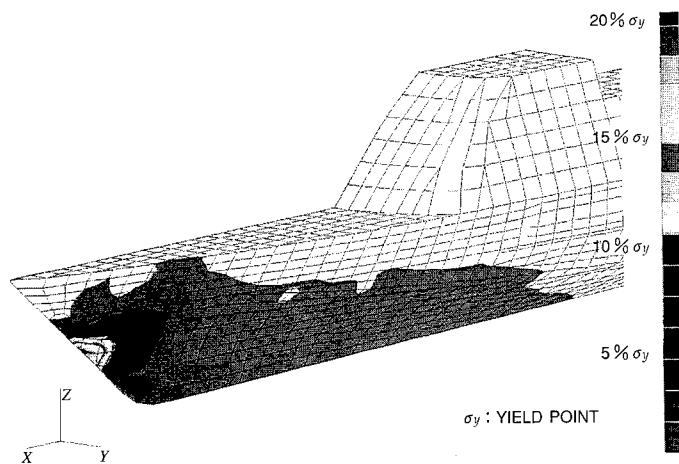


Fig. 4 Example of FEM model



**Fig. 5 Stress analysis of collision with whale**

The figure indicates the results of the estimated stresses in collision with a whale.

In order to secure comfortable habitability as a passenger ship, a flexible mounting system was adopted for not only the main engine and generator engines which are the main excitation source of vibration, but also the hydraulic equipment. In particular, vibration response analysis by FEM was performed on the complicate structural parts like the water jet ducts. Estimates were also made of noise levels by the SEA (Statistical Energy Analysis) method with respect to the special structure with the upper structures made of aluminium alloy. The results obtained served to help determine where the soundproof material should be placed.

### 3.3 Roll damping device

The wave conditions in the route between Aomori and Hakodate were examined, where the ship is engaged in order to select the most appropriate motion damping device. It was shown that the beam sea is dominant in the sea state where the wave height exceeds 3 m in the route between Aomori and Hakodate, and roll damping is most effective to improve the comfort of the ride. A non-retractable type fin-stabilizers of roll damping device was equipped near a midship after checking the effect of sufficient damping.

**Fig. 6** shows that the roll of the ship is damped by about 70% at the resonance frequency through the installation of the fin-stabilizers.

### 3.4 Propulsion plant

**Fig. 7** shows the arrangement of the propulsion plant of the

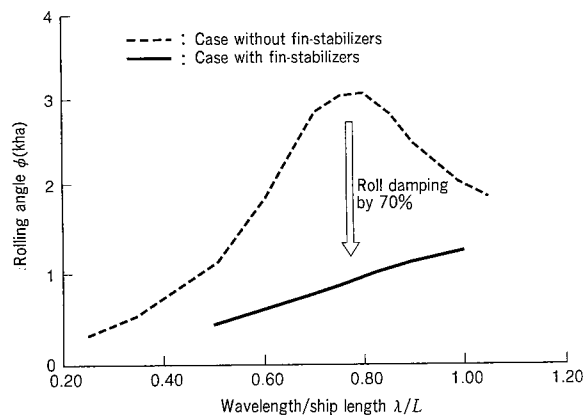


**Fig. 6 Roll damping by fin-stabilizer**

The graph shows the effect of roll damping by fin-stabilizers estimated from the results of tank tests.

ship. Four sets of high-speed diesel engines with a continuous maximum output of 6 500 kW are arranged as the main engine. There has been much experience with this type of engine in the high-speed ferries in Europe, demonstrating that they are also very reliable. Each main engine is coupled with a water jet pump through the reduction gears from the aspect of redundancy and weight reduction of the propulsion plant.

The reduction gears consist of a planetary gear system and are miniaturized in size. The casing is made of aluminium alloy. High strength nickel-chromium molybdenum steel (SNCM 439) was adopted for the material of the intermediate shaft. A two pieced ball bearing was adopted for the intermediate shaft bearing, which has been used extensively in high-speed boats. The casing for the bearing is also made of aluminium alloy in order to reduce weight.

Integrated control is performed from the wheel house by two set of engine monitoring systems and VTR cameras during navigation, and the engine room is operated in the unmanned condition.

## 4. Sea trials

Sea trials were carried out in order to check various performances of the ship which are as shown in **Table 2**.

The maximum speed during sea trials of the ship was 42.39 knots whose speed is ranked highest for diesel driven steel ships. The crash astern distance is about 580 m, and the turning circle is about 400 m (mean value for right and left turns,

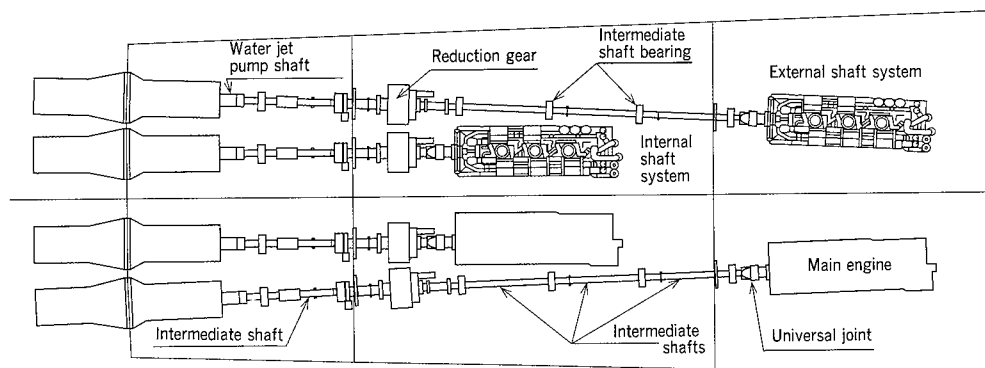


**Fig. 7 Arrangement of main engines and water jets**

**Table 2 Results of sea trial**

Items	Results of sea trial		
Speed	Maximum speed at sea trial: 42.39 kn (1/3 DW, 100% output)		
Crash astern distance	About 580 m		
Turning		Maximum longitudinal distance	Maximum transverse distance
	Left turn	About 400 m	About 440 m
	Right turn	About 370 m	About 390 m
Noise	55–67 dB(A) in whole accommodations		
Vibration	1/2 or less of the lower limit of ISO standards in whole accommodations		

equivalent to 4 times the hull length). It was confirmed that the maneuverability is far superior to that of conventional passenger and car ferries.

With regards to the results of the vibration and noise measurements, a noise level of 55 dB(A) to 67 dB(A) was achieved in accommodation areas, while the vibration level was below 1/2 of the lower level specified by ISO standards. Further, it is demonstrated that the ship is sufficiently calm.

## 5. Conclusion

The passenger and car ferry “Unicorn” is the highest speed ship of its type in Japan. It was built as a first high-speed mono-hull type passenger and car ferry, and entered regular service twice a day since June 5, 1997, playing a new main role in the route between Aomori and Hakodate. In order to ensure

high reliability which has been the initial goal, relevant data of hull stress and ship motion in waves has been accumulated in service. The resulting feedback is being applied in the design of the second and subsequent ships.

The authors wish to express their sincere gratitude to the many people of East Nihon Ferry Co. who gave the authors the opportunity of building “Unicorn” with a large number of novel factors.

## References

- (1) Kihara, k. et al., Development of Fully Submerged Hydrofoil Catamarans, Mitsubishi Heavy Industries Technical Review, Vol.32 No.1 (1995) p.1
- (2) Washio, Y., Variation and Special Features of RoRo Vessels, Bulletin of the Society of Naval Architects of Japan, Vol.797 (Nov. 1995)

# Realization of CIM Based on Systematization of Production Department

Ken Ito\*<sup>1</sup> Takashi Yoshimura\*<sup>2</sup>  
Akio Iida\*<sup>2</sup> Masahiro Sonda\*<sup>2</sup>

*For more than 10 years, the Shipbuilding Division of Mitsubishi Heavy Industries, Ltd. (MHI) has been using its own design systems, MARINE and MATES, to improve design efficiency. Recently, a new production support system has been developed and put to practical use in the Production Department. The system uses the design data supplied by MATES, and has achieved efficient production management. Furthermore, new automated facilities have been introduced by the Nagasaki Shipyard & Machinery Works, for which the design data from MATES is in a prerequisite. This has led and leads to a remarkable improvement in productivity. The successful introduction of this production support system and the automated facilities was because information is integrated from design all the way to production, and in this sense, MHI's CIM has now been constructed. This paper gives an outline of MHI's CIM, focusing on the systematization of the Production Department.*

## 1. Introduction

The increase in the rate of older employees and their wages in shipbuilding industry, as in the other industries, has accelerated the promotion of automation and computerized production system. In general, however, most of the works in shipbuilding fields are still resorted to manpower. It is, therefore, mandatory to build up a comprehensive production system taking due account of the works related to human system as well as the efficiency of each equipment.

The MHI Shipbuilding Division has developed and put into practical use, prior to the Production Department, the MARINE (Mitsubishi Advanced Realtime Initial design & Engineering system) and MATES (Mitsubishi Advanced Total Engineering system of Ships) design systems, taking into consideration the supply of information not only to the Design Department but also to the Production Department. Further, the Division has successfully developed and put into practice a production support system, aiming mainly at the improvement of control works in Production Department and the supply of accurate information to automated facilities.

With the adoption of the production support system as the foundation for field operation, and the introduction of automated facilities, the information from design to production has been integrated, thus realizing the MHI's shipbuilding CIM. This paper describes the outline of the Shipbuilding CIM, focusing on the systematization of the Production Department.

## 2. Overall view of CIM

The shipbuilding CIM configuration is given in **Fig. 1**. The shipbuilding CIM is composed of the initial design and engineering system MARINE used at the upstream, the total engineering system of ships, MATES, and the production support system to support the production works.

MARINE, an integrated CAE (Computer Aided Engineering) system to support the initial design, came under development project in 1984, and was put to practical use in 1986. The system was developed with a view to intensifying the capacity in ship dealings, improving the technical power, reducing the cost, and devising the reserve power of development.

MATES, a design CAD system covering a wide range from basic design and detail design to production design, works as a

nucleus of the shipbuilding CIM. Development on MATES started in 1983, and its application to actual ship started in 1986. Equipped with a high-degree design support function, the system greatly contributes to improving the design efficiency and shortening the design term.

The production support system, developed after an elapse of three years, has been put to full operation since 1996, supporting the Production Department in the fields of production control and parts control in different stages such as working, assembly, erection, outfitting and delivery. Further, the system is also used for supplying operation date to automated facilities such as robots, etc. and for collecting the operational records.

The shipbuilding CIM has been built up and put into practical use through a long-term development process based on aforesaid conceptions, with its application to actual ships widened, and its link with other systems enlarged to realize the commutation and integration of information.

## 3. Features of design systems

### 3.1 Features of MARINE

This system enables optimization of design under given conditions by creating the desired ship model on the basis of type ship, and promptly repeating various performance calculations, and has the features given below.

- Study of effective design due to powerful GUI (Graphic User Interface)
- Visual check and evaluation of input data and calculation results
- Groups of substantial programs to support the evaluation of lines/performance
- Smooth system operation due to various data base control functions

### 3.2 Features of MATES

A nucleus of CAD system to support basic design, detail design and production design, MATES is composed of hull system and outfitting system. The system particularly features in its rich functions to meet flexibly with diversified alterations due to trial and error in addition to the basic functions of an ordinary CAD.

The system also includes the distinctive functions given below.

\*1 Ship & Ocean Engineering Department, Shipbuilding & Ocean Development Headquarters  
\*2 Nagasaki Shipyard & Machinery Works

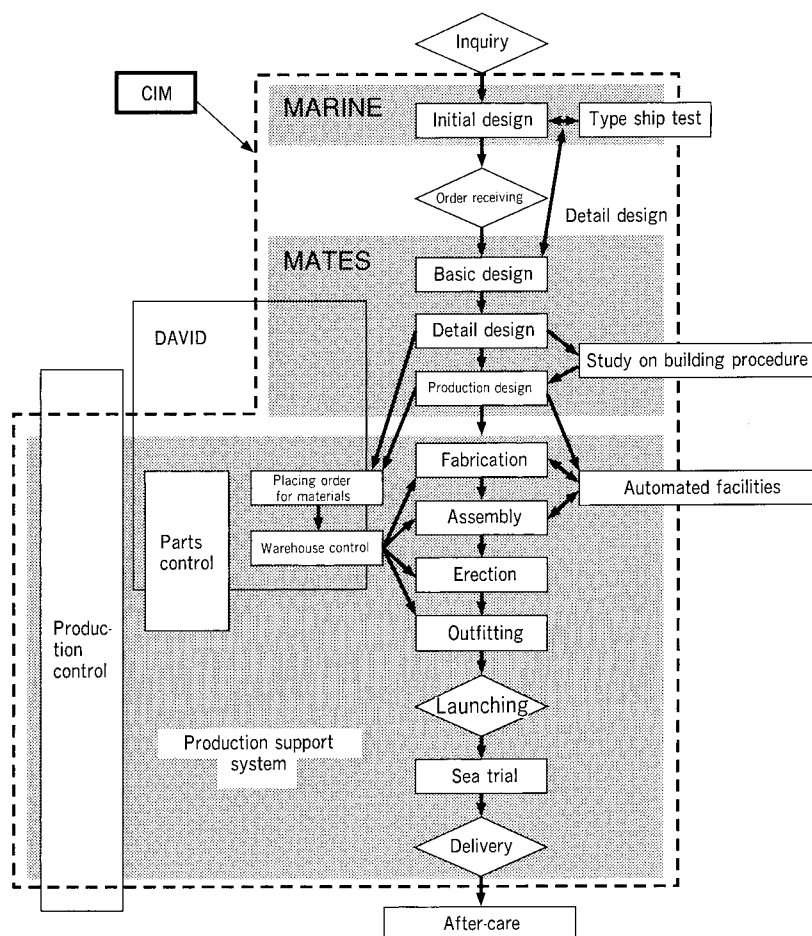


**Fig. 1 Systems coverage of CIM**

The systems and workflow in Design and Production Departments composing the shipbuilding CIM are shown.

- Various CAE functions to realize efficient design
- Substantial correcting function for diversion design
- Automatic processing function for parts making etc. in production design stage
- Data check and automatic set functions including design know-how

Furthermore, the design systems supply the material amount for production control like welding length, weight, etc., the three-dimensional structural data required for operating the automated facilities in production site, and working data to the production support system at the downstream.

#### 4. Functions and features of production support system

The unique production support system, newly developed by making use of the design data of MATES, has actually been put into practical use in Production Department, contributing drastically to the improvement in the efficiency of production management. The newly developed system extends a wide support ranging from initial production planning to detailed production control tasks: mainly the precise tasks per work type and per facility controlled by a foreman, promotes integration of production information, and is equipped with various automated functions to support the optimization of production planning. The system is developed particularly with a view to implementation of target control for task group or individual.

The design data such as welding length is fed into this system to get processed into material amounts required for production control before being used for calculating the

number of man-hour or leveling the process. Detailed design data is essential to improve precision target control. Further, the design data is also used for preparing the action data and processing data to operate the NC cutting machine, automated pipe assembly factory, high-precision assembly system, and automated facilities such as sub-assembly and welding robots, etc.

In production control, the production schedule mesh gets successively fragmented from manager or managing staff to foremen and workers, whereas the production record is subjected inversely to proceeding control as the whole factory by integrating the data obtained by the foremen.

Described below are the representative systems to support the aforesaid tasks.

- (1) Long-term scheduling system
- (2) Mid-term scheduling system
- (3) Detail scheduling/Production control system

##### 4.1 Functions and features of long-term scheduling system

This system has been developed for the manager or the staff in Production Planning Department.

The long-term scheduling calls for making plans several years ahead when the design is not yet completed. This system sum up the long-stored records regarding work types and machines, and is equipped with the following functions required for effective scheduling on the basis of parameters obtained through regression analysis.

- Scheduling function
- Personnel planning function

- Register function of sum

Fig. 2 shows an example of scheduling screen.

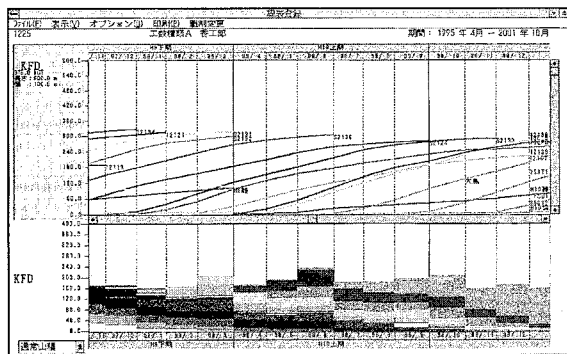


Fig. 2 Long-term scheduling system

The scheduling screen of the long-term scheduling system is shown.

## 4.2 Functions and features of mid-term scheduling system

This system, developed for the manager or the staff in Production Planning Department, is a support system for production control work involving adjustment of concrete production process some 3 to 6 months ahead based on the basic schedules made during long-term scheduling.

The system makes use of the design information such as welding length, obtained through MATES in making process adjustment, and carries out schedule adjustment by evaluating the work load, and is equipped with various functions befitting with the different scheduling methods such as optimization through simulation, etc. regarding the process adjustment and conveyor tact scheduling while making schedules for disposition places.

The mid-term scheduling system carries out various functions given below in accordance with the production control workflow, contributing to effective execution of work in each process.

### 4.2.1 Erection schedule planning function

This is a function to support the erection schedule planning for the erection block of ship in dock. The erection sequence differs according to the ship, but there exists a standard schedule depending on the type of the ship, ship model, size, etc. Systematization of these items has enabled automation and contributed to improving the efficiency of each work.

### 4.2.2 Scheduling and layout planning function

This is a function of carrying out simultaneous planning for schedule adjustment and block layout in grand assembly area around the building dock, with the adaptability between schedule and place constantly maintained through interference check function in order to prevent block overlap. (Fig. 3)

### 4.2.3 General schedule adjusting function

This function allows automatic formation of standard schedules for the preceding assembly and working processes on the basis of the building block erection day. The standard schedules are prepared, taking into consideration the block shape and assembly method, to ensure adaptability of all processes needed for one unit of block. The schedule adjustment is carried out while evaluating the workload, and the schedule thus fixed is used for determining the design drawing

submitting day or material purchase day.

The material amount, indispensable to schedule adjustment, is automatically supplied from MATES in required units to respective processes. Precisely, the applicable material amounts are: individual welding length, number of pipes, quantity of hull and outfitting parts, painting area, weight, etc.

Since it is possible to refer to the work records and proceeding information, stored in the detail schedule/production control system at the downstream, the adjustment can be made while observing the records.

### 4.2.4 Mid-term scheduling function

This function supports in making schedule adjustment for several ships per building or per equipment in the building for several months, allowing load adjustment of the concerned process while referring to the sum of the concerned building or equipment.

### 4.2.5 Assembly area layout scheduling function

This function supports simultaneous schedule making for block assembly area layout inside a building and process adjustment, allowing to make a draft of optimum layout while referring to the assembly area and total occupied area.

### 4.2.6 Conveyor tact scheduling function

It is necessary to draft optimum tact schedules for several stages such as material distribution, fitting works, welding, etc. in a conveyor type assembly area. The conveyor tact scheduling function allows to carry out simulations, with block charging sequence, personnel allotment, overtime working hours, etc. as parameters for optimization.

## 4.3 Features and functions of detail schedule/production control system

The production plan laid out in mid-term production planning is subjected to detailed monthly or weekly execution scheduling. This execution scheduling is carried out per work group or per equipment, and involves diversified fields, so that building up and operation of a support system for production control of this level is normally difficult. However, it is an essential function for supporting implementation of individual target control and improving the productivity, one of the important objects of the production support system.

This is a support system for job-wise, equipment-wise or

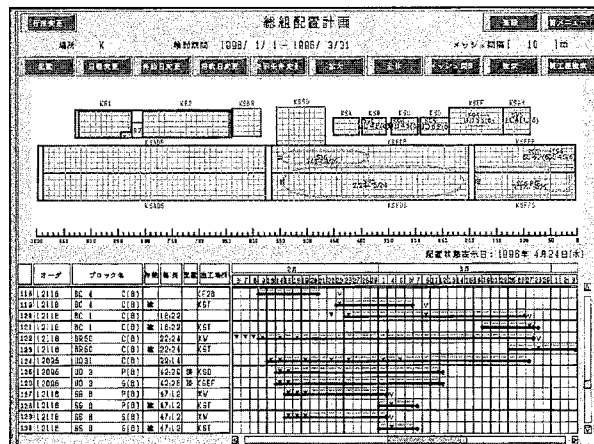


Fig. 3 Scheduling & layout planning for ground assembly blocks

The overall scheduling and layout planning for building blocks around the dock are shown.

group-wise control, one of the most important features of production support system. The main features of the system are given below.

This system is operated by means of personal computers in each control room in production field, enabling dynamic production planning and collecting daily records. Further, the personal computers are linked to the server machine through LAN, so that the input record data can be monitored at real time using any of the EWS or personal computer on the network. Further, special attention is paid to the GUI (Graphical User Interface) for foremen not accustomed to using a personal computer.

#### 4.3.1 Staff and foreman support system

The main support functions are as follows.

##### (1) Schedule adjustment

Referring to the execution schedules of the before/after processes, the state of work proceeding, and workload sum of material amount and number of man-hour can make schedule adjustment. Fig. 4 shows an example of the screen for schedule adjustment.

##### (2) Work schedule time layout

The allocation of the amount of daily work and the target time is carried out for each job and each equipment, which is used for target control of individual or group.

##### (3) Input of daily report

The foreman makes daily input of the material amount produced and the record of number of man-hour. The work records are fed into the production control server machine through the in-company LAN, and are stored there to be used for data analysis etc.

##### (4) Output of weekly report

The schedules drafted in the preceding week, and the records of the week are compared and automatically transmitted.

#### 4.3.2 Optimization simulation function

The automatic and optimized scheduling function of the 2 units of 600-t Goliath crane in the building dock is a representative simulation function for optimization. The function enables automatic drafting of crane schedule by using optimization method to minimize the crane traveling distance and block erection time, taking due account of the constraint conditions such as interference and hanging object with two cranes. The example is shown in Fig. 5.

#### 4.3.3 Individual/group target control function

The target control of individual/group is essential to realize real improvement in productivity through production control, and for this it is necessary to provide detailed information according to the object. In shipbuilding CIM, various functions have been developed for target control by using design information. Two of them are described below.

##### (1) Pipe line installation control

Each individual worker is provided with a work procedure sheet for the installation of pipes or outfitting parts for one day and the target working hours, calculated by using the three-dimensional model information of design. This enables the workers to do their jobs effectively without having to consult the complicated drawings.

Further, using the bar code put on the pipe carries out the work proceeding control.

##### (2) Painting work instruction sheet

Work instruction sheet is issued indicating the three-dimensional model diagram of the hull block drawn from design data, painting area, target number of man-hour, work procedures, etc. in order to give clear image of work, contributing to drastic improvement in the work efficiency and to preventing the error. The example is shown in Fig. 6.

#### 4.3.4 Function of solidarity with outside makers regarding production control information

The information regarding any alterations in process proceedings in the shipbuilding yard is transmitted smoothly at real time to the production control system of the maker, preventing the delay in delivery of products from the maker and promoting the just-in-time delivery of products and materials.

### 5. Operational support for automated facilities

The latest automated facilities such as high-precision assembly device, sub-assembly, installation and welding robots, etc. have been introduced mainly in Koyagi Plant of MHI Nagasaki Shipyard & Machinery Works in order to make drastic improvement in productivity. These facilities are all based on the premise of design information from MATES, and the production support system supports the operation of

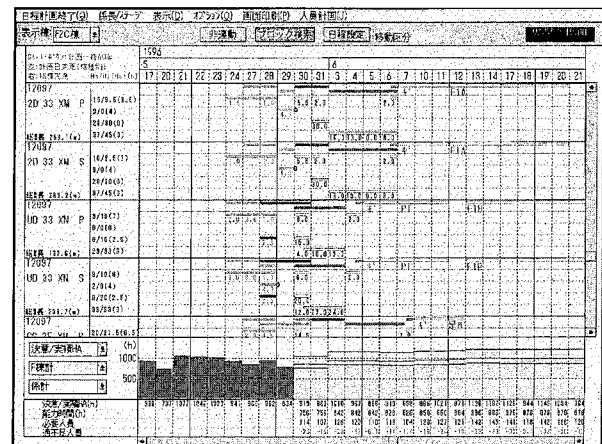


Fig. 4 Staff & foreman support system

The schedule adjustment screen for staff and foreman support system is shown.

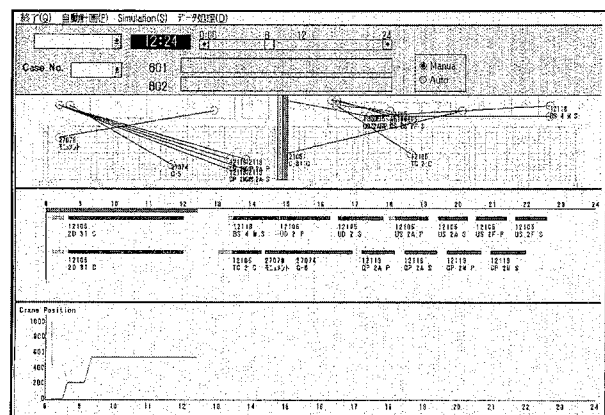
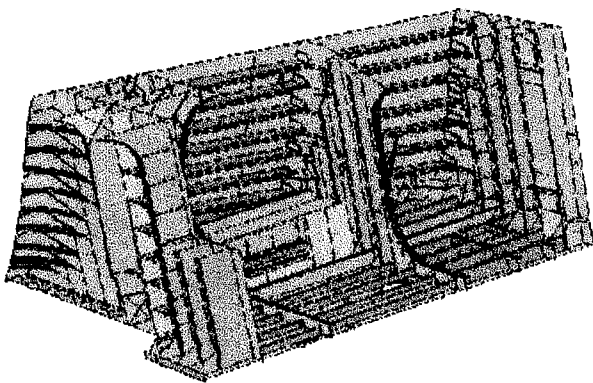


Fig. 5 Simulation system for optimization of crane scheduling

The simulation screen for automatic and optimized scheduling of two units of crane is shown.

Work name	3D31P				Process		Work start	March 24,1997
Paint name	Area	Number of cans	Film thickness	Interval	HC	HA	Fitting day	May 9, 1997
Tar epoxy	171	6.7	175	20-5				
Vinytar	171	2.5	50					
ZINC	909	13						



**Fig. 6 Work instruction sheet at painting stage**

The work instruction sheet using the three-dimensional model of the hull block is shown.

Work procedure sheet	① Standard time (h)	② Target time (h)	①-② Difference (h)	③ This time (h)	③-② Difference (h)	Measure
Initial setup before surface treatment (Vehicle, rust removal machine)	1.0	0.9	0.1			Initial setup of bilge collect car
Surface treatment (Rust removal machine, disc sander)	31.0	25.5	5.5			S/P of outside plank at P/E
Cleaning (Air blow, oil removal)	6.0	5.5	0.5			Cleaning by using bilge collect car
Inspection witness	1.0	1.5	-0.5			Repair or corrections at witness
Initial setup before painting	3.5	2.8	0.7			Material distribution of painting site
Spray painting	12.0	10.0	2.0			Spraying on outside plank at P/E
Cleaning up	3.5	2.9	0.6			
Total	58.0	49.1	8.9			

these facilities. Described below are two examples of these facilities.

### 5.1 High-precision block assembly system

The block built in Koyagi Plant of MHI Nagasaki Shipyard & Machinery Works is one of the largest size blocks in the world with width 23 m, and since the block is built by connecting several pieces of steel planks, it has been a big hurdle how to overcome the problem of the work accuracy error caused by the complicated shrinkage and deformation attributed to welding. In order to realize the high-precision assembly, the data regarding the shape and position of steel plank or longitudinal frame is used as the design data.

Further, the accuracy standards of the concerned facilities are all reviewed to improve the accuracy of supplied parts, and high-precision working and assembly are carried out on the basis of design data in preceding stage facilities for marking on steel plank and die steel, NC cutting, longitudinal assembly, etc. The improvement in block accuracy greatly contributes to the high efficiency of work in after processes.

### 5.2 Sub-assembly, installation and welding robots

Shipbuilding is an order-made production, and the parts are all produced after receiving the order, so that the robot teaching method adopted in the production field is offline teaching method.

The sub-assembly robot holds the hull members such as stiffener to be installed to the sub-assembly base plank by the centered position, carries the members to the installation place, and corrects the position by recognizing the marking line on the steel plank before carrying out temporary installation. The

working data is prepared by using the design information such as shape of hull members.

The sub-assembly and welding robot operates by preparing the robot operating data based on offline teaching method by using design information such as welding length, leg length, and shape of the concerned member, etc. The operating data is automatically prepared on the basis of the member shape so as not to cause interference between robot and member.

## 6. Conclusion

Ten years after the development started on MATES, the development of production system has at last been commenced in compliance with the original objective, and the objective has recently been achieved, bringing about the realization of shipbuilding CIM.

It has become increasingly necessary for the Design Department to make study on a flexible product model capable of representing the whole shipbuilding industry including the uncertain information, and for the Production Department to develop the aforesaid model into a CIM capable of making simulation of engineering method and shipbuilding.

On the other hand, the "LINKS project" under the sponsorship of Ship & Ocean Foundation and other main Shipbuilding Companies and the "NCALS" under the guidance of the Ministry of International Trade and Industry are briskly operating. The objects of these projects are similar to those mentioned above, so that we are determined to make close cooperation and promote harmony to make further improvement in shipbuilding CIM.

# Technical Feasibility of Ocean Sequestration of CO<sub>2</sub>

Masahiko Ozaki\*<sup>1</sup>  
Kazuhisa Takeuchi\*<sup>1</sup>

Yuichi Fujioka\*<sup>1</sup>  
Keisuke Sonoda\*<sup>1</sup>  
Yoshihiro Suetake\*<sup>2</sup>

*World-wide anxiety about global warming due to the increasing concentration of CO<sub>2</sub> in the atmosphere has been accelerating studies on countermeasures, including the capture and sequestration of CO<sub>2</sub>. The ocean sequestration of CO<sub>2</sub> is thought to be a promising option because of the huge amount of CO<sub>2</sub> to be treated, provided that the influence on the oceanic environment is acceptable. In this paper, the technical feasibility of the implementation of CO<sub>2</sub> injection into the ocean depths is studied. The conceptual outlines obtained here will be useful in the planning stage of coming research programs to model the behavior of CO<sub>2</sub> after injection.*

## 1. Introduction

Mitigation of increasing concentration of CO<sub>2</sub> in the atmosphere has become an important international problem as a countermeasure against global warming. Linked closely with the energy problem, the CO<sub>2</sub> problem calls for a scenario "how to reduce the CO<sub>2</sub> emission in the future." Among various options such as high-efficiency power generation, energy saving, switching to renewable energy or the energy with no CO<sub>2</sub> emission, promotion of natural absorption of CO<sub>2</sub>, recovery of CO<sub>2</sub> from combustion gas, etc., it is urgently required to make a thorough investigation and study in order to ascertain their roles in long term schedule.

The concept of capture and ocean sequestration of CO<sub>2</sub> from combustion gas has the following features: (1) there is no need to make a drastic change in the energy supply system, (2) the huge amount of CO<sub>2</sub> can be treated directly from the generating source, and (3) relatively low cost, etc. However, in order to pass a judgement on the issue, it is mandatory to collect the data for evaluating the duration of CO<sub>2</sub> retention in ocean and the impact on the oceanic environment, and for this it is indispensable to establish a technology capable of predicting the behavior of CO<sub>2</sub> fed into the ocean.

Under such circumstances, the "study of environmental assessment for carbon dioxide ocean sequestration for mitigation of climate change (SEA-COSMIC)," a project under the guidance of the Agency of Industrial Science and Technology of Ministry of International Trade and Industry, started in Japan in 1997, and an international joint study participated by Japan, America, Norway etc, is on the way to taking shape.

In prediction of CO<sub>2</sub> behaviors, it is important to make clear the technically feasible range of initial condition of CO<sub>2</sub> injection. In this study, therefore, an investigation is made on the basic conception of the system in order to make the concept of ocean sequestration of CO<sub>2</sub> more concrete.

## 2. Concept of ocean sequestration of CO<sub>2</sub>

In order to minimize the impact on the oceanic environment, there are two types of concepts of ocean sequestration of CO<sub>2</sub>: dissolution type and storage type.

The dissolution type is based on the idea that CO<sub>2</sub> dissolved and diluted in seawater does no more harm than slightly increasing the concentration of CO<sub>2</sub> already contained in the

seawater. The amount of carbonate contained in seawater in one form or another is equivalent to about 50 times the net amount of CO<sub>2</sub> currently present in atmosphere and, in light of the discussion made on the climatic change brought about by the CO<sub>2</sub> concentration in atmosphere getting doubled, the ocean is considered to have sufficient room for sequestration of CO<sub>2</sub>. However, it is impossible to carry out artificial dissolution of CO<sub>2</sub> in ocean uniformly throughout the world, so that it is necessary to make a technical study on whether it is all right to dissolve CO<sub>2</sub> thinly and widely in a short time, and then leave it to the dilution due to natural diffusion.

The storage type, on the other hand, is based on the idea of storing CO<sub>2</sub> in the hollow of deep sea, enabling the impact to be limited to a localized area. For example, a hollow, 50 km in diameter and 50 m in depth, could store about 100 times of the annual emission in Japan. It goes without saying that the place immediately under the CO<sub>2</sub> storage area and the surrounding sea bottoms will be affected. However, it is necessary to make investigation and study regarding the concept of localizing the affected area and thus avoiding the effect from spreading to other areas, the scientific assurance that the CO<sub>2</sub> storage over a long time causes no problem, and the quantitative evaluation of the size of the area that could be affected.

The examples of overall conceptional systems in ocean sequestration of CO<sub>2</sub> for dissolution type and storage type from the technical point of view are shown respectively in Fig. 1 and Fig. 2<sup>(1)-(3)</sup>. In both cases CO<sub>2</sub>, removed and recovered from the combustion waste gas in the thermal power plant on land, is liquefied and transported by sea to a certain area in the ocean, where the CO<sub>2</sub> is fed into the specified ocean depths through the pipes suspended from a ship or an offshore floating facility.

Transportation and dispersion of CO<sub>2</sub> using submarine pipeline is also an effective way depending on the transportation distance and dispersion depth, but it is difficult to pick out an appropriate place in the sea along Japanese coasts because of their frequent use.

## 3. Injection and dispersion in mid-ocean depth by moving ship

The injection and dispersion in mid-ocean depth by moving ship is considered one of the methods of dissolution type ocean sequestration of CO<sub>2</sub>. The system is mainly composed of temporary storage tanks on land, CO<sub>2</sub> carrier and CO<sub>2</sub>

\*1 Nagasaki Research & Development Center, Technical Headquarters

\*2 Nagasaki Shipyard & Machinery Works

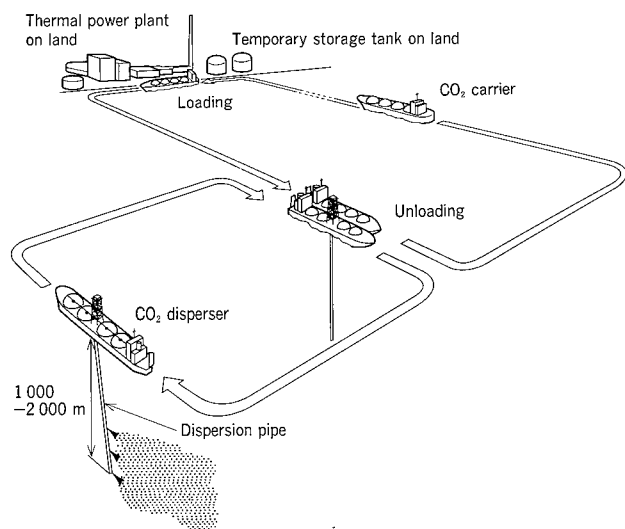


**Fig. 1 Conceptual system for CO<sub>2</sub> dispersion by moving ship**

Technical conception of dispersion type ocean sequestration of CO<sub>2</sub> is shown. The ship with suspended pipe is moved forward to accelerate dispersion and dilution of CO<sub>2</sub>.

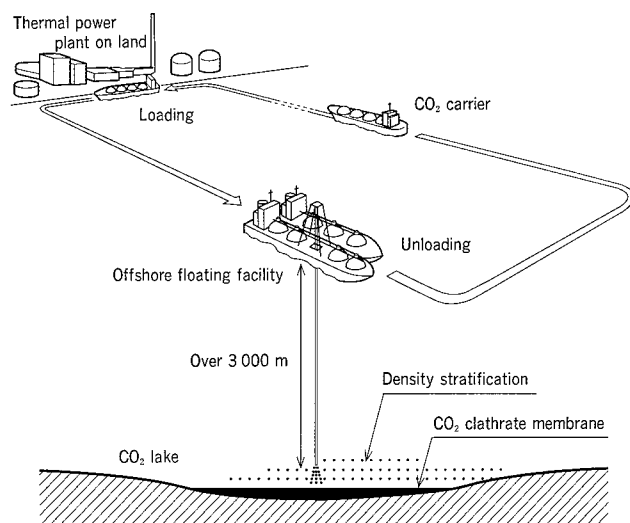


**Fig. 2 Conceptual system for CO<sub>2</sub> storage in deep sea**

Technical conception of storage type ocean sequestration of CO<sub>2</sub> is shown. Storing CO<sub>2</sub> in a hollow in deep sea localizes the effect zone.

dispenser. In Fig.1, CO<sub>2</sub> carrier and CO<sub>2</sub> disperser are illustrated to play separate and independent role, but it is also possible to use the CO<sub>2</sub> carrier jointly as a disperser. The liquid CO<sub>2</sub> is injected and dispersed deep into the sea through the bottom end of a 1 000—2 000 m long pipe suspended from the ship which keeps on moving, thus accelerating the dilution of CO<sub>2</sub> by moving the point of dispersion.

Since no artificial control can be made of the CO<sub>2</sub> after dispersion, it is necessary to pursue technical development by setting a technical target of dilution immediately after dispersion. The dilution target depends on the dilution rate set from the standpoint of environmental effect and on the degree of natural dilution due to the mixing of CO<sub>2</sub> with the water in the deep sea. The CO<sub>2</sub> is supposed to behave in the following manner in the process of dilution immediately after dispersion.

Immediately after dispersion, CO<sub>2</sub> turns into droplets in the fluctuating flow area due to the vortex formed and left behind

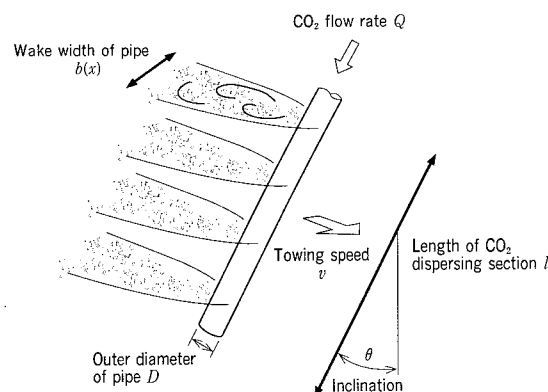


**Fig. 3 Schematic view of CO<sub>2</sub> dilution in wake of pipe**

The CO<sub>2</sub> droplets discharged from the towed pipe get rapidly dispersed in the fluctuating flow area formed behind the pipe.

the wake of pipe before getting mixed uniformly with seawater, thus taking the first step towards getting dispersed into the huge space of ocean. The simulated situation is shown in Fig. 3.

The pipe gets inclined backward against the moving direction due to the cross flow, and intermittently the wake vortex with rotational axis almost parallel to the pipe shaft is formed as the ship moves on. The wake vortex pattern differs according to the pipe shape, the condition of pipe surface, the diameter of pipe and the moving speed etc., but in the case of a steel pipe of diameter several 10 centimeters, running at the speed of several kn, the vortex is normally formed at the left and right of the pipe alternately, leaving the fluctuating flow area behind, where the mixing of CO<sub>2</sub> and seawater is considered to take place.

If CO<sub>2</sub> is dispersed almost uniformly by opening holes over the length  $l$  along the pipe bottom end as shown in Fig. 3, the width  $b$  of the fluctuating flow area and the ship running speed  $v$  can be used to express the initial dilution rate  $\alpha$  as in the equation given below.

$$\alpha = Q/(bvl\cos\theta)$$

where,  $Q$  is the CO<sub>2</sub> emission rate and  $\theta$  is the angle of pipe inclination.

For example, if  $Q = 100$  kg/s,  $l = 100$  m,  $v = 5$  kn,  $b = 2$  m and  $\theta = 30^\circ$ , then  $\alpha \approx 1/4$  300. In other words, in a very short time immediately after dispersion, each CO<sub>2</sub> droplet is surrounded respectively by seawater with volume about 4 300 times larger than its size.

The CO<sub>2</sub> droplets rise gently upward before dissolving in the surrounding seawater. With the dispersion point shifted, CO<sub>2</sub> is not supplied to the same place continuously. If the initial diameter of droplet is small, CO<sub>2</sub> gets dissolved in seawater before it rises several hundred meters up the sea level<sup>(4)</sup>. The problem left thereafter is the problem of dispersion of the seawater containing CO<sub>2</sub>.

The seawater with higher CO<sub>2</sub> content, thickness  $b$ , and width over  $l$  is formed in vertical band shape parallel to the CO<sub>2</sub> disperser before getting spread wide in the ocean mainly in horizontal direction over a long time period, and is eventually expected to gain substantial dilution rate.

#### 4. Storage in deep sea

Since the liquid CO<sub>2</sub> has higher compressibility than seawater, its density rise is relatively large against the pressure rise, so that under temperatures 2°C–5°C in deep sea, the liquid CO<sub>2</sub> becomes heavier than the surrounding seawater at depth over 3 000 m. Further, clathrate, a compound of water and CO<sub>2</sub>, is formed on the contact surface of seawater and CO<sub>2</sub>, which is experimentally found to restrain the dissolution velocity of CO<sub>2</sub> into the seawater. Hence, it is considered possible to store a huge quantity of CO<sub>2</sub> over quite a long time period if a hollow is found in deep sea of about several thousand meter depth where there is no current or tide of seawater.

The technical concept of the storage type ocean sequestration of CO<sub>2</sub> using a hollow in deep sea has much similarity with the aforesaid injection and dispersion in mid-ocean depth by moving ship. The system is mainly composed of temporary storage tanks on land, CO<sub>2</sub> carrier and offshore floating facility, with the liquid CO<sub>2</sub> injected and fed into the storage area using more than 3 000 m long pipe suspended from the offshore floating facility keeping the specified position.

Since withdrawing a long pipe needs quite a lot of time, it is necessary that the offshore floating facility keeps a stand-by position even in storm with the pipe suspended in order to obtain feasible operation factor. Fig. 4 shows the calculated diameter and length of the pipe possible to remain suspended in rough seas from the standpoint of strength<sup>(5)</sup>. The feasible pipe length for a ship type offshore structure of 80 000-ton class is supposed approximately to be under 5 000 m, and under 6 000 m when a semi-submersible offshore structure with excellent sea-keeping performance is used.

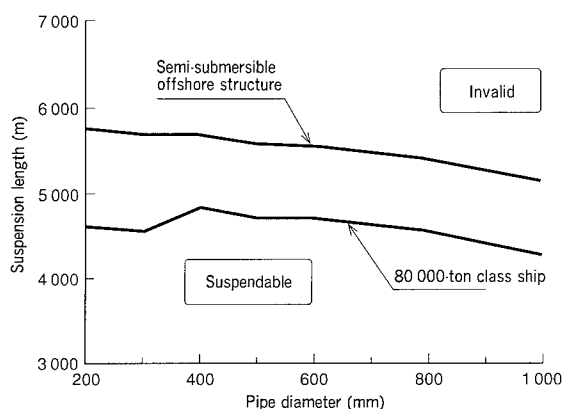


Fig. 4 Length of vertical pipes under ship or platform in rough seas

It is possible to suspend a pipe under 5 000 m in length for a 80 000-ton class ship, and under 6 000 m in length for a semi-submersible offshore structure.

#### 5. Component elements and technical problems

##### 5.1 Temperature and pressure of CO<sub>2</sub> under treatment

The component elements of the system differ according to the temperature and pressure of CO<sub>2</sub> to be treated. It is comparatively easy and convenient for the storage and treatment of a huge quantity of CO<sub>2</sub> if the pressure condition for

keeping the liquid phase of CO<sub>2</sub> is set to low level (for example –55°C, 6 bars), but lowering down the temperature of liquid CO<sub>2</sub> consumes a huge amount of energy. It is, therefore, mandatory to make optimization through a comprehensive evaluation of the system including CO<sub>2</sub> recovery, CO<sub>2</sub> liquefaction, etc.

##### 5.2 Temporary storage tank on land

A CO<sub>2</sub> carrier visits the harbor from time to time to load CO<sub>2</sub>, but in the plant on land, CO<sub>2</sub> is captured continuously, so that temporary tanks for CO<sub>2</sub> storage are needed on land. A skirt supported spherical tank, shown in Fig. 5, is considered suitable for CO<sub>2</sub> storage. The upper capacity limit of the spherical tank capable of withstanding 6 bars is 20 000 m<sup>3</sup> per unit from the present standard of production technology. The materials for the tank are the steels for low temperature use, also adopted for LPG tanks, with the temperature inside the tank prevented from rising by means of the outer heat insulating material.

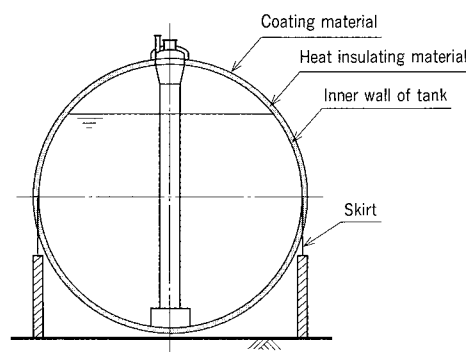


Fig. 5 Storage tank of liquid CO<sub>2</sub> on land

The skirt-supported spherical pressure vessel is considered as a suitable large-capacity CO<sub>2</sub> storage tank.

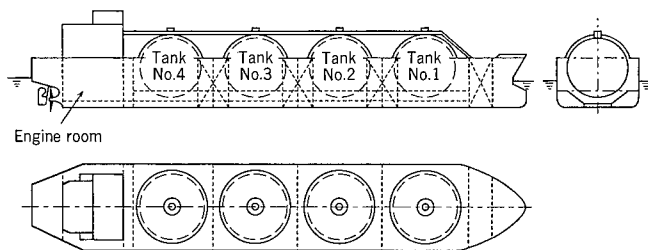
A tank for CO<sub>2</sub> storage with such a huge capacity has not yet been produced, but it is possible to apply the technologies used for making LPG/LNG tanks or piping facilities.

CO<sub>2</sub> is a gas originally contained in atmosphere, and has no toxicity. However, it is dangerous when the concentration exceeds a certain level. Odorless and heavier than air, CO<sub>2</sub> is less diffusive, so that it is indispensable to take a through measure against leakage.

##### 5.3 CO<sub>2</sub> carrier

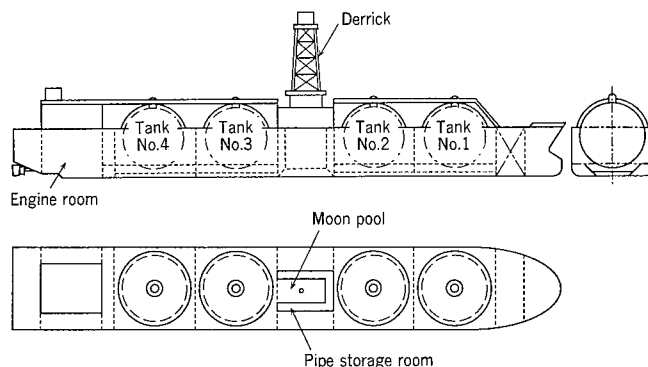
A CO<sub>2</sub> carrier is a ship equipped with pressure vessels for liquid CO<sub>2</sub>, and is similar to carriers of liquid gases such as LPG, LNG, etc. Generally a small-size LPG carrier carries the liquid gas at room temperature and under high pressure, whereas a large-size LPG or LNG carrier at low temperature and under normal pressure. There are also so-called SEMI-REF type carriers designed to carry the cargo under the state from low temperature, normal pressure to room temperature, high pressure in order to provide flexibility in operation, though such carriers have small capacity. Hence, there are not many elements of new development regarding the construction of CO<sub>2</sub> carriers.

Fig. 6 shows an example of conceptual design of a CO<sub>2</sub> carrier, with several skirt-supported, spherical tanks mounted on her.



**Fig. 6 Rough arrangement of CO<sub>2</sub> carrier**

A liquid gas carrier similar to an LNG carrier, with several pressure tanks mounted on her, is shown.



**Fig. 7 Rough arrangement of CO<sub>2</sub> disperser**

A ship almost same in size and type as a CO<sub>2</sub> carrier and equipped with loading/unloading facility for injection pipe is considered suitable as a CO<sub>2</sub> disperser.

#### 5.4 CO<sub>2</sub> disperser and offshore floating facility

A CO<sub>2</sub> disperser (or offshore floating facility) basically has the same size and capacity as a CO<sub>2</sub> carrier. Equipped with pressure vessels to store CO<sub>2</sub> received from the CO<sub>2</sub> carrier, the mooring and unloading facilities to handle the liquid CO<sub>2</sub>, and the suspended pipes for CO<sub>2</sub> injection. The conceptual design of a CO<sub>2</sub> disperser is shown in Fig. 7.

There are following technical problems regarding the construction of a CO<sub>2</sub> disperser. First, it is required of a CO<sub>2</sub> disperser to stay put in a certain sea area by detecting its position by itself in the vast ocean with no objects in the surrounding, and to get linked with a CO<sub>2</sub> carrier in a scheduled manner. It is, therefore, necessary to build up an operating system by making use of the information from satellites.

One of the problems to improve the operation factor is the mooring and unloading facilities for the CO<sub>2</sub> carrier and CO<sub>2</sub> disperser. It is difficult to moor two ships safely without collision in the vast sea where there is nothing to shield from the waves, and no quays or piles to moor the ships. Further, it is necessary to develop a device capable of loading/unloading the liquid CO<sub>2</sub> at low temperature and high pressure preferably in a short time. It is also necessary, in a system of injection and dispersion in mid-ocean depth where a carrier is jointly used as a disperser, to develop a new technology to allow the carrier to install and withdraw the long pipes promptly on the site.

Further, in order to tow a CO<sub>2</sub> disperser suspending 1 000—2 000 m long pipes in the case of injection and dispersion in mid-ocean depth, it is necessary to develop a fixation system to fix the upper end of the pipe to the ship. There is a need of a mechanism that keeps the ship free from the pipe bending

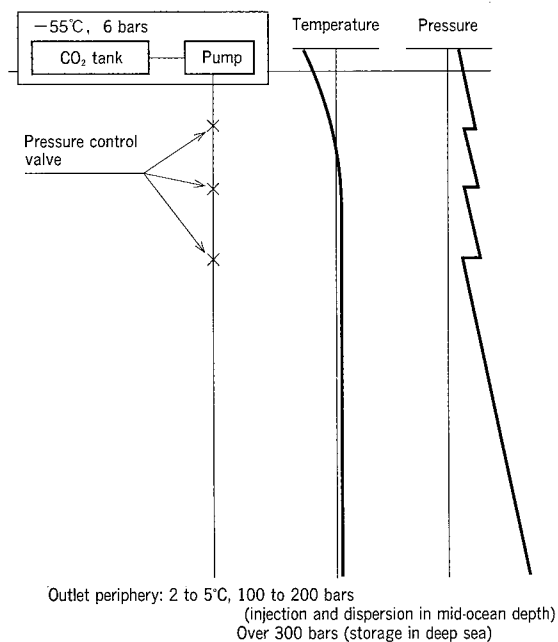


**Fig. 8 Vertical change of CO<sub>2</sub> condition in pipe**

The temperature rises due to the heat received from the surrounding water. It is necessary to adjust the pressure at the inlet port since the outlet pressure cannot be made higher than the surrounding water pressure.

load while keeping the pipe weight and dragging force intact, allowing safe passage without any leakage of the low-temperature, high-pressure liquid CO<sub>2</sub>.

#### 5.5 CO<sub>2</sub> carrying technology using suspended pipes

As for the technology of liquid CO<sub>2</sub> injection through pipe, the existing technology and equipment for handling liquid gas are applicable, but then there are some special items in this technology: the transportation is carried out vertically in downward direction, and the replacement is made with seawater not with air<sup>(6)</sup>.

Fig. 8 shows the conceptional vertical distributions of temperature and pressure of CO<sub>2</sub> inside the pipe during continuous injection. The CO<sub>2</sub> temperature inside the pipe rises as the gas passes through the long pipe due to the heat received from the surrounding seawater, while the CO<sub>2</sub> pressure shows a linear rise from the pressure on the sea surface due to its self-weight. However, it is impossible to make the CO<sub>2</sub> outlet pressure higher than the surrounding water pressure, so that it becomes mandatory to adjust the pressure on the way. When there is a need of preventing CO<sub>2</sub> evaporation due to rise in temperature around the surface layer, the pipe has to be coated with heat insulating material up to a certain depth where the desired pressure is secured. Moreover, it is important to grasp thoroughly the condition inside the pipe at the time of injection start-up or shut-down in order to study the operating procedures and equipment. Hence, it is necessary for the planning of pipes and equipment to find an established method<sup>(7)</sup> for prediction of CO<sub>2</sub> condition inside a pipe.

#### 6. Conclusion

Various investigations and researches are required for the evaluation of different impacts on oceanic environment before making a judgement on whether the ocean sequestration of

CO<sub>2</sub> can be used as a promising option for controlling the sharp increase of CO<sub>2</sub> concentration in the atmosphere. This paper extracts the subjects of development, and describes the study made on the basic concept of ocean sequestration in order to clarify the initial conditions required for predicting the behavior of CO<sub>2</sub> after injection. Conceptual as the study is, it has revealed technical feasibility for obtaining several thousand times higher initial dilution rate by using injection and dispersion in mid-ocean system without any difficulty. Further,

in the system of storage in deep sea, the study has shown the technical feasibility for injecting CO<sub>2</sub> into a hollow of ocean about 5 000—6 000 m deep by using suspended pipes. As for the detailed study on the technical subjects, it will be precisely dealt with after the achievements in the prediction of CO<sub>2</sub> behavior are fed back, and the specifications are clarified for items such as injection depth, flow rate, initial size of CO<sub>2</sub> droplet, ship running speed, etc.

#### References

- (1) Nakashiki, N. et al., Technical View on CO<sub>2</sub> Transportation onto the Deep Ocean Floor and Dispersion at Intermediate Depths, Direct Ocean Disposal of Carbon Dioxide, edited by N. Handa and T. Ohsumi, TERRAPUB Tokyo (1995) p.183
- (2) Ozaki, M., CO<sub>2</sub> Injection and Dispersion in Mid-Ocean Depth by Moving Ship, Int. Symp. on Ocean Disposal of Carbon Dioxide Tokyo (1996)
- (3) Asai, K. et al., Transportation System for CO<sub>2</sub> into Deep Sea (2nd report), J. of the Society of Naval Architects of Japan, Vol. 171 (1992) P.135
- (4) Haugan, P. M. et al., Dissolution of CO<sub>2</sub> in the Ocean, Energy Convers. Mgmt Vol.36 No.6—9 (1995) p.461
- (5) Ozaki, M. et al., Length of Vertical Pipes for Deep-Ocean Sequestration of CO<sub>2</sub> in Rough Seas, Energy Vol.22 No.2—3 (1997) p.229
- (6) Ozaki, M. et al., Sending CO<sub>2</sub> into Deep Ocean with a Hanging Pipe from Floating Platform, Energy Convers. Mgmt Vol.36 No.6—9 (1995) p.475
- (7) Ozaki, M. et al., Study on Technical Method for Sending CO<sub>2</sub> into Deep Ocean with Pipe from Floating Platform, J. of the Society of Naval Architects of Japan, Vol.175 (1994) p.171

# Construction of EDSA LRT Turnkey System in Manila City

Noritsuka Terabayashi\*<sup>1</sup>  
Syunichi Shimamura\*<sup>1</sup>

Yoshiharu Watanabe\*<sup>1</sup>  
Fumio Tomikawa\*<sup>1</sup>

*The EDSA LRT SYSTEM is now under construction in Manila in the Philippines. This is a full turnkey project which includes civil works such as the guideway, station building and all electrical and mechanical works that are firstly challenged as a Japanese manufacturer. At present the engineering is approaching the final stage and the construction works have been proceeding energetically since October 1996 with the target for handing over to the customer being 1999.*

## 1. Introduction

Epifanio de los Santos Avenue (EDSA) is the principal highway of Metro Manila; every day, 300 000 vehicles carry more than a million people on this road with its five or six lanes on either side. However, owing to recent rapid urbanization, traffic jams on EDSA have become a serious problem in Manila.

A proposed solution to the traffic problem of EDSA is the construction of railway system as a means of mass transportation, and the Department of Transportation and Communications (DOTC) of the Philippines granted the right to develop such a system to the Metro Rail Transit Corporation (MRTC).

This railway construction is called the EDSA LRT project; it is a "build, lease and transfer" (BLT) project by which the MRTC builds the system and releases it to the DOTC for 25 years. However, its "operation" is directly governed by the DOTC.

Against this background, Mitsubishi Heavy Industries, Ltd., jointly with Sumitomo Corp., has contracted with the MRTC for total system construction including civil engineering as a turnkey project.

## 2. Outline of the project

This project consists of two phases of construction. The present contract is for phase I, which includes the total railway distance of 16.9 km from Taft Avenue Station to North Avenue Station, and the Depot located at the intersection of EDSA and North Avenue Station. In phase II, a 5.2 km extension is planned from North Avenue Station to Monumento Station. A map of the route is shown in **Fig. 1**.

Upon completion of phase I, the daily transportation capacity is expected to be about 450 000 people on weekdays, and about 28 000 pphpd (one-way traffic per hour in peak time). Trains will be operated in pinched loop operation communicating between terminal stations on double tracks. The round trip time will be about 60 minutes, the minimum operational headway 150 seconds, the standard train formation will consists of three cars, and high-density operation is planned in spite of the manual operation system.

In phase II, minimum operational headway of 120 seconds and standard train formation of four cars are planned. The construction of phase I includes the station platform length and overhead contact system (OCS) facilities applicable to such extension.

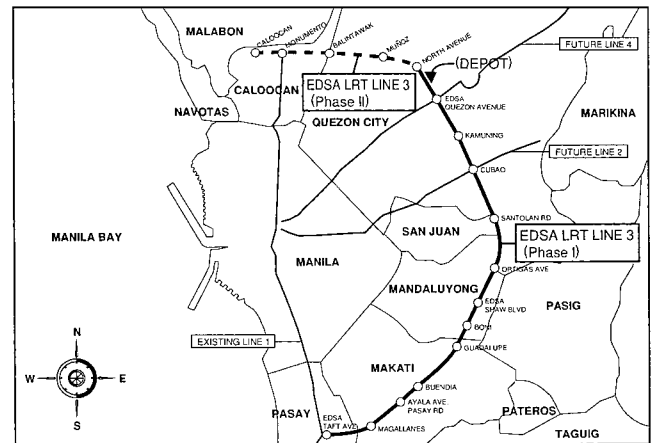


**Fig. 1** Route map of EDSA LRT (line 3, phase I, II) in Manila City

The line extends from EDSA Taft Avenue to North Avenue.

## 3. Outline of subsystem specifications

### 3.1 Guideway

The guideway is located in the center of EDSA, except for one section near Ortigas Avenue Station. It is an exclusive track occupying the standard width of 10.5 m in double track structure, and there are no level crossings for automobile traffic. In consideration of crossing with existing automobile traffic, 48% of the structure is elevated, 41% is at grade, and 11% consists of tunnel or underpass.

A nominal sectional view is given in **Fig. 2**. At grade, a concrete retaining wall is set up to give isolation from the automobile traffic, and a fence is installed in the upper portion. In both partition walls, OCS columns, emergency walkway in case of vehicle fires, cable trough, and a drain system are installed. The support post in the elevated section is a bored pile, and the superstructure has three continuous PC beams in the standard section.

A steel bridge will be built over the existing highway bridge crossing the Pasig River that flows between Guadalupe Station and Boni Avenue Station. This steel bridge will be a Langer bridge with an attractive parabolic profile, weighing 735 tons and extending over a distance of 135 meters.

### 3.2 Track

The gauge is standard 1 435 mm. At grade, concrete ties are laid on the ballast. The elevated section is a close couple track with rails connected directly to the plinth. UIC 54 rail are to be used.

\*1 Mihara Machinery Works

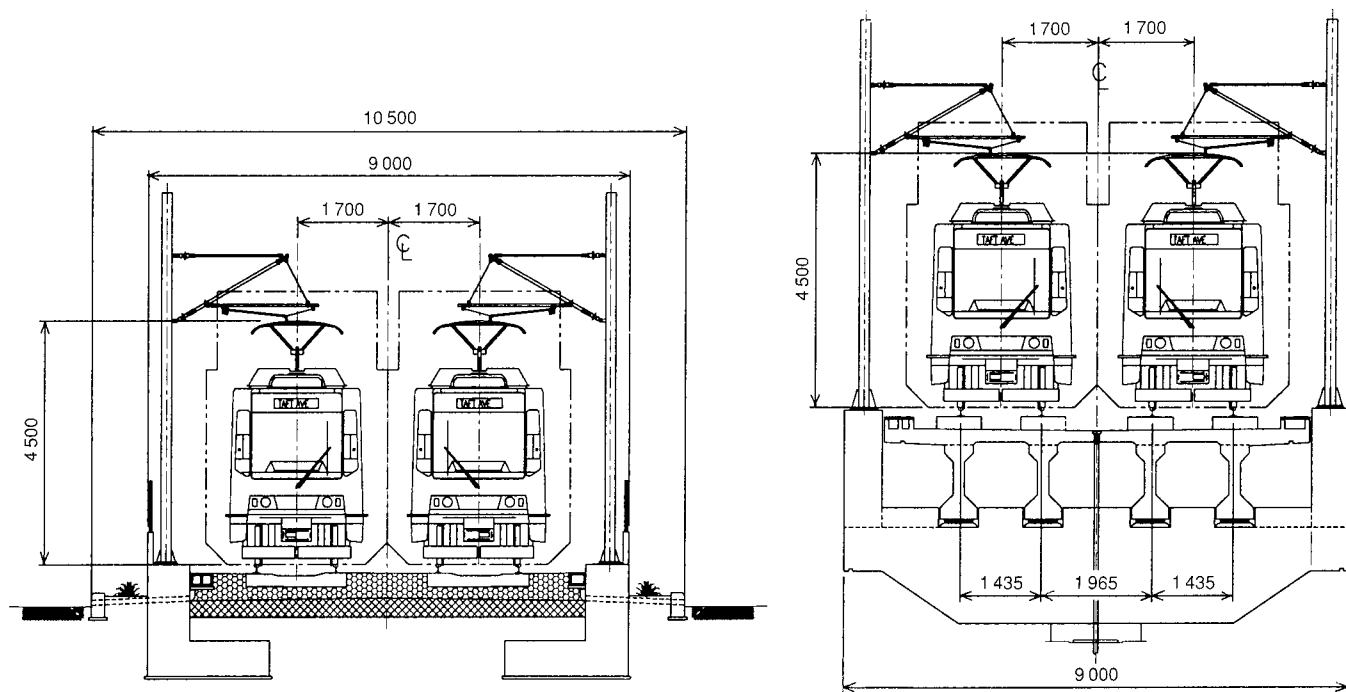


**Fig. 2 Nominal sectional view of at-grade and elevated tracks**

Sectional view of standard width in the portion having OCS posts on at-grade and elevated tracks.

### 3.3 Stations

Thirteen stations will be constructed in total to serve passengers. Regarding structure, there are elevated stations and at-grade stations depending on the track structure to be connected. Platforms are either opposed or island platforms, depending on the siting conditions. The average distance between stations is 1.34 km, ranging from about 800 m at minimum to 2.3 km at maximum.

At elevated stations, escalators, stairs and elevators will be installed to give access from the sidewalk to the station.

At entrances, the automatic fare collection system using a prepaid magnetic card will be installed to give access to the platform and for collecting fares, and efficient passenger movements will thus be assured.

The platforms will in principle have a barrier-free flat structure, and a safety area at least 2 m in width will be provided from the end of the platform. Passenger facilities will include communication equipment, CCTV, public address system, and various sign boards.

### 3.4 Depot

For the functions of both nighttime parking and maintenance of vehicles, a Depot will be built in a triangular area of 16 ha at the corner of North Avenue and EDSA (the Depot occupies an area of 8.5 ha, and the remaining space is to be used for the access line from the main track and commercial development zone).

For effective utilization of the land, the Depot will be built as an underground structure, and installed at a level several meters below the EDSA road surface. An artificial ground of a thick concrete layer will be erected above the Depot, and large commercial development facilities will be constructed on it. The maximum vehicle parking capacity will be 120 cars (90 cars in phase I).

### 3.5 Signals

Signal facilities are security facilities relating to train operation. A safe distance between trains is maintained by the facilities, and entry of trains into dangerous areas is avoided.

All facilities are fail-safe systems, and in case of trouble, they always incline to the safe side.

The signal facilities comprise the following four devices.

#### (1) Train detecting system

Function: To detect the presence of train at every block.

Method: The rail is used in part of an electric circuit, and an audible frequency signal from transmitter to receiver is interrupted by the presence of a car, so that its presence on the track is detected. Riding comfort is enhanced by employing the non-insulated track circuit in which an insulator is not inserted in every track circuit.

#### (2) ATP system

Function: At every block, the predetermined allowable speed and allowable running speed of each car in view of the train's present situation are transmitted to the cab to notify the driver. If it is exceeded by mistake, the brake is applied automatically.

ATP signal types: 65 km/h, 40 km/h, 30 km/h, 15 km/h, 0<sub>1</sub> (0 km/h), 0<sub>2</sub> (no signal).

#### (3) Interlock device

Function: On the basis of the signal from the train detecting system, a decision is made as to whether the next block section for a train to advance is free or not. Ground signals consist of a blue or red lamp of the track-side signal, and the cab signal consists of an ATP signal that is displayed to set the train direction.

Redundancy system: Dual type (One is in operation, another is standby)

#### (4) CTC system

Function: In the central control room installed at North

Avenue Station, the train's present situation and power device status are monitored, and the point machine is manipulated.

### 3.6 Communication

The communication equipment is composed of the following five facilities.

(1) Automatic telephone exchange system (PABX)

The telephone exchange of EDSA LRT system, having a capacity for 150 circuits.

(2) Radio communication system

A communication system between the center and the train driver, and two channels for the main track and one channel for the vehicle base are provided.

(3) Station public address system (station PA)

There is a public-address system from station clerk to passengers or staff members. A maintenance PA system is also installed in the vehicle base.

(4) Cab public address system (cab PA)

There is a PA system from the train driver to the passengers. This system is also usable for internal communication between the driver and conductor in the same train.

(5) CCTV facility (monitor camera facility)

The station CCTV facility enables the behavior of passengers to be monitored by the station clerk and driver. Cameras are installed on the platform, elevator and other places. The Depot CCTV facility is for monitoring the performance of trains in the Depot.

### 3.7 Electric power supply equipment

The electric power is received at eight substations at 34.5 kV from MERALCO, the local electric power company in Manila. The received power is distributed into the two sub-systems.

(1) Power feed sub-system to train (T system)

(2) Facility power supply system to auxiliary equipment and lighting (A system)

The entire system configuration is shown in Fig. 3.

**Table 1 Main features of power supply equipment**

Device	Capacity/unit	Voltage	No. of units
Transformer/rectifier unit	3 000 kW	AC 34.5 kV/DC 750 V	9
Transformer	1 000/750 kVA	AC 34.5 kV/11 kV	8
Auxiliary transformer	1 500 kVA	AC 34.5 kV/480 V	2
Auxiliary transformer	400/300 kVA	AC 11 kV/480 V	13
Emergency battery power source	50/30/20 kVA	AC 220 V	14
Battery charger	200/150/48 kA	DC 110 V	14
Emergency generator	550/150 kVA	AC 480 V	2

The capacity of the principal facilities and the number of units are shown in Table 1.

The electric power transmission line will be an overhead catenary system (OCS) composed of 170 mm<sup>2</sup> contact wire supported by droppers suspended from two 150 mm<sup>2</sup> messenger wires, and two 250 mm<sup>2</sup> feeders. Between some stations, two 250 mm<sup>2</sup> feeders are also used. Posts for OCS will be installed at intervals of 30 to 60 m at both ends of the up and down tracks. The electric power is supplied to the train through the contact wire and is returned to the substation negative pole through the track rail.

### 3.8 Cars

The cars have two articulations in the middle of the body, and the center bogie are connected at the points for supporting both car body sections. This structure has the advantage to be able to negotiate with a turning radius of 20 m. Eight DC motors are driven by the chopper control unit employing insulated gate bipolar transistors (IGBT). The regular brakes are electric brakes, and stopping and parking brakes are disc brakes. The electric brakes usually function as regenerative brakes, but the moment the catenary voltage reaches the maximum operating voltage (DC 900 V), they are changed over to rheostatic brakes. The regenerative power are consumed within this rail system only, not to the other utilities. The emergency brake consists of an electric brake and a track brake.

The main specifications are shown in Table 2, and an outline drawing is given in Fig. 4.

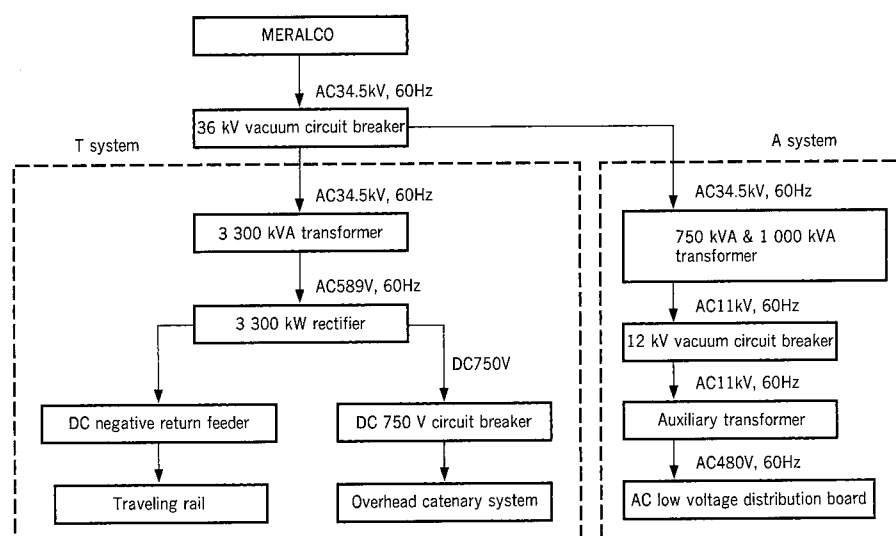


**Fig. 3 Schematic diagram of electric power supply system**

Power received from MERALCO is distributed to train driving and station facilities.

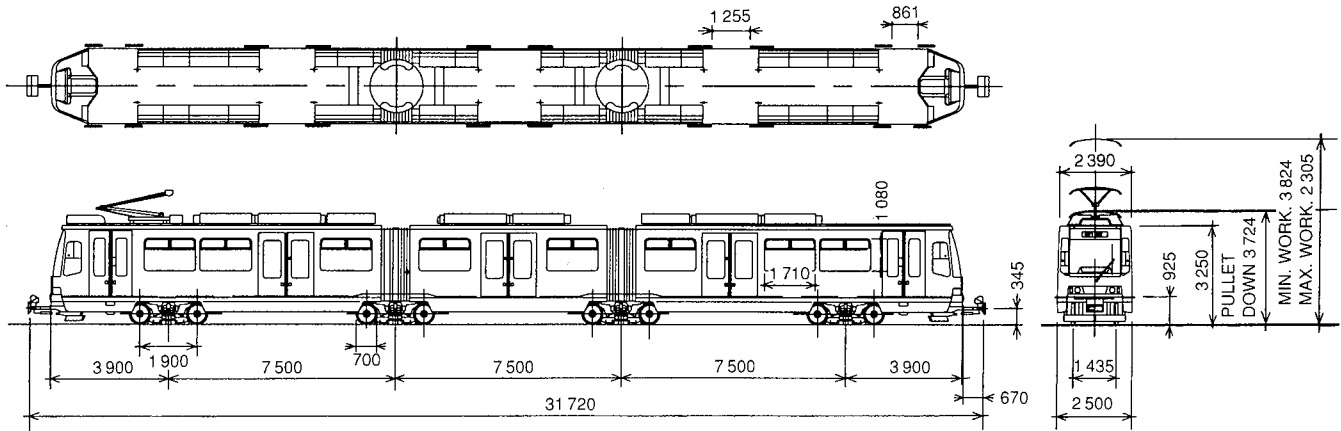


Fig. 4 Eight-axle DC motor driven Light Rail Vehicle

Table 2 Main vehicle data

No. of cars	73
Type	8 axles motor driven of 4 bogies, a three-section articulated car (including two articulations)
Drive system	Chopper driver (IGBT transistor) 64.5 kW DC shunt motor $\times$ 8 units
Brake system	Regenerative/rheostatic changeover type electric brake Track brake Disc brake
Operation control	Manual operation by driver 7-step powering, 8-step braking (including emergency brake)
Maximum speed	65 km/h
Minimum turning radius	20 m
Supply power	DC 750 V + 150 V - 250 V
Passengers	274 (specified), 394 (full capacity)
Car dimensions	L 30 300 $\times$ W 2 500 $\times$ H 3 550 mm
Car weight	46.8 t (empty), 70.4 t (fully occupied)

#### 4. Present situation of construction

Construction of the present project began in October 1996 and is going ahead rapidly as of March 1998 in the middle of dry season. Construction scenes are shown in Fig. 5 and Fig. 6.

The construction site is a narrow urban area as indicate by the following figures, and is large in terms of weight and quantity of materials.

- Construction site: about 17 km long, and vehicle base of 8.5 ha
- Amount of concrete: 154 000 cubic meters
- PC girders (I type): about 2 000

Since the EDSA is in the most congested area of Manila, and the construction site is the central traffic island, the work is carried out under the strict traffic control which is characteristic of urban traffic projects.

- (1) The road width available for work is limited, and access of heavy-duty construction machinery is limited to nighttime.
- (2) Temporary isolation fences have been set up to avoid contact with vehicles running on other lanes not used in work to prevent accidents, and the safety of the workers inside must be considered at the same time.

The authorities are attempting to calm down the complaints of citizens regarding traffic jams caused by the work by setting up detour route maps and other sign boards at the sites.

A further problem is that water works and sewers are

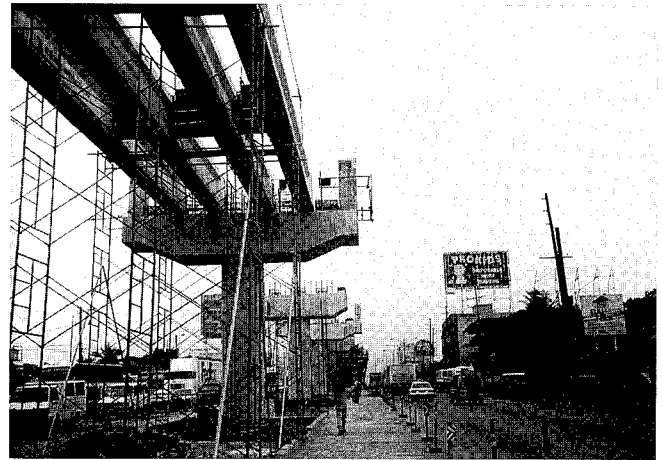


Fig. 5 Guideway under construction at Santolan area  
Elevation of PC girder (I type) was started at Santolan.

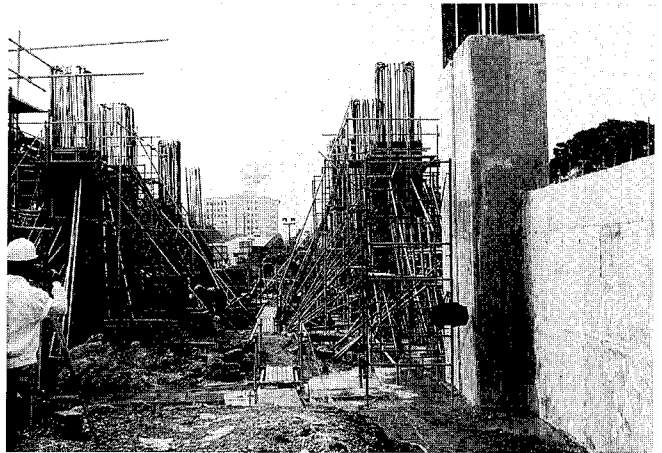


Fig. 6 Kamuning Station foundation and pier construction

buried under the ground and electricity and telephone wires are erected overhead. In order not to interfere with these facilities, various measures are always taken, including their temporary removal. In addition, even if the structures are similar at the design stage, the actual construction works may be different depending on the location, and the process must be varied depending on the circumstances.

Accidents at the construction site may be disastrous including civilian casualties, so safety and traffic control plans

are very important. In this regard, too, through proper prior negotiations, various risks can be predicted, and all necessary measures are taken in daily activities. So far, few accidents have occurred since the beginning of the construction work.

Meanwhile, manufacture of various facilities for installation and maintenance of electric power, signaling and the Depot is being implemented by the manufacturers, and certain devices are already at the plant test stage.

## 5. Conclusion

At present, the civil engineering works have been finished in 70% of the total distance, and the present situation of

progress of the project is reported herein together with the main specifications of the system, whose design is in the final stage.

This is a national project for the Philippines, and its achievement will bring direct benefits to citizens in their daily lives. The site of construction is in the center of the capital, and the significance and responsibility of promoting the work in view of the high expectations and keen attention of the citizens are great. As we imagine the departure of the first blue-and-white train from the platform under the blue sky of Manila in 1999, we are determined to concentrate all efforts of the project team on completion of this dream.

# Automated People Mover for Airports

Hiroyuki Mochidome\*<sup>1</sup>

Michio Koizumi\*<sup>1</sup>  
Masuo Takahashi\*<sup>1</sup>

Recently, as the size of each airport has grown a track transportation system inside the airport for passengers has become indispensable. Under such circumstance, Mitsubishi Heavy Industries, Ltd. (MHI) have received an order for APM system, which is a completely automated rubber tired vehicle, to be installed at the new airport in Hong Kong. The core of the APM vehicle system is designed based on the vehicles of the domestic (Japanese) new transportation system. In order to apply the system to the airports, we had various issues to solve including automatic train control system improvement of safety functions, stopping accuracy and so on. In this report, we explain outline of the work we did during design and manufacture stages. We have tested the completed APM vehicle on our test track. As a result of the test, we confirmed that the vehicle had come up to the target level.

## 1. Introduction

Recently, construction of airport hubs and the expansion of the existing airports have become popular in the world, mainly in Southeast Asian countries. As the size of each airport has grown, the movement of passengers inside and in the areas surrounding airports tend to increase, and the distance that passengers must move across also tends to be longer. Therefore, new transportation systems, has become indispensable in such large-sized airports.

MHI has received an order for an Automated People Mover System (APM system) for the new Hong Kong airport as the first transportation system for use at an airport. Construction of the entire system has been completed and the system is currently undergoing final adjustment in preparation for the opening of the airport in July 1998. This report presents on overview of the Automated People Mover Vehicle (hereinafter referred to as APM vehicle) which serves as the core of the APM system (Fig. 1).

## 2. Outline of APM system

The APM system for the new Hong Kong airport connects the airport terminal building and the remote gates. It is used inside the airport for passengers. This APM system, as shown in Table 1, consists of several sub-systems such as an operation control system, signaling system, communication system, automatic operation system, power distribution system, track, station equipment and maintenance equipment. This contract is the first phase of new airport project which consists of an about 700 m long double track between two stations in an underground tunnel of the entire length. Transportation

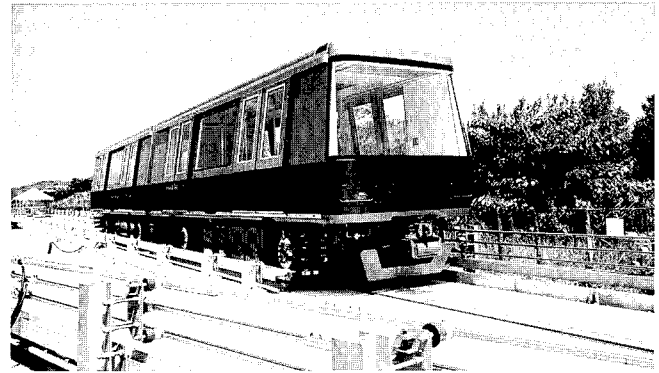


Fig. 1 Vehicle on MHI test track

The APM vehicle under completely automated operation on MHI test track is shown here.

capacity of the system is a maximum of 5 270 Passengers Per Hour Per Direction (PPHPD).

The operation of the vehicles consists of a completely automated operation using an Automatic Train Control (ATC) system. The ATC system consists of an Automatic Train Protection system (ATP), Automatic Train Operation system (ATO) and Automatic Train Supervision system (ATS). The ATP system employs an on-board signal aspect system, a check-in/check-out system, and controls the route through a Solid State Interlocking (SSI) system. The ATO has a programmed station stop function using an on-board arithmetic system. Further, a station ATO system for cooperative control of vehicle doors and platform doors as well as an ATO data transmission system between vehicle and on-land equipment are installed as part of the APM system. The ATS system has the functions of supervising and implementing the operational

Table 1 Sub-system of APM system

Sub-system	Main component	Function
Vehicle	Vehicle	Transport unit
Operation control system	Operation control unit	Operation and control of entire system
Signalling system	ATP/TD unit	Signal and safety function
Communication system	ATO transmission unit, LCX transmission unit	Communication between ground and train
Automatic operation system	On-board ATP/ATO unit, Station ATO unit	Automatic train operation
Power distribution system	Transformer, electric overhead line	Supplying power to system and vehicle
Guideway	Running surface, guide rail, switch	Running track of vehicle
Station equipment	Platform door	Securing safety of passengers
Maintenance equipment	Maintenance equipment	Maintenance equipment of vehicle

Note: ATP/TD Automatic Train Protection/Train Detection

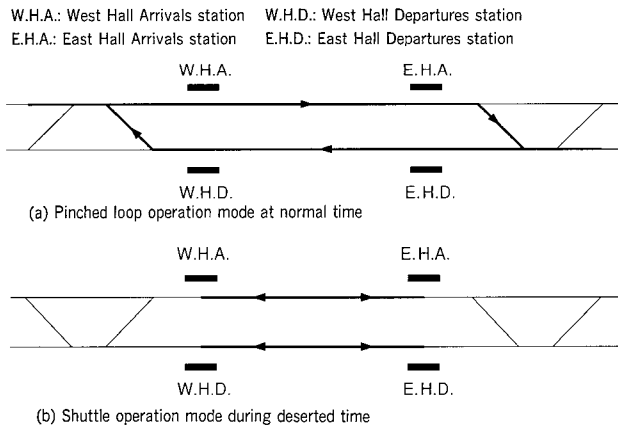


**Fig. 2 System operation mode**

Basic operation mode of the APM system is shown.

command of the system, monitoring and recording of system operations and is installed in the airport operation control center. The command console consists of a touch-screen type CRT operation system and is designed to control the operation by one operator except in the case of an emergency.

As airports are operated 24 hours a day, the APM system must also be operated for 24 hours. In order to meet such variations in demand, two main types of operating modes have been adopted. Four trains are used on the tracks and loop operation is performed during peak times [Fig. 2(a)] and, while shuttle operation using two train formations to meet demand have been implemented at the times when the airport is comparatively deserted such as at mid-night [refer to Fig. 2(b)]. Furthermore, five operation modes other than the above are set to deal with maintenance and failure of the sub-systems such as vehicles, power system and tracks. Completely automated operation of the ATC system is possible in these operation modes. The operation modes including the number of train formations are designed to be automatically changed through CRT operation in the central operation command room. This system is designed to achieve a high rate of operation [Fault Tree Analysis (FTA) result 99.9 %] as an APM system by flexibly setting and selecting the operation modes and improving reliability of the sub-systems.

### 3. Development of APM vehicle

#### 3.1 Overview of APM vehicle

APM vehicles have been improved and altered in design to adapt to the special needs of passenger transport inside the

**Table 2 Specifications of APM vehicle**

Item	Specification
Vehicle formation	Two-cars fixed formation
Passenger capacity (person)	76 (inclusive of 5 seats)/car × 2 cars
Tare weight (tf)	11.8/vehicle
Vehicle dimensions (mm)	9 850 long × 2 700 wide × 3 510 high/car
Guidance system	Side guide 2-shaft, 4-wheel steering system
Electric system	3-phase, A.C. 600V, 50 Hz
Gauge (mm)	Tred 1 700, guide rail span 2 800
Vehicle performance	Maximum speed: 70 km/h Acceleration: 3.5 km/(h·s) Deceleration Maximum service: 3.6 km/(h·s) Emergency: 5.4 km/(h·s)
Control system	Thyristor leonard phase shift control (with load compensating device and regenerative brakes)
Brake system	Electric command electro-pneumatic straight air brake system (with safety brake and parking brake)

airport based on the rubber tired vehicle of the new transportation systems so far delivered in Japan. Fig. 3 shows the vehicle formation and Table 2 summarizes the main specifications of the vehicle.

The vehicle formation consists of a fixed formation of two cars and can be formed up to three vehicles for completely automated operation. The sizes of the vehicle are enlarged based on the vehicles of the new transportation system used in Japan taking into consideration the increase in transportation volume of the system and improvement in the degree of comfort in the vehicles. Passenger capacity per vehicle formation has been increased to 152 persons.

The vehicle body consists of a welded structure of aluminum alloy in order to reduce weight. The bogie is a steering bogie with side guiding equipment consisting of a driving bogie a trailing bogie. A set of the driving bogie and trailing bogie is equipped on each vehicle. Type tests of the vehicle and continuous running for 800 km under completely automated operation of the vehicle were performed during which time its performance and reliability were confirmed.

#### 3.2 On-board ATC system

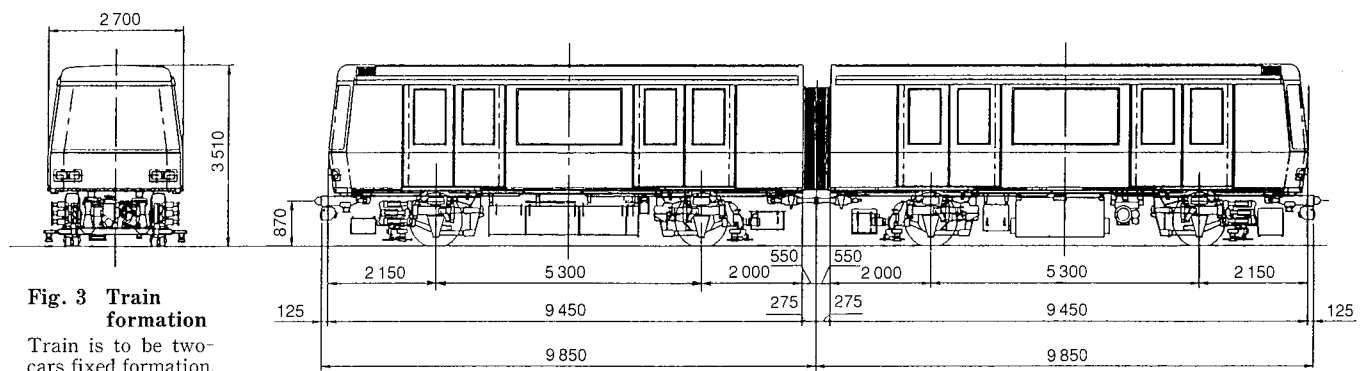
Fig.4 shows the block diagram of the on-board ATC system.

##### 3.2.1 Automatic operation system

The automatic operation system consists of the following equipment based on the new transportation systems used in Japan.

##### (1) ATO unit (onboard)

The target operation speed of the system is set based on ATP signal given from ATP receiver, and the function of



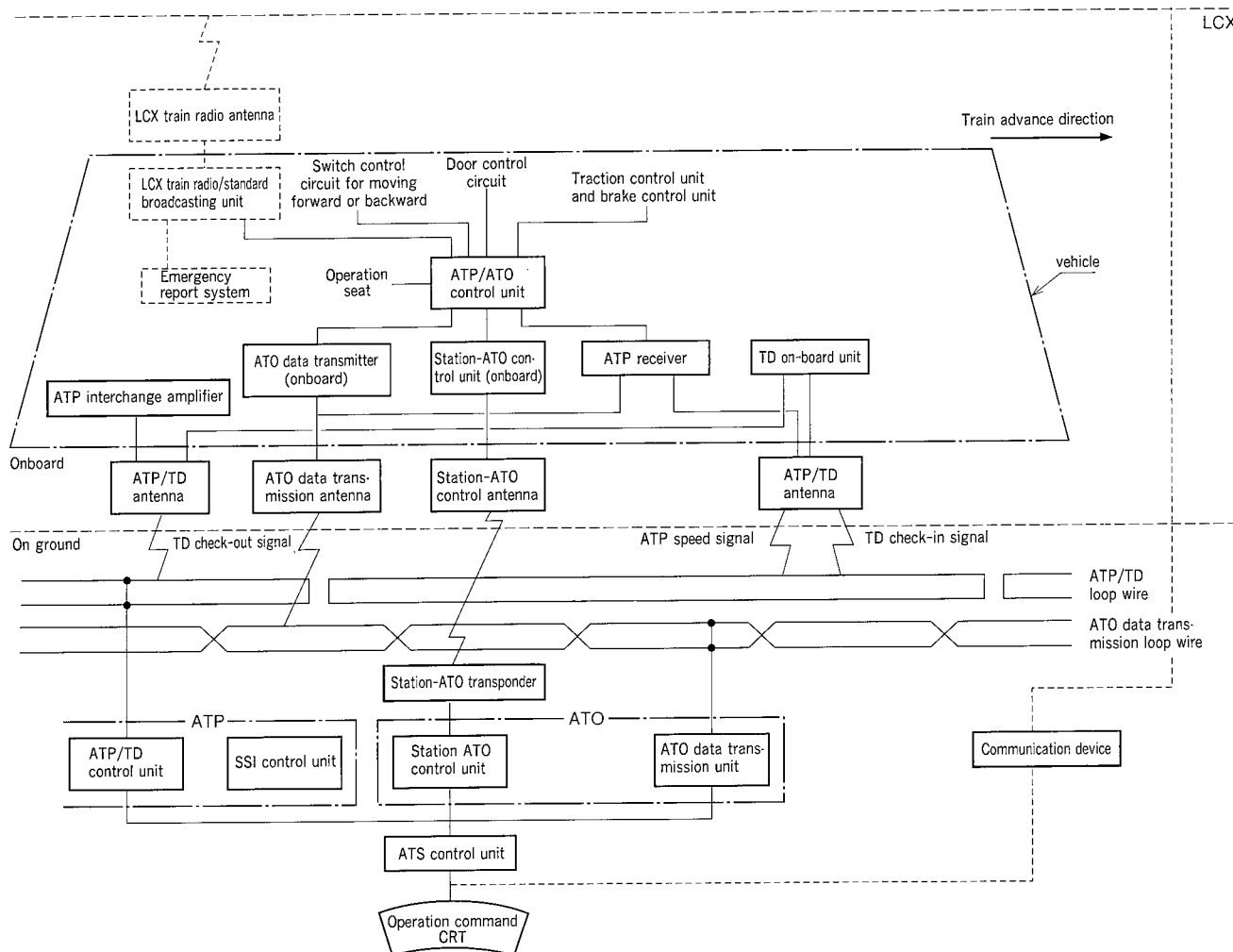


**Fig. 4 Block diagram of on-board ATC system**

Configuration of on-board ATC system and relation with on-land ATC system are shown.

constant speed operation control and the function of the programmed station stop based on the spot signal received by the station ATO control onboard unit are given to this system. Measures for improving accuracy for programmed station stops were taken as described in Section 3.4.

(2) Station ATO control unit (onboard)

The onboard antenna receives the door control command from the ground unit installed on each station. Further, the function of transmitting train control state signals from onboard at each station is given to the station ATO control unit.

(3) ATO data transmitter (onboard)

The function of the onboard ATO data transmitter is to make contact between the central command station and the train. The central command station transmits the control command to various units in the system, while at the same time the state information such as operation and failure of each unit is transmitted to the central command station from the vehicle.

### 3.2.2 Safety system

Safety and communication systems are also based on the new transportation systems used in Japan.

(1) ATP system

The ATP system continuously transmits the control

speed signal to the inductive loop installed on land which is continuously received and decoded by the onboard antenna. Information such as speed limit and stopping of the train is given to the ATP control system. Further, in the APM vehicle, switching of directions of the vehicle and distinctions for opening the side doors which were previously the functions of the station ATO system, etc. were integrated in the safety function of the ATP system in order to improve safety.

(2) TD system (onboard) (Train Detection: TD)

This system gives information regarding train track position to the ATP system (on ground) and is a continuous transmit-receive type system.

### 3.2.3 Communication system

The train radio system employs an LCX system, and two emergency speaking devices are installed in each vehicle so that passengers can communicate and speak with the central command station in case of an emergency.

On-ground and onboard connection tests as well as automatic operation running tests were performed on the MHI test track for the above onboard ATC system. It was confirmed that the functions and performance characteristics achieved the expected target values. In addition, the software of the entire ATC system including the on-land system was examined

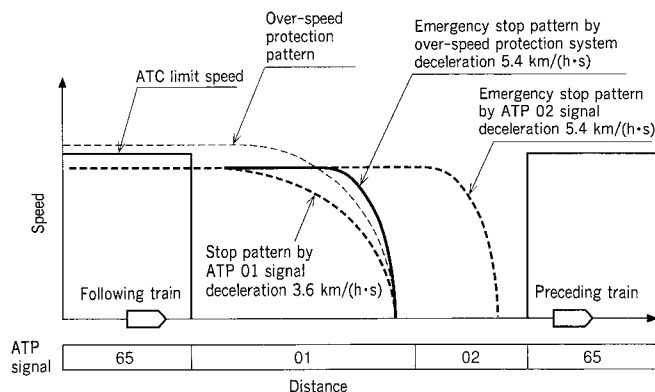


**Fig. 5 Conceptual drawing of over-speed protection**

An emergency stop is executed at the expected stop position even if the over-speed protection pattern is touched in the ATP 01 signal section. The ATP 02 signal section may possibly be omitted when the over-speed protection system is installed.

by the Railway Technical Research Institute for safety based on IEC 1508 "Functional Safety: safety-related systems (part 1 to 7)" according to which the safety was confirmed.

### 3.3 Over-speed protection

The ATP system of the safety system on ground was employed as an operation safety system in this APM system. Further, an over-speed protection function was newly added as an on-board-related operation safety system, in order to improve the redundancy of the operation safety system and reduce train operation intervals. Fig. 5 shows a conceptual drawing of the over-speed protection.

As shown in Fig. 5, the tracks on which the vehicles run is fixedly divided into a constant section (block section) for safety and ATP signals (limiting speed signal and stop signal) are given to each section based on the relative position between trains and restrictions on the tracks such as curvature. The train is automatically operated according to these ATP signals received from the ground. The stop signal (0 signal: 01 or 02) is given to the rear section of the preceding train. The function which decelerates and stops the following train by the ATP brakes [service maximum deceleration 3.6 km/(h·s)] when it enters the 01 signal section, and decelerates and stops the train by the emergency brake [deceleration 5.4 km/(h·s)] when it enters the 02 signal section, is set to the ATP system. Further, when the train exceeds the ATP signal during constant speed running according to the speed signal, the train is decelerated to less than the ATP signal by the service maximum brake. These safety functions are given by the ATP system on the ground. However, the ATP system based on such fixed block establishes the fixed safety intervals which are always required by the brake performance of the train between the preceding train and the following train. As a result, this system hampers high density operation of the trains.

However, in this system the emergency stop pattern was set in the outside of the ATP signal from the ground as shown in Fig. 5. This function is in which after the train enters the ATP 01 signal section, the emergency stop pattern is generated in the onboard control unit and the presence or absence of touch with this pattern is verified by the running distance and speed of the train itself. When presence of such touch is verified, the emergency brake is actuated.

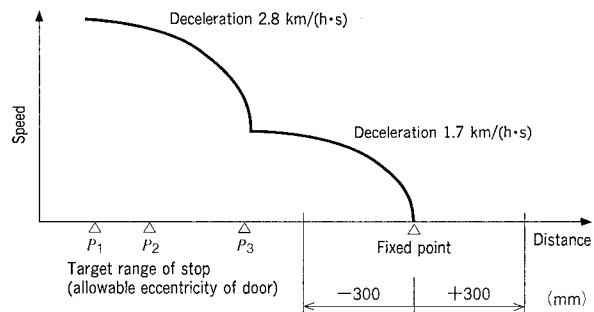


**Fig. 6 Train automatic stop control pattern**

The typical deceleration and stop pattern of a train which stops at a station is shown here. The train is controlled in such fashion as to be automatically decelerated and stopped according to a two stage pattern.

The emergency stop pattern is set such that the emergency stop pattern is generated in the onboard ATP control unit in the ATP 0 signal section. Even when the train is not decelerated with the specified ATP brake by the 01 signal, the train is stopped by the emergency brake at the specified stop position by the ATP brake. At the same time, the absolute limiting speed line in the ATP limit speed signal section is established above the limiting speed. When the train speed exceeds this line, the function of emergency stop [deceleration 5.4 km/(h·s)] is added to the emergency stop pattern. The operation safety system using such onboard control system is called over-speed protection.

As described above, safe and high-density operation became possible in the completely automated operation through the addition of over-speed protection function to the existing ATP function. The verification test for this function was performed on the MHI test track. From such results, it

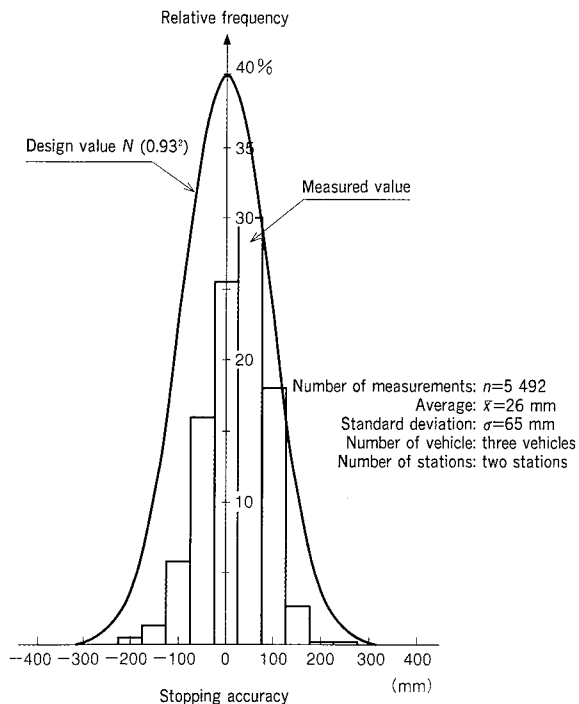


**Fig. 7 Result of measuring of stopping position**

The results of measurements of stopping accuracy at the MHI company test track is shown by a histogram. From this figure, it can be seen that a good result of 195 mm ( $=65 \times 3$ ) against the target of  $3\sigma = 300$  mm was obtained. The solid line shows the design value.

was confirmed that minimum operation intervals of approximately 100 seconds in the APM system for the new Hong Kong airport could be realized.

### 3.4 Improvement of stopping accuracy

It is a necessary condition that a completely automated train stops accurately at each station. In the APM system for the new Hong Kong airport, the customer's specifications required that a stopping accuracy of 150 mm at  $\sigma$  of a generation probability of 68.3% and 300 mm at  $3\sigma$  of generation probability of 99.7% from allowable eccentric values between the train access door and the station platform door.

**Fig. 6** shows the train automatic stop control pattern at the station. The stop control pattern is generated in the automatic train operation control system between the point  $P_1$  (about 250 m before the stop position) and the expected stop position (the fixed point). The train is decelerated and stopped by the specified stop control pattern based on the speed and running distance detected on the train. On the way, the absolute position between the point  $P_2$  and the fixed point is detected by the transponder in the ATO system of the station to support the stop control.

The factors related to the stopping accuracy for such existing stop controls were analyzed and their degree of contribution was simulated. The stopping accuracy was improved based on the above results as shown in **Table 3**.

**Fig. 7** shows the distribution of the stopping accuracy. The solid line shows the simulated results (design values) of the stopping accuracy after improvement, and the histogram shows the measured values of the stopping accuracy on the MHI test track. It can be understood that 300 mm at  $3\sigma$  of the

**Table 3 Improvement of stopping accuracy**

Factor	Measures
Speed and distance detecting accuracy	Improvement of speed resolution by changing speed sensor output to total wave rectification system
	Determination of accurate distance and speed by adding automatic compensating function of tire diameter
Absolute position detecting accuracy	Exact determination of point position by employing carrier detection system in spot signal input
Brake force controlling accuracy	Smooth brake control just before stop by changeability of brake notch for prevention of rolling

specified stopping accuracy could be attained by improving of the stopping accuracy shown in Table 3 using the above results.

### 4. Conclusion

The new Hong Kong airport will be opened in July of 1998. At the same time, the first APM system of MHI will start operation. In this report part of the outline of the APM train and its development are introduced. Currently the system is undergoing final adjustment, but every effort is being made to finish the system more completely until commencement of the operation. It is the strong hope of everyone involved in the project that many people will use the system effectively after opening of the new airport and that the expected objective of the APM as a transportation system can be attained.

In conclusion, the authors wish to express their special thanks for the valuable external support which they have had to date, particularly from the companies concerned who supplied the sub-systems.

# Development of Non-Stop Toll Collection System

Hideyuki Murakoshi\*<sup>1</sup>

Michio Hamana\*<sup>2</sup>

Kazumasa Miyamoto\*<sup>3</sup>

*The Non-stop Toll Collection System can ease traffic congestion, reduce cost of manpower and improve customer service by cashless tolling. Also, it can bring about environmental improvements by reducing the exhaust gas and noise emitted as vehicles start or accelerate from toll plazas. Therefore, its application to toll roads has been increasing especially in foreign countries. This report covers the elemental technology and system technology needed for the Non-stop Toll Collection System and the result of system operation tests in Malaysia and Singapore. Mitsubishi Heavy Industries, Ltd. (MHI) started the development of this system in 1984, and has received orders for the system from the countries mentioned above. The system employs elemental technology and system technology using radio frequency communication (RF communication) and image processing obtained by many years of research.*

## 1. Introduction

The aim of the electronic toll collection (ETC) system is to collect tolls at toll plazas by RF communication without requiring the passing vehicles to stop at the plazas. The system is expected to improve the environment by reducing emissions and lowering engine restarting noise, and to bring about economic effects by saving fuel and shortening driving time. This system, which has been already installed widely in Europe and America, has recently been planned and introduced in Asia, and use of the system is becoming a global trend. MHI started its research and development in 1984, and received orders for the ETC system from Malaysia, and also for an electronic road pricing (ERP) system from Singapore as a toll collection system which limits traffic flow into the urban area.

This papers give an outline of the ETC system and elemental technologies including the RF communication, image processing, and system integrating. As practical examples, trial operation reports of the systems for Malaysia and Singapore are also included.

## 2. Outline of ETC system

The ETC system allows vehicles to pass without stopping or manual operation by collecting the toll through RF commu-

nication between a roadside antenna installed at the toll plaza and an RF communication unit mounted on the vehicles. The system consists of the antenna for RF communication, antenna controller, vehicle presence detector for detecting the presence of vehicles on the lane, equipment to block the passing and capture the image of vehicle with invalid onboard equipment (OBE), and a lane controller for integrating and controlling these devices. The ETC system may be classified into the single-lane ETC system and multi-lane ETC system depending on the lane type of the toll plaza. The former collects tolls on every lane as in existing toll plazas, and basically performs a sequential transaction for each vehicle. The latter collects tolls from a number of vehicles simultaneously traveling along several lanes, as on an expressway. Each system is described below.

### 2.1 Single-lane ETC system

#### 2.1.1 System configuration

The single-lane ETC system is applied in place where the lanes are completely separated, as in existing toll plazas, and is designed to collect toll from each vehicle on every lane entering the toll plaza. An example of this system configuration is shown in Fig. 1. As shown in the diagram, the single-lane system is composed of a roadside antenna, a vehicle presence detector, indicator and others, but the toll collection

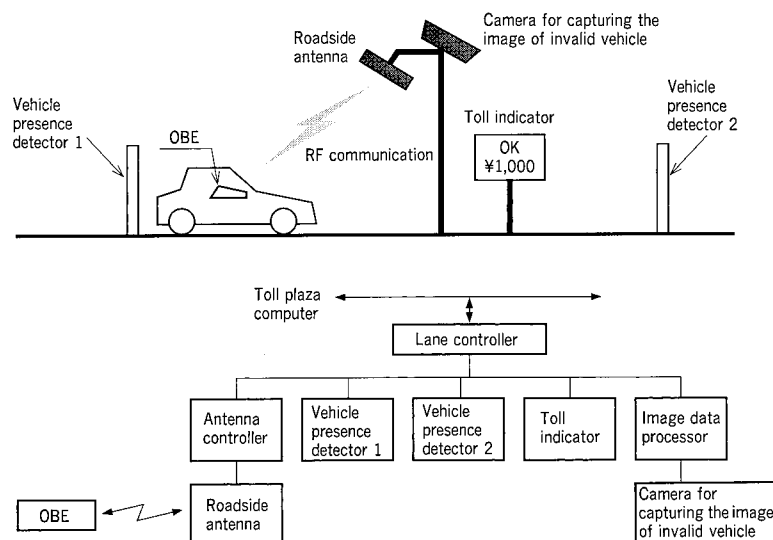


**Fig. 1 Example of system configuration of single-lane ETC system**

An example applied to toll plaza and lane is shown.

\*1 Kobe Shipyard & Machinery Works

\*2 Takasago Research & Development Center, Technical Headquarters

\*3 System Technology Center, Electronics Research & Development Department

function on lane differs between the toll lane of the open system collecting the same toll from each type of vehicle, and the closed system collecting different tolls depending on the traveling distance and vehicle type. Thus, the system configuration also varies with the lane of the open system, the entry and exit lane of the closed system.

### 2.1.2 System functions

In most instances of the single-lane ETC system, the ETC equipment is additionally installed to existing manual toll plaza, and the system is therefore often integrated with the existing toll collection system equipment (vehicle presence detector, lane barrier, indicator, and other lane control devices having interface between the roadside equipment and the host equipment for totalizing the tolls).

As mentioned above, these existing toll system arrangements vary with the lane type—e.g., open system and closed system (entrance and exit toll plaza)—and also the toll plaza type. The basic functions of the single-lane ETC system are:

- Detection of vehicle entry, and start of RF communication
- Toll collection by RF communication with OBE (writing and reading of entrance toll plaza number, time, and collection of toll)
- Display of collected amount
- Detection of vehicle passage
- Capturing the image of license plate number of vehicle having invalid OBE

## 2.2 Multi-lane system

### 2.2.1 System configuration

The multi-lane ETC system is a system applied in place where a number of vehicles travel on several lanes simultaneously as on the main lanes of a tollway, and is designed to handle a number of vehicles entering the toll plaza simultaneously.

An example of this system configuration is shown in Fig. 2. As shown in the diagram, the multi-lane system is composed of the equipment installed on a gantry straddling several lanes, such as several roadside antennas, vehicle presence detectors, a camera for capturing the image of vehicle with invalid or no

OBE.

### 2.2.2 System functions

In the multi-lane ETC system, since the ETC equipment is installed on the main lane of the tollway, the traveling speed of the vehicle is fast, and it is necessary to determine the position of the moving vehicle on the lane, unlike the single-lane system installed on the toll plaza lane.

Therefore, there is a need for both high-speed processing to deal with the vehicles traveling at high speed on several lanes simultaneously, and short-range communication band of roadside antennas for identifying the vehicles from which toll are collected. The functions of multi-lane ETC system are given below.

- Toll collection by RF communication with OBE (writing and reading of entrance toll plaza number, time and collection of toll)
- Detection of vehicle passage position on the lane by vehicle presence detector
- Locating the position of the vehicle communicated with the antenna
- Capturing the image of license plate number of vehicle having invalid OBE by the camera at the detected position

## 3. Elemental technologies of ETC

Construction of ETC system requires various elemental technologies including RF communication technology. It also requires a system technology to integrate these elemental technologies. As principal elemental technologies of the ETC system, the RF communication technology, vehicle detection technology, and technology for enforcement are briefly described below.

### 3.1 RF communication technology

#### 3.1.1 Requirements for RF communication

##### (1) High reliability

Since financial information is handled in the ETC system, high reliability is required in the RF communication.

Usually, the data bit error rate is required to be  $1 \times 10^{-5}$

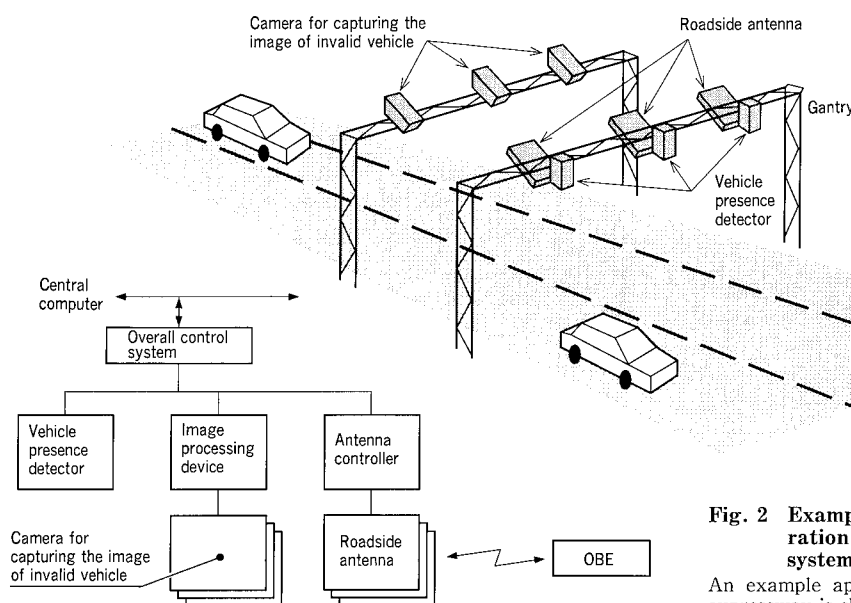


**Fig. 2 Example of system configuration of multi-lane ETC system**

An example applied to main lane of expressway is shown.

**Table 1 Specifications of RF communication equipment**

Item	Specification	Remarks
Roadside antenna		
Frequency band	2 450 MHz band* <sup>1</sup>	* 1 Frequency band and output vary with each local situation
Output	300 mW or less* <sup>1</sup>	
Polarization	Circularly polarized wave	
Data transmission speed	600 kbps or more* <sup>2</sup>	* 2 Varies with the applicable system
Modulation method	ASK* <sup>3</sup>	* 3 Amplitude shift keying
Communication area	3 m (transverse direction) × 4 m (traveling direction)* <sup>4</sup>	* 4 Supposing vehicle mounting height to be 1 m
Onboard equipment		
Method	Passive method (backscatter)	
Modulation method	PSK* <sup>5</sup>	* 5 Phase shift keying

or less.

(2) Limitation of communication area

To obtain the high reliability mentioned above, sufficient radio transmission intensity must be provided, but if the antenna output is too high, it may cause interference with the antenna of the adjacent lane or communication with the vehicle ahead or behind by mistake. For this reason, the directivity of antenna must be controlled and the communication area must be limited. The communication area of roadside antennas used in this system is about 3 m × 3 m (transverse direction × traveling direction), corresponding to the size of a vehicle.

(3) High speed data transmission

To assure sufficient reliability and to transmit and receive a huge volume of data even in such a limited communication area, high speed data transmission is needed. The data transmission speed is determined by the vehicle speed and the data volume, and often required to be more than 500 kbps.

### 3.1.2 Main specifications of RF communication

For data communication of the ETC system, infrared ray communication and RF communication are considered to be the media that satisfies such requirements. We employ RF communication in semi-microwave band or microwave band, because they are less affected by the dirt on antennas and so on.

An example of the specifications of this RF communication equipment is shown in **Table 1**.

## 3.2 Vehicle detection technology

### 3.2.1 Requirements for vehicle detection

(1) High reliability

Similar to the RF communication technology mentioned above, in the ETC system, high reliability is also required for vehicle detection. The vehicle detection error rate is often required to be  $1 \times 10^{-3}$  or less.

(2) Separation of vehicles

It is necessary to separate vehicles traveling bumper to bumper or side by side accurately, and to detect the position and the number of passing vehicles correctly. Usually, the ability to detect vehicle separation is required to be several hundred millimeters or less.

(3) Dealing with vehicles traveling at high speed

To detect and identify the vehicles on the lane accurately, high-speed response of sensor and high-speed processing are required. It is particularly important to detect vehicles travelling at high speed on the main lanes of tollways.

### 3.2.2 Main specifications of vehicle presence detector

There are various methods for the vehicle detection, such as optical sensors, loop coils, treadles and others. As an example applicable to both the single-lane and the multi-lane system, specifications of overhead type vehicle detector are shown in **Table 2**.

**Table 2 Specifications of vehicle detector**

Item	Specification	Remarks
Sensor unit	One-dimensional camera	
No. of pixels	2 048	
Driving clock	8 MHz	
Detecting range	4 800 mm (transverse direction)* <sup>1</sup>	* 1 Varies with the applicable system
Accuracy of separation	250 mm (transverse direction and traveling direction)* <sup>1</sup>	
Control unit		
Response time	30 ms or less	

## 3.3 Technology for enforcement

Since the aims of the ETC system are to realize an automatic toll collection at toll plazas and to pick up invalid vehicles, it is necessary to install the enforcement devices such as lane barriers and cameras. Requirements and specifications for enforcement are described below.

### 3.3.1 Requirements

(1) Accurate detection of invalid vehicle

At the toll plaza, since vehicles with no or invalid OBE and vehicles with normal OBE travel together successively or adjacently, it is necessary to detect with accuracy the invalid vehicles only. Cameras for capturing the image of invalid vehicle must have sufficient resolution and illumination to be able to capture the image of high quality.

(2) Dealing with vehicles traveling at high speed

To detect vehicle traveling at high speed on the main lane of tollway, the vehicle sensor is required to have high-speed response and high-speed processing.

### 3.3.2 Main specifications of equipment for capturing images of invalid vehicles

Equipment for enforcement applied in the ETC system includes lane barriers and cameras. In view of the non-stop toll collection, which is the principal part of the ETC system, the camera is appropriate. The camera specifications are shown in **Table 3**.

## 4. ETC system technology

For the ETC system, together with the elemental technologies, such as RF communication technology and vehicle detection technology mentioned above, a system technology

**Table 3 Specifications of equipment for capturing the image of invalid vehicle**

Item	Specification	Remarks
Sensor unit	CCD camera	
Visual field	2 500 mm × 2 500 mm	
No. of pixels	1 024 pixels × 1 024 pixels	
Resolution	2.5 mm/pixel	
Control unit		
Image compression time	500 ms or less*	* 1 At image compression rate of about 1/10.

for integrating these elemental technologies is necessary to realize the functions of toll collection and detection of invalid vehicle.

This system technology performs sequential transaction for each vehicle in the single-lane system, but an advanced system technology is needed in vehicle identification and others on the lanes permitting coexistence of vehicles having no OBE.

On the other hand, in the multi-lane system, in order to handle a number of vehicles traveling on several lanes simultaneously, an advanced system technology is required to identify the position of the vehicle communicated with the antenna, to identify invalid vehicles and so on.

Requirements for the system technology are summarized below.

(1) Single-lane ETC system

- Accurate and smooth execution of vehicle sequential transactions (avoidance of reversed processing order and so on)
- Integration of existing equipment, if any
- Avoidance of radio interference with adjacent lanes

(2) Multi-lane ETC system

- High-speed processing to deal with a number of vehicles travelling at high speed simultaneously
- Locating the traveling position of the vehicle communicated with the antenna
- Avoidance of radio interference with adjacent antennas

Although the equipment construction of the ETC system varies with the required specifications, a more advanced system can be constructed by adding functions, such as license plate number detector and vehicle classification, to the system configuration mentioned above.

## 5. Examples of trial operation

### 5.1 Trial operation of ETC system in Malaysia

#### 5.1.1 Outline

As an example of a single-lane ETC system application, the ETC system in Malaysia is described. In Malaysia, a non-stop toll collection system, which takes the place of the conventional manual toll collection, was planned to install. The trial operation of the system was conducted on North Klang Valley Expressway from November 1994. In this operation, in order to verify the effect of the ETC system, the OBE was distributed to about 2 000 vehicle drivers including those other than the parties, and the test was continued for two months. MHI received the order for this trial system in March 1994. After this trial, we also received orders for the installation of ten toll plazas and 25 000 units of the OBE for commercial operation.

An outline of the trial system is given below.

- Service district: From Subang to Jalan Duta

- Toll system: Closed system
- Number of lanes: (1 ETC entry lane/1 ETC exit lane) × 2 toll plazas; by modification of the existing toll plazas and lanes
- Payment system: Pre-paid system
- OBE: One-piece type

#### 5.1.2 Effect of ETC system

To investigate the effect of the ETC system, in the trial operation, the processing time for one lane and the number of vehicles using the ETC lanes were measured. The on-lane processing time by ETC system was found to be about one third of manual collection, and a notable effect of the system was confirmed. The number of users on the daily average amounted to about 1 600 vehicles in the total of two toll plazas, and the rate of use by the 2 000 OBE users was very high. It also ensured that the convenience of the system was widely approved by the users.

(1) Processing time at exit lane

- Manual toll collection lane: 14.7 s/vehicle
- ETC lane: 4.1 s/vehicle

(2) Number of vehicles

- Subang toll plaza (exit lane) : Approx. 700 vehicles/day
- Jalan Duta toll plaza (exit lane) : Approx. 900 vehicles/day

### 5.2 ERP system in Singapore

#### 5.2.1 Outline

As an example of the multi-lane ETC system application, the electronic road pricing (ERP) system in Singapore is described. Road pricing, a system to charge vehicles for entering the city, is intended to limit the volume of traffic entering, and differs from the toll collection on the tollway. In Singapore, the license system was introduced in 1975 as a road pricing system to limit the traffic flow into the city.

This system involved problems in the purchase procedure of licenses and the allocation of inspectors. To solve such problems, it was planned to introduce an electronic road pricing system by RF communication.

This project was offered by international tender in 1991. Ten consortia applied and three of them were chosen, and after the evaluation tests conducted in 1994 and 1995, MHI's system as shown in **Fig. 3** was finally adopted.

The required specifications of this system are given below.

- Applicable to various driving forms on public roads without divisional strips.
- Identifying and capturing the image of invalid vehicle are feasible.
- Collecting tolls from an IC card placed in an OBE is feasible.
- Applicable to all vehicles including motorcycles.
- Maximum vehicle speed for toll collection: 120 km/h
- Invalid vehicle detecting speed: 180 km/h
- Transaction error rate:  $10^{-5}$  or less
- Accuracy of vehicle separation: 250 mm (all around of the vehicle)

#### 5.2.2 Test results

This trial system was tested by using a total of 8 000 vehicles from May to July 1995. The principal results are shown below, and they were found to satisfy all of the customer's specifications, described in each parentheses.

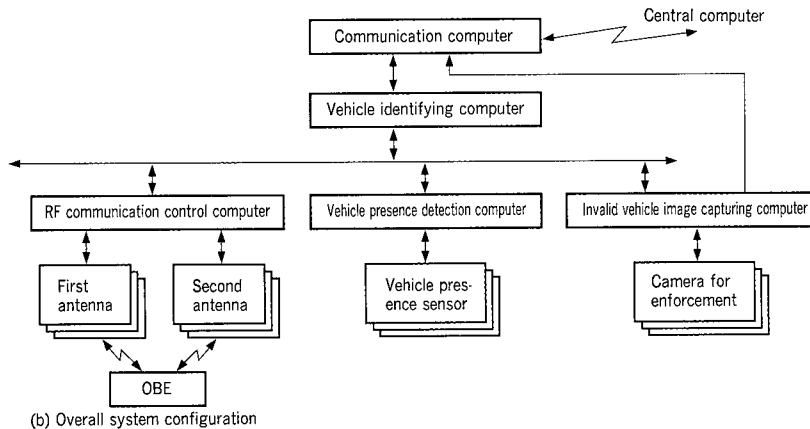
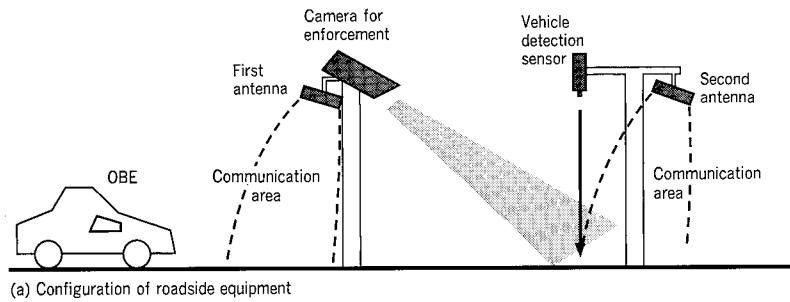


**Fig. 3 Configuration of ERP system**

An example introduced in Singapore is shown.

- Accuracy of toll collection: 100% (customer's specification: error rate  $10^{-5}$  or less)
- Detection rate of invalid vehicles: 100% (customer's specification: 99% or more)
- Recognition rate of license plate number: 97% (customer's specification: 95% or more)

Furthermore, in the system evaluation tests conducted in 1997, the conformity with the customer's specifications was successfully verified by using more than 1 million vehicles in total.

## 6. Conclusions

The demand for the electronic toll collection system on tollways and the electronic road pricing system for traffic volume control in urban districts is expected to be on the increase in future. We obtained valuable know-how concern-

ing future system developments by the experience in the development of the systems for Malaysia and Singapore. Henceforth, by making use of such experience, we shall continue to promote development of the new ETC system as a measure for solving environmental problems, seeking a greater contribution to society. As the standard relating to the ETC system, ISO/TC 204 has been established, and an attempt is being made to establish the standard for TICS (Transport Information and Control System) in it. In particular, WG 5 (AFC: Automatic Fee Collection), WG 1.3 (AVI: Automatic Vehicle Identification), and WG 15 (DSRC: Dedicated Short-Range Communication) of this ISO/TC 204 are closely related to the ETC, and MHI is planning to participate and cooperate in the development of equipment complying with the international standards.

# Development of Double Medium Corrugated Fiberboard Production Machine

Hiroshi Ishibuchi\*<sup>1</sup>  
Yukiharu Hattori\*<sup>1</sup>

Kazukiyo Kohno\*<sup>1</sup>  
Yukuharu Seki\*<sup>2</sup>  
Makoto Ando\*<sup>2</sup>

There has been an increasing demand in the corrugated fiberboard industry for a new type of corrugated fiberboard with high compressive strength and high shock-absorption, accordingly a double medium corrugated fiberboard which has high and low flutes is proposed. In order to produce this new fiberboard, accurate flute position control technology is required. A double medium corrugated fiberboard production machine, which incorporates a technique to measure the position difference between the high and low flutes and a method of accurate sheet tension control, has been developed. The correct sheet tension is calculated by using the measured position difference and the extension rigidity of the paper. As a result of production tests of the newly developed machine, a maximum position difference within  $\pm 3\text{mm}$  has been successfully achieved at the maximum machine speed of 180 m/min, using liners from 150 g/m<sup>2</sup> to 300 g/m<sup>2</sup>.

## 1. Introduction

Conventional corrugated fiberboard has a structure consisting of multi-layer single-faced corrugated fiberboard using single-layer corrugating medium. However, when a structure of double layer corrugating medium which has different flute height is employed, it is possible to achieve a functional corrugated fiberboard which has both shock-absorption properties not found in double faced corrugated fiberboard and a higher compressive strength than that of double wall corrugated fiberboard.

In order to produce such specific corrugated fiberboard, the flute position of two corrugating mediums having different flute heights should be adjusted so as to be mated and pasted together. However, since the single faced corrugated fiberboard having corrugating medium tends to shrink when heated and becomes elongation due to variations in tension, a suitable means is necessary to address such problems during the production process.

In this research a high precision flute position measurement technique and flute position correction technique have been devised, and the first double medium corrugated fiberboard production machine has been developed at the world. These accomplishments are reported on in this paper.

## 2. Features of double medium corrugated fiberboard and outline of the production machine

### 2.1 Features of double medium corrugated fiberboard

The double medium corrugated fiberboard, as shown in Fig. 1, has a structure in which two layers consisting of low-flute and high-flute corrugating mediums of equal flute pitch and different flute heights are arranged between the linerboards.

Fig. 2 shows an example of some flat compression test results obtained for double medium corrugated fiberboard. Fig. 2 also shows the flat compressive behavior of double faced corrugated fiberboard and double wall corrugated fiberboard for comparison. Compressive load accompanied by an increase in the compressive deformation of the double medium corrugated fiberboard is equal to that of double faced corrugated

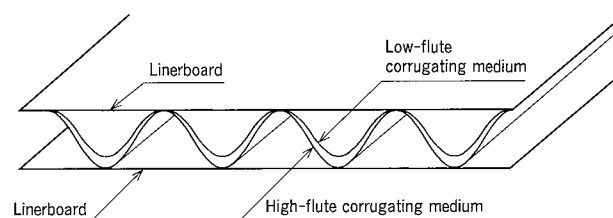


Fig. 1 Shape of double medium corrugated fiberboard

Double medium corrugated fiberboard has a double corrugating medium of equal flute pitch and different flute heights between the linerboards.

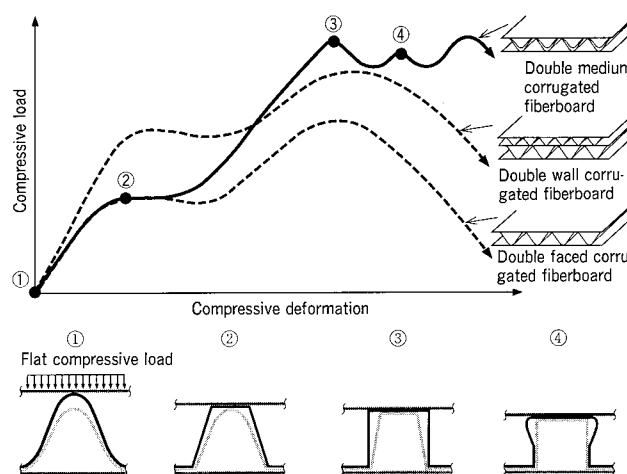


Fig. 2 Flat compressive characteristic of double medium corrugated fiberboard

Double medium corrugated fiberboard has the characteristics of both good shock-absorption effect, which is not in the double faced corrugated fiberboard, and greater maximum compressive strength than that of double wall corrugated fiberboard.

fiberboard until the high-flute corrugating medium comes into contact with the low-flute corrugating medium. However, thereafter the compressive load is higher than that of double faced corrugated fiberboard, and the maximum compressive load becomes higher than those of double faced and double wall corrugated fiberboard.

As shown in Fig. 2, the flat compressive deformation

\*1 Hiroshima Research & Development Center, Technical Headquarters  
\*2 Mihara Machinery Works

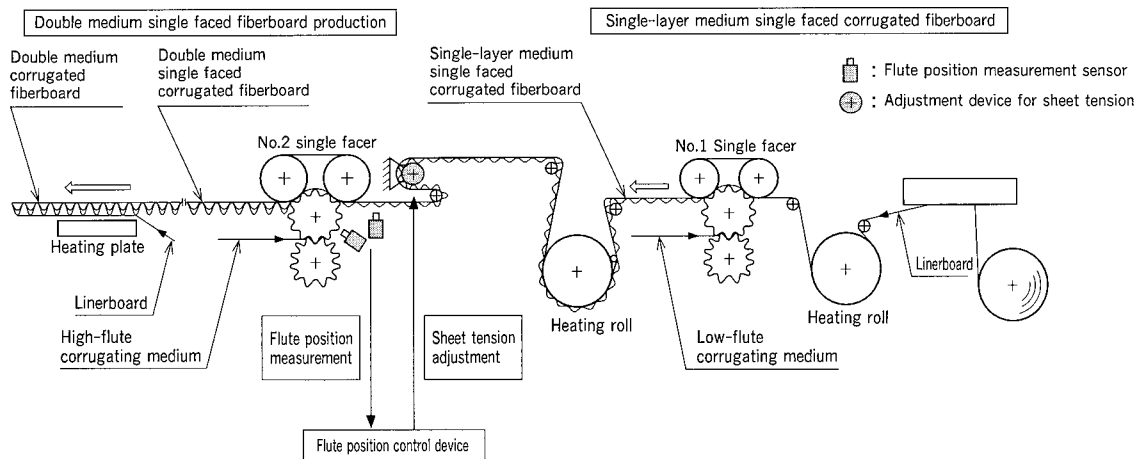


**Fig. 3 Schematic view of double medium corrugated fiberboard production machine**

Single-layer medium single faced corrugated fiberboard is produced by the No.1 single facer. Then double medium single faced corrugated fiberboard is produced by controlling the flute position of high-flute corrugating medium at the No.2 single facer.

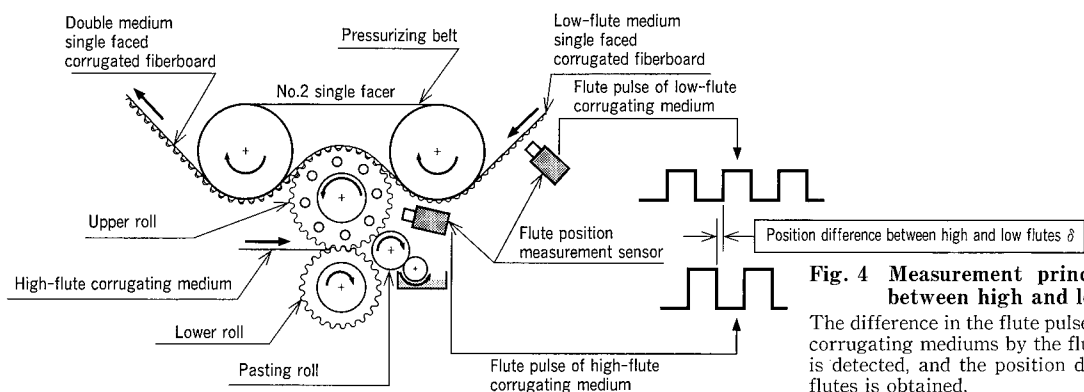


**Fig. 4 Measurement principle of position difference between high and low flutes**

The difference in the flute pulses of the low-flute and high-flute corrugating mediums by the flute position measurement sensor is detected, and the position difference between high and low flutes is obtained.

behavior of the double medium corrugated fiberboard can be described as follows. The high-flute corrugating medium becomes trapezoidal in shape in stage ②, and the compressive load shows its first peak due to contact of the high- and low-flute corrugating mediums. Thereafter, the compressive load increases with an increase in the compressive deformation, while in stage ③ the high-flute corrugating medium becomes rectangular in shape and the low-flute corrugating medium becomes trapezoidal in shape resulting in the maximum compressive load producing a second peak. After exceeding stage ③, the compressive load decreases somewhat due to buckling of the high-flute corrugating medium. However, since the low-flute corrugating medium becomes rectangular in shape, a third peak of the compressive load is produced as shown in stage ④.

From the above, it can be seen that the double medium corrugated fiberboard has shock-absorption properties which are not found in double faced corrugated fiberboard and has a higher maximum compressive strength than that of double wall corrugated fiberboard. Another feature of double medium corrugated fiberboard is that it has one less liner sheet compared with double wall corrugated fiberboard.

## 2.2 Outline of double medium corrugated fiberboard production machine

Fig. 3 shows a schematic view of the double medium corrugated fiberboard production machine. First, single-layer

medium single faced corrugated fiberboard is produced by pasting low-flute corrugating medium faced with the linerboard at a No.1 single facer. Second, the flute position difference between the low-flute corrugating medium of the single-layer medium single faced corrugated fiberboard and the high-flute corrugating medium faced is detected by a flute position measurement sensor. Sheet tension is then calculated to correct differences in the flute position by using a flute position control device. The tension of the single-layer medium single faced corrugated fiberboard is varied with an adjustment device for sheet tension. Thereafter, double medium single faced corrugated fiberboard is produced by pasting single-layer medium single faced corrugated fiberboard with high-flute corrugating medium by using a No.2 single facer. The double medium corrugated fiberboard is then produced by pasting it with the linerboard on a heating plate<sup>(1)(2)</sup>.

The existing facer can be used by utilizing the above production method. Double faced corrugated fiberboard and double wall corrugated fiberboard other than the double medium corrugated fiberboard can be produced by changing the sheet path.

The key point in such a production method is that the position difference between high and low flutes in the high-flute and low-flute corrugating mediums can be continuously corrected. For this purpose, a high-precision flute position control technique which includes the capability of measuring

flute position differences and adjusting sheet tension is needed.

### 3. Flute position measurement device and adjustment device for sheet tension

#### 3.1 Flute position measurement device

Fig. 4 shows the measurement principle for determining the flute position difference between high- and low-flute corrugating mediums by using the flute position measurement device. The flute pulse of the low-flute medium single faced fiberboard and the flute pulse of the high-flute corrugating medium faced are detected by the flute position measurement sensor, and the differences in both pulses are averaged at constant measurement interval in order to obtain the flute position difference  $\delta$ .

#### 3.2 Adjustment device for sheet tension

Fig. 5 shows a schematic view of the adjustment device for sheet tension. The low-flute medium single faced corrugated fiberboard is wound on the guide-roll for braking so that the flute side of the corrugating medium faces the guide-roll. The tension of the low-flute medium single faced corrugated fiberboard can be adjusted by varying the torque of the guide-roll for braking by using the brake via the driving belt.

The maximum sheet tension,  $T_{MAX}$  at the exit side of the guide-roll for braking occurs just before the sheet tension adjustment is disabled due to slippage of the low-flute medium single faced corrugated fiberboard on the guide-roll for braking.  $T_{MAX}$  is shown by the following equation.

$$T_{MAX} = T_0[\exp(\mu\theta)] \quad (1)$$

where,

$T_0$ : Sheet tension at the entrance side of the guide-roll for braking

$\mu$ : Coefficient of friction on the surface of the guide-

roll for braking

$\theta$ : Angle of contact of the single faced corrugated fiberboard on the guide-roll for braking

$T_{MAX}$  increases with an increase in the coefficient of friction  $\mu$  of the roll surface and the angle of contact  $\theta$  of the single faced corrugated fiberboard on the guide-roll and, the sheet tension adjustment range of the single faced corrugated fiberboard becomes broader.

### 4. Flute position control method

#### 4.1 Flute position control theory

Fig. 6(a) shows the method for calculating the sheet tension in order to correct the flute position difference. When the flute position difference is measured  $N$  times and the first average measured value of the flute position difference is  $f(\delta_1, N)$  and the second average measured value of the flute position

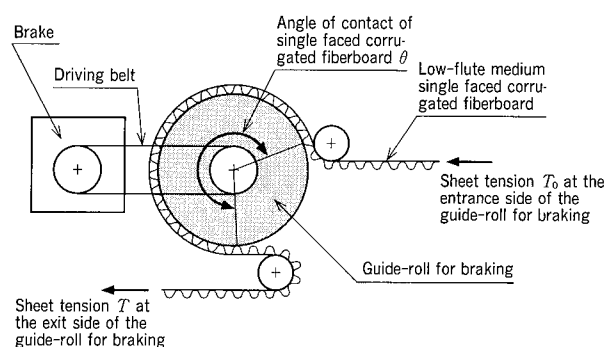
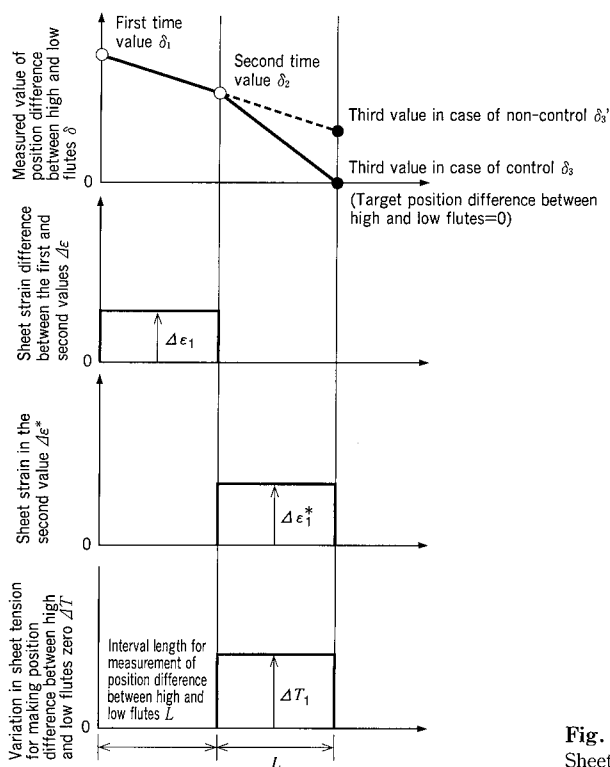
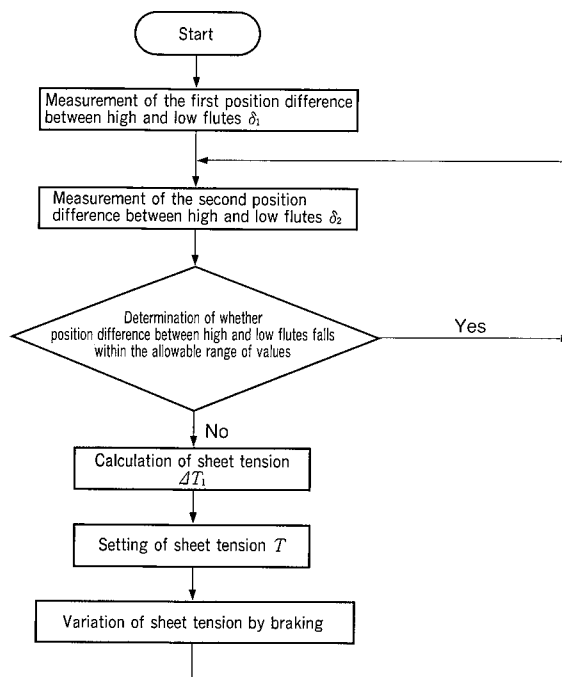


Fig. 5 Schematic view of adjustment device for sheet tension

The tension of the low-flute medium single faced corrugated fiberboard is adjusted by varying the torque of the guide-roll for braking.



(a) Calculation principle of sheet tension for correcting the position difference between high and low flutes



(b) Flow chart of flute position control

Fig. 6 Concept of flute position control and flow chart of control

Sheet tension for correcting the third position difference between the high and low flutes is calculated from the first and second position differences between high and low flutes.

difference is  $f(\delta_2, N)$ , the following equation shows the difference in sheet strain  $\Delta\epsilon_1$  between the first and second measured values.

$$\Delta\epsilon_1 = \frac{f(\delta_1, N) - f(\delta_2, N)}{L} \quad (2)$$

where,

$f(\delta_1, N)$ : First average measured value of flute position difference by  $N$  times measurements

$f(\delta_2, N)$ : Second average measured value of flute position difference by  $N$  times measurements

$L$ : Length of interval in measurement of flute position

The following equation shows the sheet strain  $\Delta\epsilon_1^*$  corresponding to the second measured value of the flute position difference.

$$\Delta\epsilon_1^* = \frac{f(\delta_2, N)}{L} \quad (3)$$

From equations (2) and (3), the variation ( $\Delta T_1$ ) of the sheet tension for correcting the third flute position difference  $\delta_3$  can be obtained by the following equation.

$$\Delta T_1 = \frac{[2f(\delta_2, N) - f(\delta_1, N)]\phi_\delta}{f(K_P, P)L} \quad (4)$$

where,

$\phi_\delta$ : Tension relaxation coefficient

$f(K_P, P)$ : Sheet strain by tension 1 kgf/cm corresponding to weight  $P$ /sheet of 1 m<sup>2</sup>

Thus, when in Fig. 6(a) the sheet tension for correcting the flute position difference shown in equation (4) from the first measured value  $\delta_1$  and the second measured value  $\delta_2$  of the flute position difference is varied, the third measured value is to be  $\delta_3$ . However, when there is no variation in the sheet tension, the third measured value is to be  $\delta_3'$ .

Fig. 6(b) shows the flow chart of flute position control. After the first flute position difference  $\delta_1$  is measured, the second flute position difference  $\delta_2$  is measured and a determination is made as to whether or not the value falls within the allowable range of values.

When the value falls within the allowable range of values, the third flute position difference is measured. When the value is not within the allowable range of values, the sheet tension  $\Delta T_1$ , for correcting the flute position difference shown in Fig. 6(a) is obtained from equation (4). The sheet tension  $T$  is set, and the sheet tension is varied by the brake.

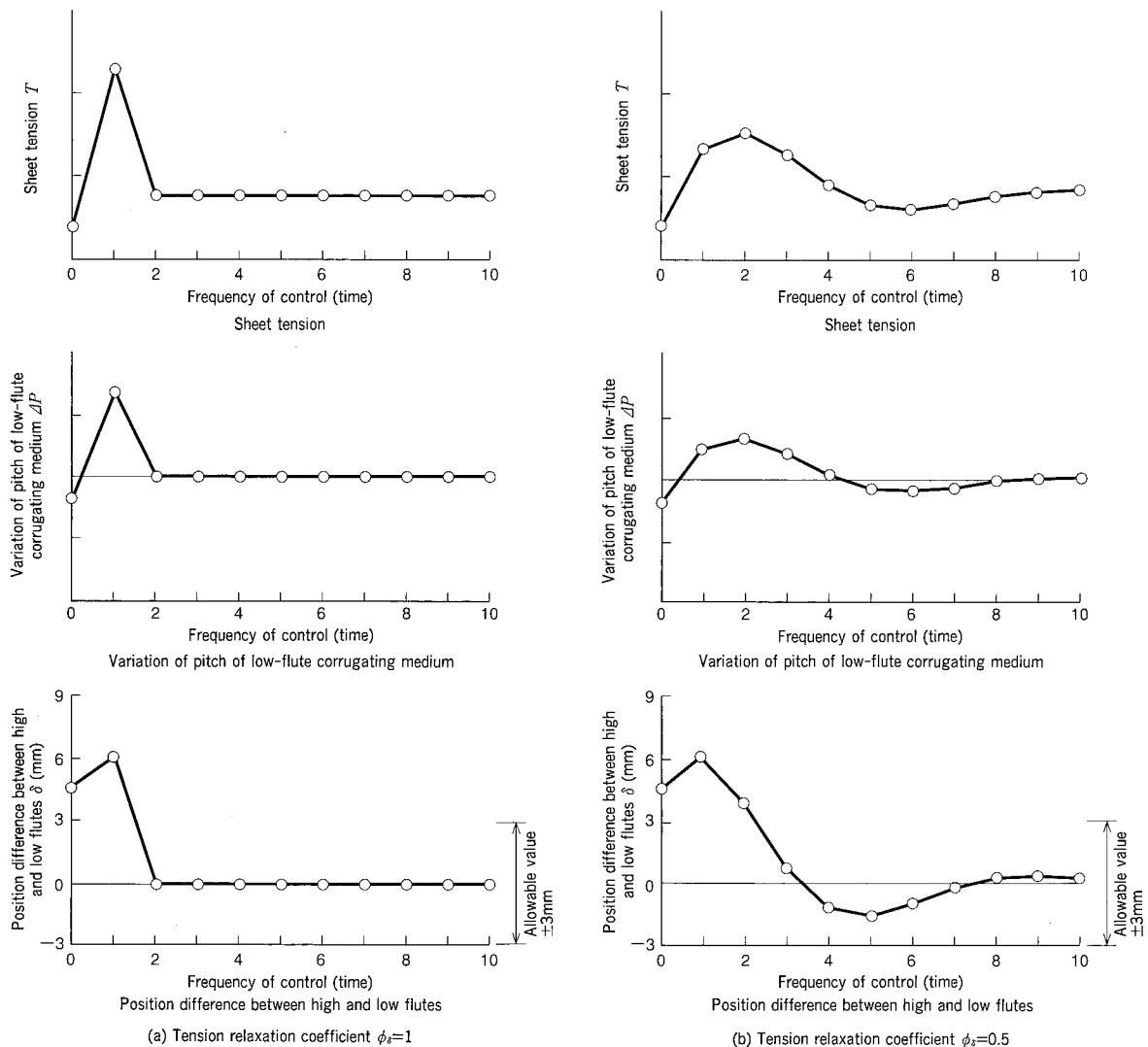


**Fig. 7 Results of flute position control simulation**

It is better to control the flute position by reducing the tension relaxation coefficient  $\phi_\delta$  and restraining variation of sheet tension in consideration of sheet tension load on the guide-roll for braking.

The above method is sequentially carried out at every length of interval  $L$  in order to measure flute position thereby making high-precision flute position control possible.

#### 4.2 Flute position control simulation

Simulations were performed to verify the effectiveness of the flute position control theory. Assuming that the pitch of a flute in a low-flute corrugating medium is shorter than that in a high-flute corrugating medium. And assuming that differences in flute position occur, the sheet tension  $T$ , variation of the pitch of a flute  $\Delta P$  in the low flute corrugating medium and flute position difference  $\delta$  were simulated in cases where the tension relaxation coefficient  $\phi_s=1$  and 0.5 as shown in Fig. 4.

Fig. 7(a) shows the simulation results in the case where  $\phi_s=1$ . When the new flute position difference is not occurred during the flute position control, variations in the pitch of a low-flute  $\Delta P$  and the flute position difference  $\delta$  can be made to be 0 mm by varying the sheet tension  $T$  two times.

This means that by measuring the first flute position difference  $\delta$ , the sheet tension  $T$  for adjusting the second flute position difference  $\delta$  to 0 mm is actuated the first time.

In the case where  $\phi_s=1$ , the flute position difference can be theoretically adjusted to 0 mm by implementing the flute position control two times. However, it is considered that various difficulties will arise such as rupturing of the sheet on the guide-roll for braking, crushing of flutes and slippage occurring easily because of significant variations in tension during control in the actual operation of the machine.

Fig. 7(b) shows the simulation results in the case where  $\phi_s=0.5$  for restraining variation of the sheet tension.

This is the case in which variations in tension is only half of the target tension by  $\phi_s=0.5$ . It is found that variations in tension per time is reduced and convergence of the flute position difference  $\delta$  is delayed compared with the case where  $\phi_s=1$ , as can be seen in Fig. 7(a).

Even in this case, the flute position difference  $\delta$  is reduced to within an allowable value of  $\pm 3$  mm after three times of control frequency. Although control frequency increases to some extent by relaxing variations of the tension as described above, differences in flute position can be corrected by reducing variations in the tension.

From these simulated results, it was confirmed that the flute position control theory was effective.

#### 5. Verification of actual machine performance

Verification of the actual machine consisted of measuring, machine speed under acceleration, deceleration and constant speed conditions, as well as sheet tension and differences in flute position when the type of paper and paper width of the linerboard and corrugating medium are changed and also when

**Table 1 Performance of double medium corrugated fiberboard production machine**

Maximum flute position difference	Within $\pm 3$ mm
Maximum machine speed	180 m/min
Maximum sheet width	1 800 mm
Grammage of linerboard used	150 to 300 g/m <sup>2</sup>
Grammage of corrugating medium used	120 to 200 g/m <sup>2</sup>

the machine speed varied.

Table 1 shows the performance of the double medium corrugated fiberboard production machine obtained from verification of an actual machine. It was confirmed that a maximum flute position difference of the double medium corrugated fiberboard is within  $\pm 3$  mm at the maximum sheet width of 1 800 mm and a maximum machine speed of 180 m/min. for almost all grammages, including a linerboard grammage, of 150–300 g/m<sup>2</sup> and a corrugating medium grammage of 120–200 g/m<sup>2</sup> which are in current use can be produced. Further, it was found that the flute position difference is significantly small even in poor pasting of single faced corrugated fiberboard sheets and also at the paper joint point.

#### 6. Conclusion

MHI has recently completed development of a double medium corrugated fiberboard production machine equipped with a flute position control device. The following conclusions can be obtained regarding the performance of this machine.

- (1) A high-precision flute position control technique has been developed by obtaining the proper tension taking into strain caused by tension from measurements of the flute position difference for the corrugating mediums having flutes of different heights.
- (2) Double medium corrugated fiberboard having a grammage of linerboard from 150 g/m<sup>2</sup> to 300 g/m<sup>2</sup> and a maximum flute position difference within  $\pm 3$  mm can be produced at the maximum machine speed of 180 m/min by using the newly developed double medium corrugated fiberboard production machine.

The first machine was introduced in 1996 and was highly evaluated by the customer. In the future, we will endeavor to realize a machine capable of higher speeds and a reduction in the amount of waste paper.

#### References

- (1) Seki, Y., Production Machine of Double Medium, Seminar on the Development of New Packaging Material Proceeding, (1996-12) p.35
- (2) Ishibuchi, H. et al., Production Machine of Corrugated Fiberboard, Pat. Pend.8-222041 (1997)

# Superplastic Forming of Titanium Matrix Composite (TMC)

Takeshi Yamada\*<sup>1</sup>

Hiroaki Sato\*<sup>1</sup>

Takayuki Tsuzuku\*<sup>1</sup>

*The high strength to density ratio and stiffness of titanium matrix composites (TMC) are attractive for aerospace structural applications. Some TMC model parts have already been developed, but most of them are not for practical use. TMC parts have been expensive because they have to be shaped before being consolidated. In order to reduce the production cost of TMC parts, high formability TMC sheets and a superplastic forming process have been developed. By using this new material and process, it has been demonstrated that stringer- and blade-shaped TMC models can be fabricated successfully.*

## 1. Introduction

Continuous fiber reinforced titanium matrix composites are expected to be applied in aerospace structures as heat-resistant materials with high specific strength and stiffness. Their application in discs, blades, other engine parts, as well as in wing skins, landing gear and other structural parts are being studied. Hitherto, parts made of these composites have been manufactured as shown in Fig. 1(a). Titanium alloy foils are processed by hot preforming before being consolidated, while reinforcement fibers and preformed titanium foils are laminated alternately and compounded by Net-Shape consolidation using the hot isostatic pressing (HIP) process. However, both the hot preforming process and Net-Shape consolidation process require complicated exclusive jigs and are very expensive, and the resultant high cost of parts manufacturing has been an insuperable barrier to practical use. So far, titanium matrix composites have been considered as not being applicable to plastic forming. However, if forming by plastic processing is possible, it does not require hot preforming, and complicated jigs can be substantially simplified, thereby reducing the cost of parts manufacturing significantly. It seems that even continuous fiber type composites could be formed plastically, without damaging the reinforcement fibers, by sufficiently enhancing the plastic flow of the matrix.

This paper reports on the development of titanium matrix composites which have excellent processing characteristics through the use of superplastic material for the matrix, and the development of low-cost manufacturing technology utilizing superplastic forming as shown in Fig. 1 (b).

## 2. Development of titanium matrix composite applicable to superplastic forming

### 2.1 Selection of matrix material

In the plastic forming of titanium matrix composite components, the matrix material must undergo all manner of plastic deformation. Accordingly, it is extremely important to use a matrix material having excellent plastic flow characteristic — i.e., superplastic characteristics. Moreover, in the fiber/matrix consolidating process and subsequent superplastic forming process, heating is maintained for a long period of time while maintaining contact between the fiber and matrix. Thus, in order to prevent formation of a surface reaction layer and deterioration of the fiber, the matrix material should present a superplastic nature at the lowest possible tempera-

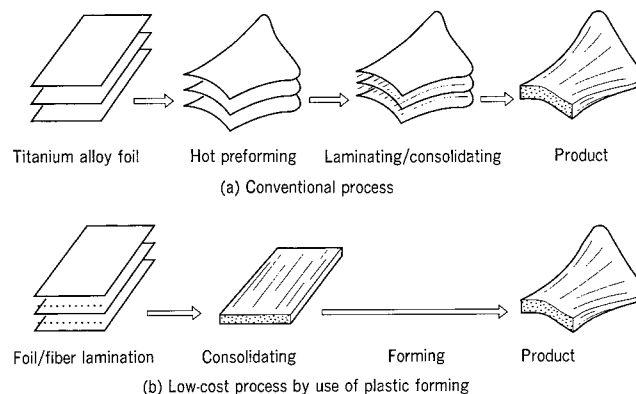


**Fig. 1 Comparison of conventional and new fabrication process for titanium matrix composite components**

By omitting the hot preforming process, costs are lowered compared with conventional processes.

ture. In the commercial titanium alloy sheets registered in various standards,  $\alpha+\beta$  alloys such as Ti-6 Al-4 V alloy, Ti-6 Al-6 V-2 Sn alloy, and Ti-6 Al-2 Sn-4 Zr-2 Mo alloy exhibit excellent superplasticity, and the superplastic forming temperature is about 1173 K. On the other hand, among recently developed titanium alloys, Ti-4.5 Al-3 V-2 Fe-2 Mo alloy (SP 700), which is a  $\beta$ -rich  $\alpha+\beta$  alloy, has attracted attention as a material displaying a superplastic nature at low temperature. The SP 700 shows a maximum elongation of more than twice that of the Ti-6 Al-4 V alloy at a temperature lower by about 150 K, and the  $m$ -value (strain rate sensitivity exponent: the closer to 1 the better for superplastic forming) is about 0.6, which is similar to that of Ti-6 Al-4 V alloy at 1173 K. Accordingly, the SP 700, which is capable of lowering the forming temperature by about 150 K without sacrificing superplasticity, was selected as the matrix material.

### 2.2 Selection of reinforcement fiber

Chemical vapor deposition (CVD) fibers such as boron (B), BOROSIC (B/SiC), boron carbide (B/B<sub>4</sub>C), and silicon carbide (SiC) have been widely used as reinforcement fibers of titanium matrix composite. Above all, the SiC fiber is excellent in its chemical compatibility with titanium alloy, exhibits minimum fiber/matrix interface reaction, and is high in strength in terms of the fiber itself. Therefore, compared with other fibers, the strength characteristics of the composite are excellent. As a result, the SCS-6, a CVD type SiC fiber manufactured by Textron (USA) was selected as the reinforcement fiber in this study. A woven preform, consisting of SiC fibers 140  $\mu$ m in

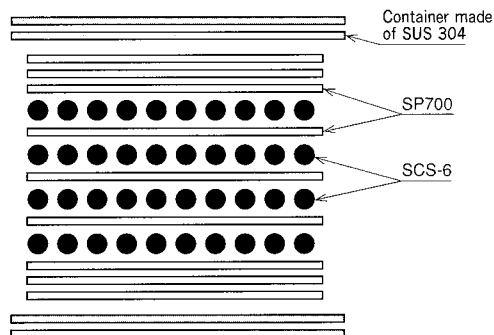


**Fig. 2 Layer structure of SiC/SP 700 composite**  
A schematic view of the layer structure of SiC/SP 700 composite is shown in the figure.

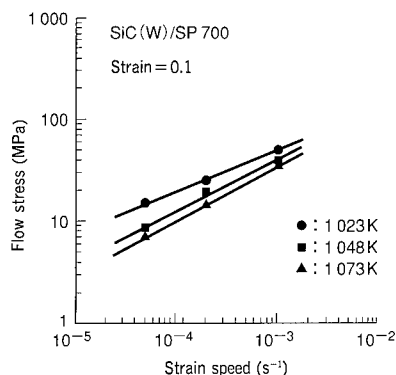


**Fig. 3 Deformation properties of SiC/SP 700 composites consolidated at various temperatures (fiber orthogonal direction)**

Plastic deformation properties of SiC/SP 700 composites consolidated at three temperatures in the fiber orthogonal direction are shown.

diameter arranged in one direction and woven by Ti-Nb alloy foil of about 100  $\mu\text{m}$  in width, was used.

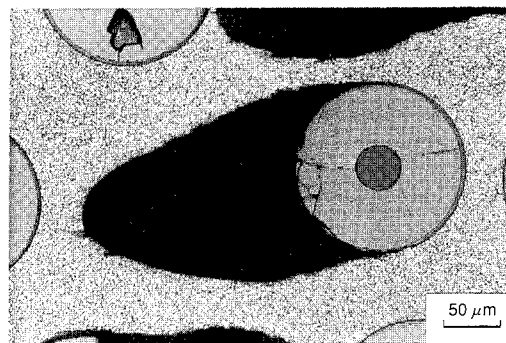
### 2.3 Setting of consolidating condition

In order to set appropriate consolidating conditions for the selected combination of fiber and matrix material, observations of the microstructures of the material were conducted by changing the consolidating temperature in the range from 973 to 1 073 K in 25 K increments. The specimen was prepared by alternately laminating four layers of SCS-6 woven preforms and three layers of SP 700 sheets of 150  $\mu\text{m}$  in thickness, as shown in Fig. 2, and overlaying three SP 700 sheets of the same thickness on each outer side. The laminated composite was vacuum-packed in a stainless steel container at 723 K and HIP processed. The pressure and holding time were set at 150 MPa and 2 hours, respectively, on the basis of the preliminary tests of the diffusion bonding of SP 700 sheets. After observing the microstructure of the sample materials, the diffusion bonding was ascertained to be insufficient at 998 K or less, and excellent at 1 023 K or more. In addition, since the grain size becomes larger along with a rise in the consolidation temperature, the consolidation temperature was set at 1 023 K with a view to maintaining the super-fine microstructure necessary for superplastic characteristics.

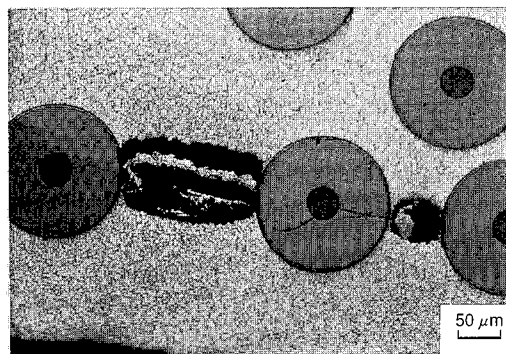
## 3. Plastic deformation behavior of SiC/SP 700 composite

### 3.1 Plastic deformation properties

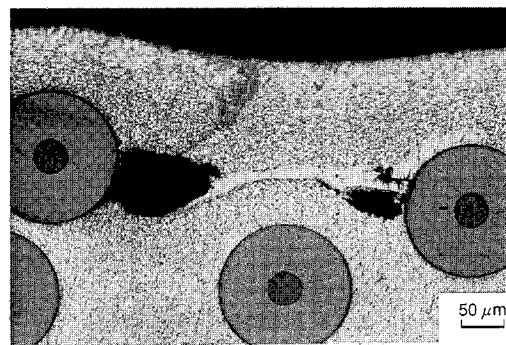
In order to evaluate the deformation properties of the SiC/SP 700 composite (hereinafter-called superplastic composite) fabricated above, the plastic deformation characteristics of the material were investigated in the orthogonal direction of the



(a) Type I



(b) Type II



(c) Type III

**Fig. 4 Defects of various types observed in specimens after deformation**

Three types of separation defects were observed during observation of the sectional microstructure of the material after plastic deformation of SiC/SP 700 composites.

fiber. Using specimens having gauge dimensions of 40 mm in length, 6 mm in width and 1.2 mm in thickness, high temperature tensile tests were conducted at three temperatures of 1 023, 1 048, 1 073 K in a strain rate range from  $5 \times 10^{-5}$  to  $1 \times 10^{-3} \text{ s}^{-1}$ .

As shown in Fig. 3, a high  $m$  value of about  $m = 0.6$  was obtained at 1 048 and 1 073 K, as in the matrix of the composite, and deformation properties with adequate applicability to superplastic forming were confirmed. From this result, the forming temperature of this material was set at 1 048 to 1 073 K.

### 3.2 Occurrence of defects due to superplastic forming

The deformation properties of the newly developed superplastic composite were excellent, and a fundamental outlook was obtained with respect to the establishment of expected low-cost forming process. However, the occurrence of separation defects was detected at the fiber and matrix interface

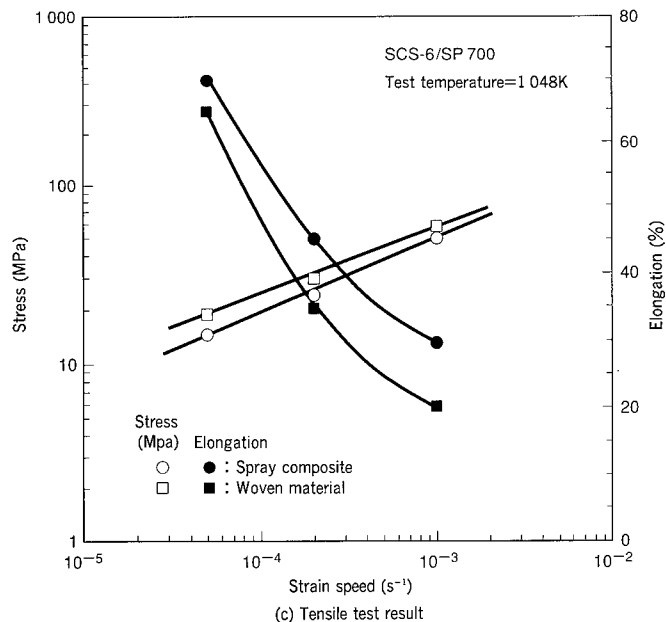
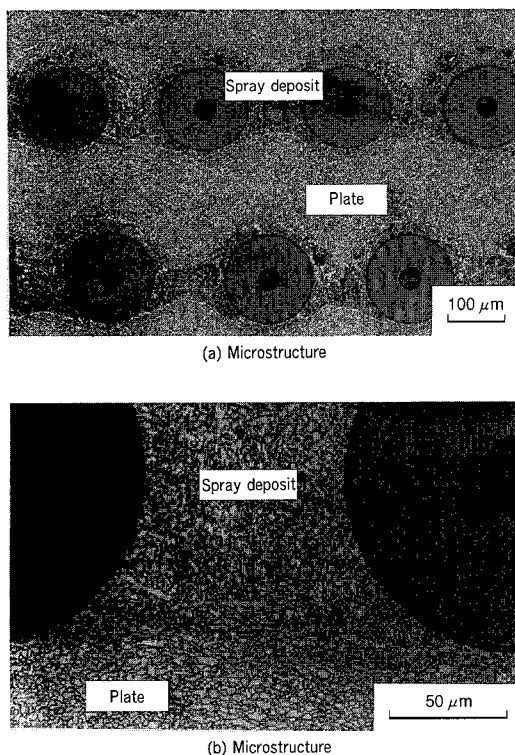


**Fig. 5 Microstructure and deformation properties of SiC (spray)/SP700 composite**

The spray deposit also has an adequately fine structure, and deformation properties are equivalent to or better than those for woven material.

during deformation. This effect was found more when the deformation stress was higher and the strain was larger. Possible deterioration of the strength characteristic of this composite after forming was thus recognized. Defects could be classified into three types as shown in **Fig. 4**. Type I is a separation defect at the fiber/matrix interface due to application of a stress which is higher than the interfacial bonding strength. Type II is a defect caused by detachment of contacted fibers. Type III is a defect derived from TiNb ribbon for fixing the fibers. Of these, types II and III are intrinsic defects less related to the forming conditions, and are considered to be preventable by controlling the fiber array and not using weaving ribbons. On the other hand, type I is a defect related to the forming conditions. It can be decreased by widening the fiber intervals for reducing the stress concentration around the fibers, or by forming at low deformation stresses<sup>(1)</sup>.

Hence, it was planned to develop a spray preform in order to control the fiber interval and to fabricate a superplastic composite not using weaving ribbons for fixing fibers.

#### 4. Development of superplastic composite by spray preform

##### 4.1 Manufacture of superplastic composite by spray preform

A low-pressure plasma spraying method with low contamination from the spraying atmosphere was selected. Preforms were fabricated by spraying SP 700 powder with the size of 53  $\mu m$  or less manufactured by the atomizing method on the SiC fibers (SCS-6) wound on a drum 500 mm in diameter. To lower stress around the fibers that occurs during deformation, the SiC fiber interval was set to 100  $\mu m$  in the spray preform, twice that of the woven preform. In consolidating, as in **Fig. 2**, four layers of spray preforms were enclosed with SP 700 sheets of

150  $\mu m$ , and the HIP process was applied under the conditions of 150 MPa, 1048 K  $\times$  2 hours. To enhance the bonding strength between the fiber and matrix so that almost no separation can occur, the processing temperature of the superplastic composite was set 25 K higher than the previous HIP processing condition. **Fig. 5** (a) and (b) show the microstructure of the superplastic composite by spray preform (hereinafter called spray composite). The spray deposit locates around the fibers, and the other part of the matrix is the sheet portion. When observed at low magnification, the boundary between each layer could be clearly seen, but when observed at high magnification, the spray deposit also shows a uniform and fine structure. It was therefore considered that the superplastic properties had not been lowered.

##### 4.2 Superplastic deformation properties of spray composite

Using specimens of the same shape as used in paragraph 3.1 above, tensile tests were conducted in the range of strain rate from  $5 \times 10^{-5}$  to  $1 \times 10^{-3} s^{-1}$  at 1048 K. The results are shown in **Fig. 5** (c) in comparison with woven material. The deformation stress of the spray composite was slightly lower than that of the woven material, and the elongation to failure tended to be larger. The  $m$ -value of the spray composite was slightly higher than that of the woven composite, and the improving effect of spray preform on plastic deformation properties was confirmed.

##### 4.3 Defect forming behavior and strength properties of spray composite

Spray composites and woven materials manufactured under the same consolidating conditions (150 MPa, 1048 K  $\times$  2 hours) were used as specimens. Defect forming behavior and strength properties of the material after forming were examined. A stringer model as shown in **Fig. 6** (a) was superplastic-formed by gas pressure loading at a forming temperature of 1048 K

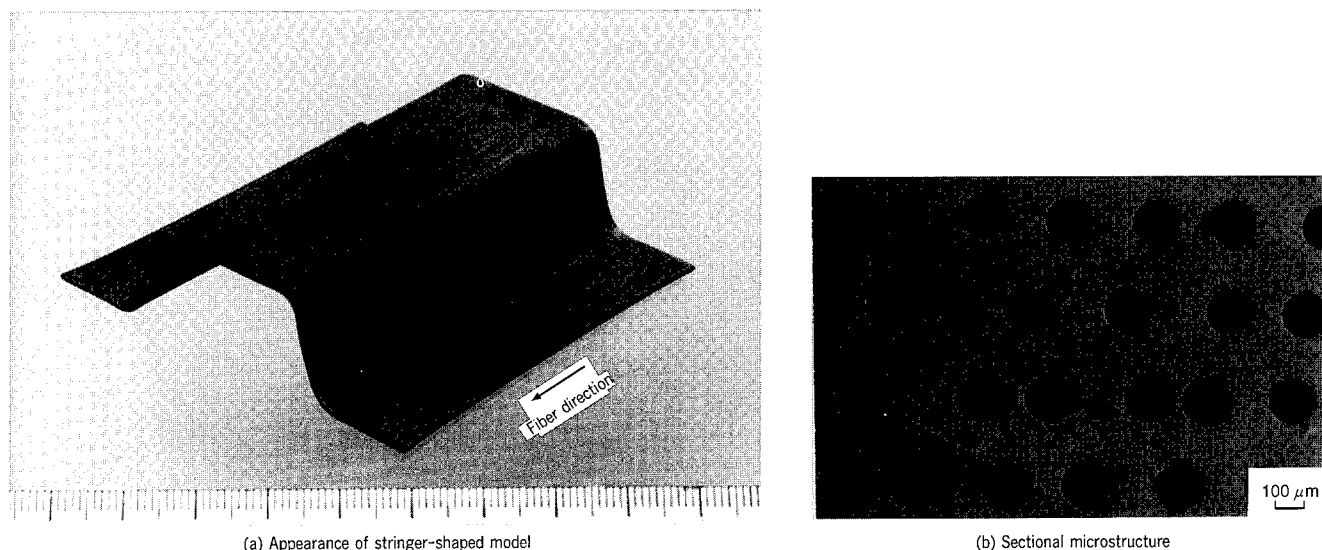


**Fig. 6 Appearance of stringer-shaped model part made of SiC (spray)/SP 700 composite and microstructure of this model**  
SiC/SP 700 composite was successfully formed into a stringer-shaped model by gas pressure loading. Only type I separation defects were observed.

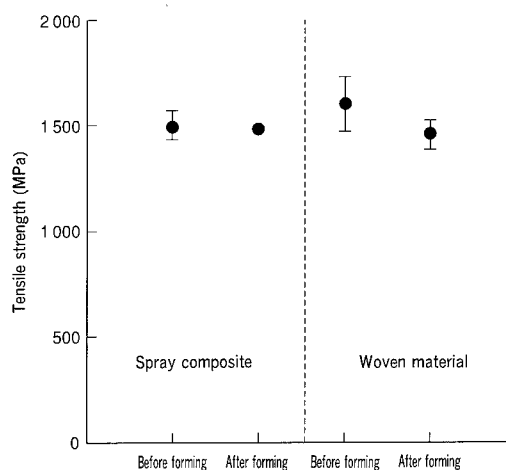


**Fig. 7 Influence of deformation on tensile strength (at R.T.) of SiC/SP 700 composite**  
Room-temperature tensile strength was not significantly lowered after forming with a strain of about 10%.

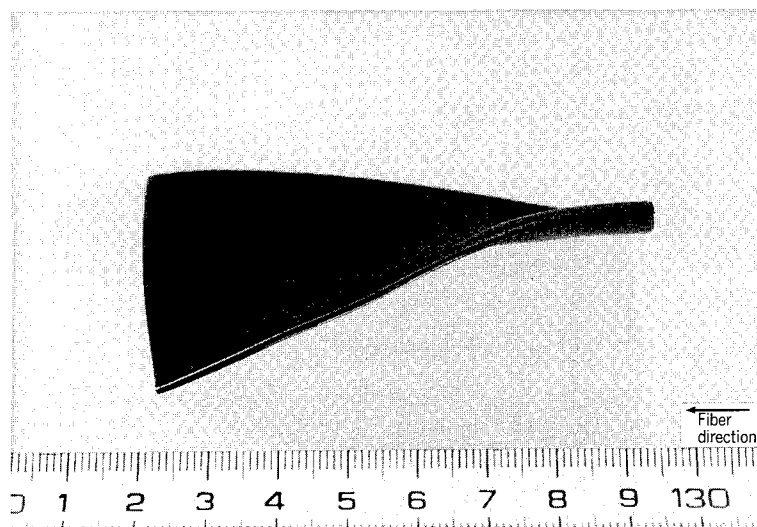


**Fig. 8 Appearance of part of blade-shaped model made of SiC (spray)/SP 700 composite**  
SiC/SP 700 composite was successfully formed into a blade-shaped model by gas pressure loading.

and a strain rate of  $5 \times 10^{-5} \text{s}^{-1}$ . Specimens were cut out from the bottom of the model, and microstructural observation and a room-temperature tensile test was conducted. Fig. 6 (b) shows the sectional microstructure of the bottom of the spray composite formed into the stringer model. In this part, the strain was about 10%, and no large defects were observed. No mutual contact of fibers was noted and the fibers were arranged uniformly, while the effect of spray composites to reduce the types II and III defects was confirmed.

A room-temperature tensile test was conducted using a specimen obtained from the bottom of the same model. The strength of the specimen was little lowered as compared with the strength of the spray or the woven composite before forming, as shown in Fig. 7.

## 5. Studies for parts forming process

The most promising application of the superplastic composite developed from the present research seems to be for aircraft

engine fan blades. Fan blades have a complicated multi-curvature shape, and in order to apply the developed composite, it is necessary to clarify the curvature forming property of this material. As a method of forming into the multi-curvature shape, gas bulge forming using a driving sheet was employed. In this method, the composite was not fixed directly by a forming jig, but the composite was sandwiched between two driving sheets. Indirect forming of the composite was attempted — i.e. the upper driving sheet pressed the composite to the female mold. Fig. 8 shows the appearance of the model formed into a multi-curvature shape by this method. The forming temperature was 1 048 K, the strain rate was  $5 \times 10^{-5} \text{s}^{-1}$ , and the spray composite was used as the specimen. Although the blade tip is of relatively simple shape while the blade root is complicated, the designed shape was formed. Almost no defects were observed in the model even at the blade root in spite of the large strain amount of 7 to 14% in thickness. The defects in the blade-shaped model are smaller than those in the

stringer-shaped. This can be caused by keeping the gas pressure less than 4 MPa during model forming. Because forming had been performed by extending the time when the load gas pressure in calculation exceeded 4 MPa, it was thought that the actual strain rate was lower than  $5 \times 10^{-5} \text{s}^{-1}$ , thereby resulting in the suppressed occurrence of defects. Moreover, as a result of forming without directly fixing the composite, a large tensile force was not built in the composite, and this is thought to be another reason for the favorable characteristic.

## 6. Conclusion

In order to lower the cost of manufacturing parts made of titanium matrix composites, composites applicable to superplastic forming were developed, and blade-shaped models were successfully manufactured by gas bulge forming. Henceforth, further technical developments will be promoted with the aim

of realizing practical application of these composites and processes.

## Acknowledgements

Finally it is noted with thanks that part of the research and development reported herein was entrusted to Mitsubishi Heavy Industries, Ltd., from the New Energy and Industrial Technology Development Organization of Japan, through the Foundation of Chubu Science and Technology Center as a part of Large-scale Regional Projects for States of the Art Technology of MITI.

## References

- (1) Sato, H. et al., SUPERPLASTIC DEFORMATION PROPERTIES OF FORMABILITY TITANIUM-MATRIX COMPOSITE, Proceeding and Fabrication of Advanced Materials V, Edited by T. S. Srivan and J. J. Moore, TMS (1996), p. 303.

## new products

### Low-Noise, Low-Vibration Spiral Compressor

Air compressors are mounted on rolling stocks to supply compressed air used for brake control to stop the cars safely and for air springs to provide comfortable ride. In recent years, low-noise and low-vibration spiral compressors are increasingly demanded to improve the room environment on a rolling stock.

Mitsubishi Heavy Industries, Ltd. (MHI) Mihara Machinery Works has conventionally been manufacturing reciprocating compressors for rolling stocks. In order to meet with the recent demand, MHI has successfully developed a new type rotary spiral compressor making use of the long-stored manufacturing technology of pneumatic brake equipment for rolling stocks and MHI's high-precision machining technique.

The outline of the newly developed spiral compressor is introduced below.

#### 1. Outline

The external appearance of the compressor is shown in Fig. 1, the compression mechanism in Fig. 2, and the basic

Table 1 Basic specifications

	Spiral type (newly developed)	Reciprocating type (conventional type)
Model	RC 1500	C 2000 L
Compression type	Single-stage compression Rotary Spiral type	Two-stage compression Single-acting Reciprocating type
Delivery air volume	1 090 Nl/min	1 401 Nl/min
Delivery air pressure	9.0 kgf/cm <sup>2</sup>	9.0 kgf/cm <sup>2</sup>
Rated rotational frequency	1 750 rpm	1 160 rpm
Rated time	Continuous	30 min
Lubricating oil	Oil exclusively used for rotary compressor	Oil exclusively used for reciprocating compressor
Noise (at 1.5 m from machine side)	68 dB	76 dB
Vibration transmission force (rated)	±2 kgf	±10 kgf

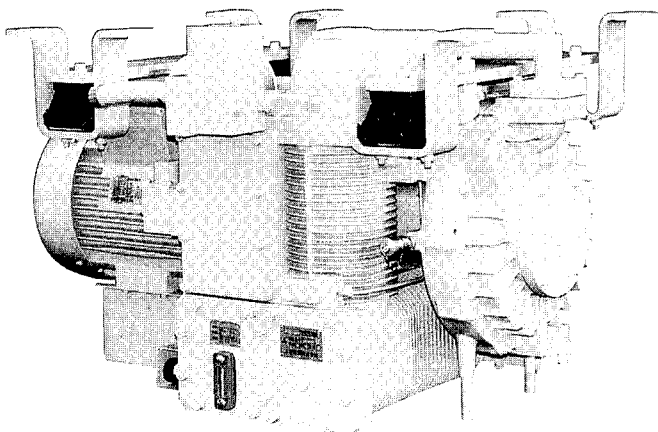


Fig. 1 External appearance

specifications in Table 1.

#### 2. Features

- (1) The simultaneous progress of suction, compression and discharge causes less variation of torque, less noise and less vibration.
- (2) The small pressure difference between compression chambers causes less air leakage, increasing the volumetric efficiency.
- (3) Because of rotation orbit movement, the relative speed of the sliding surfaces is small, causing less mechanical loss.
- (4) The capacity is larger than that of the compressor used for air conditioner, etc.

#### 3. Compression Mechanism

The compression mechanism fundamentally exists of two spirals ; one fixed ,and the other orbiting. The orbiting spiral is placed by being turned by 180° relative to the fixed spiral, which forms compression chambers. Specifically, air is taken into at the periphery of the spirals and is compressed in accordance with the chambers getting smaller by orbiting motion; meanwhile, since the volume occupied by the air becomes progressively smaller, the air pressure steadily increases, finally, the air is discharged from a discharge port located near the center of the fixed spirals. Since the air is discharged continuously, there is lower noise and vibration rather than a reciprocating compressor.

Air generates high temperature when compressed, so that lubricating oil, working as a lubricant and seal, is injected into the compression chambers to cool off, creating a situation close to the isothermal compression to prevent the compressive force from getting increased.

The fixed spiral wall and orbiting spiral wall are designed not to come in contact with each other, and the small space between the two spiral walls is sealed by means of lubricating oil.

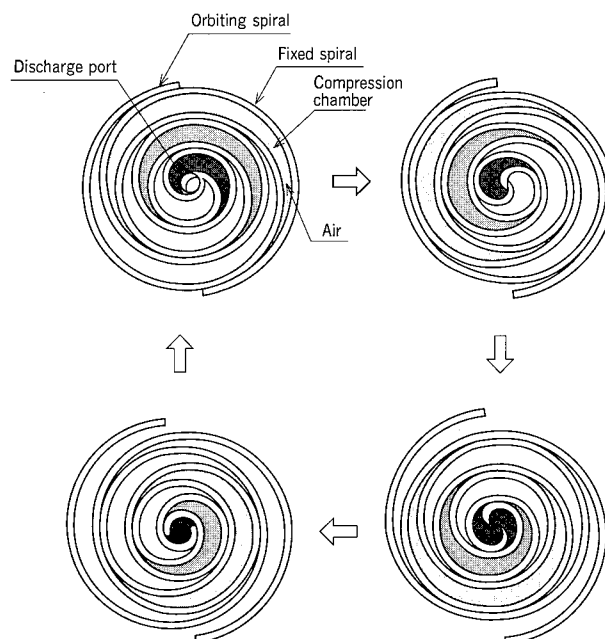


Fig. 2 Compression mechanism

The fixed and orbiting spirals come in contact with one another at the thrust bearing portion at the outer periphery of the spiral wall. Because of the lower sliding speed due to

## Three Dimensional Inspection System of Road

Mitsubishi Heavy Industries, Ltd. Nagoya Guidance & Propulsion Systems Works has developed and put on sale of road surface inspection system for road pavement companies. This system have capability for automatic measurement and analysis of road surface conditions such as rut depth, roughness, crack and forward view image.

We have successfully developed a new three-dimensional inspection system, the outline of which is given below.

### 1. Outline

This system carries out three-dimensional inspection of road surface. It is combined a device to measure the cross-sectional shape of the road, and an inertial navigation system to measure the self-position of the vehicle on which the system is mounted.

Table 1 Features & performance

Items		Features & Performance
Main measuring instruments	Cross-section measurement	Cross-sectional shape measuring device with the lane mark as the base
	Self-position measurement	Inertial navigation system
Measuring width		3.8 m
Measuring velocity		0—80 km/h
Measuring accuracy		$\pm 5 \text{ mm}$ ( $1\sigma$ ) (When survey data per 50 m is fed.)

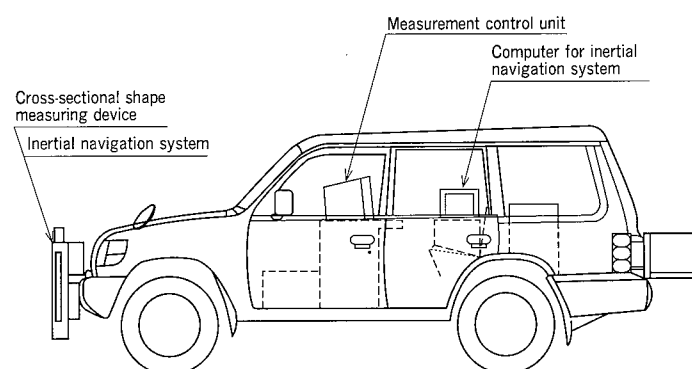


Fig. 1 System configuration

the rotation orbit movement rather than that of the reciprocating compressor, and because of the low surface pressure, the spiral compressor has less wear.

Further, the system provides the cut and overlay plan accuracy by input of the survey data on the lane mark (white line).

The features & performance of the system are given in Table 1, the system configuration in Fig. 1, and the example of output in Fig. 2.

### 2. Features

#### 2.1 Labor-saving and high mobility

The three-dimensional inspection of road has conventionally been made through analysis of the regarding longitudinal survey and cross-sections survey of the road. The newly developed system enables three-dimensional inspection by driving an inspection car (equipped with the system), realizing labor saving and high mobility.

#### 2.2 High accuracy

The system ensures high accuracy of measurement by compensating the data, transmitted from the inertial navigation system, with the measuring speed, gravitational acceleration when the car stands still (zero velocity update).

#### 2.3 Others

Adding an inertial navigation system and a computer to the road inspection system enables simultaneous measurement of three-dimensional shape in addition to the rut depth, roughness and crack of the road.

### 3. Future Prospect

The newly developed system is expected to be applied in the field of road maintenance for cut and overlay plan, measurement of joint-step, cross fall, curve radius, etc.

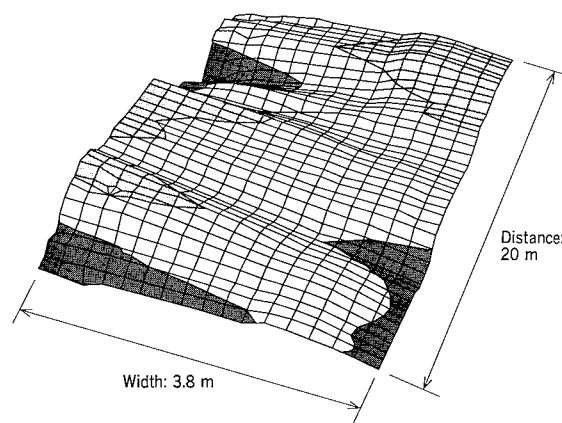


Fig. 2 Example of output (cross-country road)

## ECU for Automobile (Front ECU)

With the increase and diversification of electronic appliances in the automobile, the wiring harness for connecting these appliances is getting more and more complexed and diversified, causing the development of multiplex-control command by serial communications (LAN) and of the ECU (Electronic Control Unit) for the system to get accelerated among the automobile makers with a view to reducing the cost through simplification of wiring harness.

In order to meet with the aforesaid need, Mitsubishi Heavy Industries, Ltd. Nagoya Guidance and Propulsion Systems Works together with Mitsubishi Motors Corporation has developed a "Front ECU." This ECU applies the technology of Ruggedized-HIC (Hybrid Integrated Circuit) to the ECU for automobile, making it possible to put in the engine room with extremely severe condition. The outline of front ECU is introduced as follows.

### 1. Configuration

The configuration of front ECU is shown in Fig. 1, and the external appearance in Fig. 2.

The Front ECU is composed of seven relays that drives each loads: head lamp, tail lamp, front wiper motor, front washer motor, etc., and an electronic circuit board that controls the each relays according to the serial data transmitted from serial data bus.

Table 1 Specification of Front ECU

Item	Performance
Main function and performance	
Communication specification	Bit rate: 5kbps Transmission system: Bi-phase system Error detection: CRC check
Control items	Head lamp, tail lamp, front wiper, front wiper washer, head lamp washer
Operating voltage	8 to 16 V
Standby current	Below 0.1 mA
External dimensions (mm)	55 × 90 × H 55
Environmental performance	
Operating temperature range	−40 to +110°C
High temperature dynamic (operating) life	Over 110°C, 1 500 h
Thermal Shock tolerance	Over 1 000 cycle (−40°C ↔ 125°C)
Moisture resistance	95%
EMC	Over 100V/m
Transient Voltage	Power lines: +100 V/−120 V Signal lines: +40 V/−60 V

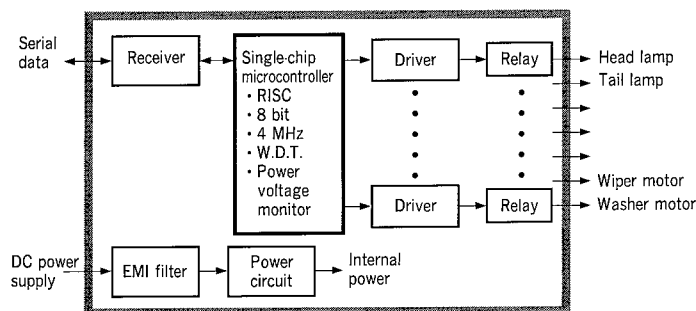


Fig. 1 Configuration

### 2. Specifications

The main functions and performance elements of the Front ECU are shown in Table 1.

### 3. Features

Front ECU is an automobile appliance put in the engine room; therefore that is required for low cost and high quality. It is described as follows that we applied the main technical points to ensure heat resistance (125°C), low cost and high quality.

#### (1) Environmental resistance (endurance)

The most noticeable performance of Front-ECU in severe environment is the long-term reliability regarding high temperature (110°C) dynamic life, thermal shock tolerance and moisture resistance.

First of all, the newly developed ECU has the low power consumption in the circuit by optimizing circuit constants. And the Joule heat and thermal resistance are reduced due to thick conductive printed pattern in order to ensure requirement of high temperature dynamic life.

As for the improvement of thermal shock tolerance, measures are taken against broken through-holes in a printed wiring board, thermal stress of electronic devices is released by adopting small surface-mounting device, and thermal shock resisting solder is used as a measure against solder crack.

The moisture resistance is obtained by using low migration substrate, cleaningless low residue soldering flux and coating.

#### (2) Low cost and high quality

In order to realize the environment resisting performance in item (1) at a low cost, the material cost is reduced by adopting heat resisting resin substrate and using common electronic parts, and the reduction of production cost and improvement of product quality are obtained through simplification of production process and adoption of the structure that allows automation.



Fig. 2 External appearance

## Tunnel Inspection System

An inspector walks through a tunnel to make a regular inspection by checking for crack or water leakage through visual observation, and for delamination through tapping. The results of inspection have so far been summed in a hand-drawn (tunnel) defect map.

In recent years, however, with the length of newly built tunnel getting extended, the superannuation of existing tunnel advancing, and the number of skilled inspector decreasing, the following problems have come to draw attention.

- Difficulty in tapping (delamination) inspection throughout the whole surface
- Shortage of inspection time and inspector

In order to solve the aforesaid problems, Mitsubishi Heavy Industries, Ltd. has developed jointly with Teito Rapid Transit Authority a new self moving tunnel inspection system, the outline of which is given below.

### 1. Outline

The tunnel inspection system (hereafter "the system") heats the tunnel wall while moving to obtain the visible and infrared images of the wall. The obtained data is then subjected to offline image processing and the various deteriorations and defects shown in Table 1 are automatically detected, with the analyzed data transmitted automatically in the (tunnel) defect map.

The system is shown in Fig. 1, and the data analyzer in Fig. 2.

Table 1 Specifications

Items	Specifications
Inspection speed	4 km/h
Inspection width	2 m
Detected thickness of delamination	1 cm (at inspection speed: 1 km/h) 5 mm (at inspection speed: 4 km/h)
Detected crack width	1 mm
Detected deterioration and defect wise	Crack, delamination, water leakage, lime, dirt, etc.

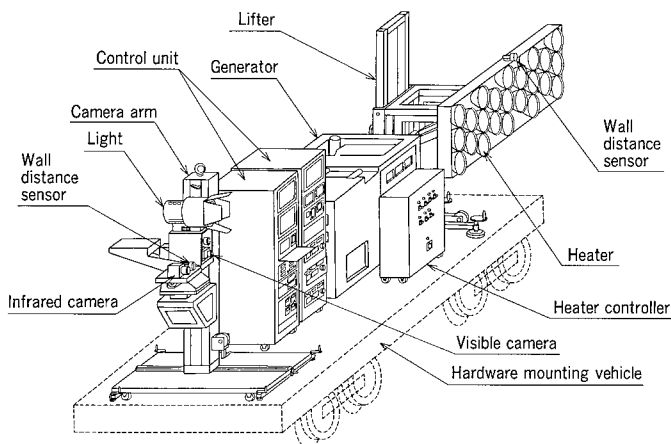


Fig. 1 Tunnel inspection system

### 2. Specifications

The specifications for the tunnel inspection system are shown in Table 1.

### 3. Features

- (1) Thorough detection of internal delamination of wall

The system takes infrared photographs after heating of the tunnel wall to detect the delaminated section with surface temperature higher than the normal section, enabling a thorough detection throughout the whole surface, which was not possible through tapping (in which case only spot detection was possible).

- (2) Labor-saving due to self-moving inspection system

This system is self-moving type, and carries out inspection automatically, so that one inspector and one driver can make an inspection team which was conventionally made of 3-4 persons, contributing to labor saving.

- (3) Automatic preparation of defect map through image processing

The (tunnel) defect map in conventional inspection system was manually made on the basis of visual and tapping inspections, needing a large amount of labor for map making. The new system prepares the defect map automatically through image processing of the obtained data using a data analyzer.

- (4) Tunnel wall inspection data base

The system carries out digital recording of the obtained visible image, infrared image, analyzed defect map, various statistic data, etc. as a data base, ensuring easy maintenance and data control, and at the same time enabling to learn the proceeding degree of defect in time sequence.

Further, the data base being a data base for personal computer, it is highly flexible, and can be easily connected with other data bases.

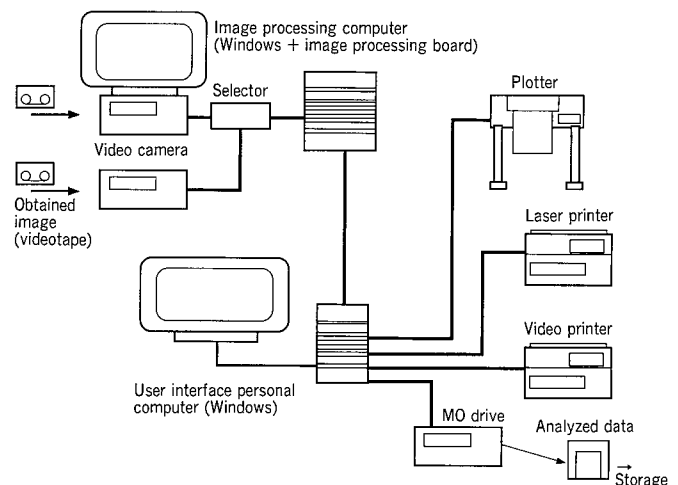


Fig. 2 Data analyzer

# Automatic Guided Vehicle for Hot Stainless Coil and Slab

Mitsubishi Heavy Industries, Ltd. Sagamihara Machinery Works delivered a 30-ton automatic guided vehicle for hot stainless coil and slab to Nippon Metal Industry Co., Ltd. Kinuura Factory in March 1997. The outline of the vehicle is described below.

## 1. Outline

### (1) Scope of supply

- Automatic guided vehicle for hot coil (AGV-S): 3 units
- Automatic guided vehicle for hot slab (AGV-L): 1 unit
- Navigation system: 1 set
- Ground side guiding, safety equipment and automatic battery charger: 1 set
- Coil transship stand: 7 units
- Slab transship table: 1 unit

(2) This is an epoch-making integrated transportation system for carrying hot slab from steel making factory to transship table in hot rolling factory using AGV-L, and further for carrying the coil, subjected to hot rolling in the after process, to cold rolling factory using AGV-S.

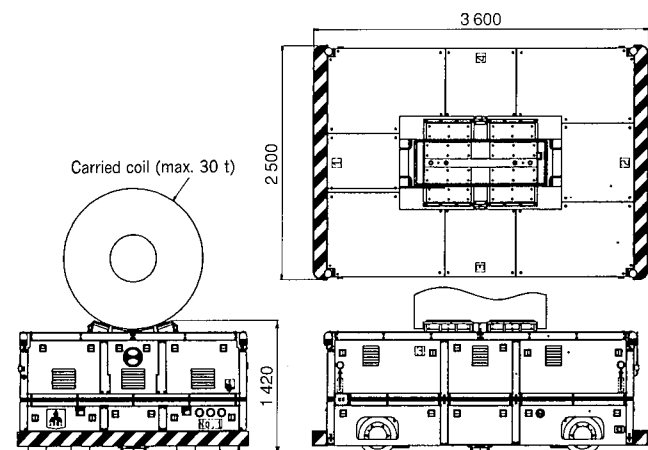


Fig. 1 External appearance of AGV-S

Table 1 shows the main specifications of AGV, Fig. 1 and Fig. 2 the external appearances of AGV-S and AGV-L respectively.

## 2. Features

### (1) Applicable to hot coil and slab

The best-fit adiabatic design, based on thermal analysis due to finite-element method, and model experiment have enabled the vehicles to carry out continuous transportation of slab at 800°C (AGV-L) and coil at 300°C (AGV-S).

### (2) Optimum navigation system

The optimum navigation has been realized from the engineering workstation (EWS, the sequencer in case of AGV-L) by using the data from ground facility composed in the sequencer network.

### (3) Adoption of radio remote controller

In order to cope with the increasingly large size of vehicle (AGV-L) and for easy transfer of vehicle at the time of maintenance, the joystick capable of remote control (manual mode) is adopted.

### (4) Man-machine interface

Touch panels are adopted in machine side operating panel and AGV, giving easily visible display of operating conditions, alarm information, etc.

### (5) All-weather AGV system

Since the AGV is designed for outdoor use, both the ground facilities and AGV are all-weather type.

Table 1 Main Specifications

Items	AGV-S	AGV-L
Overall length (mm)	3 600	14 800
Overall width (mm)	2 500	3 890
Overall height (mm)	1 420	2 060
Vehicle weight (t)	Approx. 10	Approx. 50
Loading capacity (t)	30	30
Maximum speed (m/min)	66	91
Power source	Ni-Cd battery	Ni-Cd battery
Guiding type	Magnetic guiding	Magnetic guiding
Communication type	Bilateral optical communication	Bilateral optical communication
Steering type	Full mode	Full mode

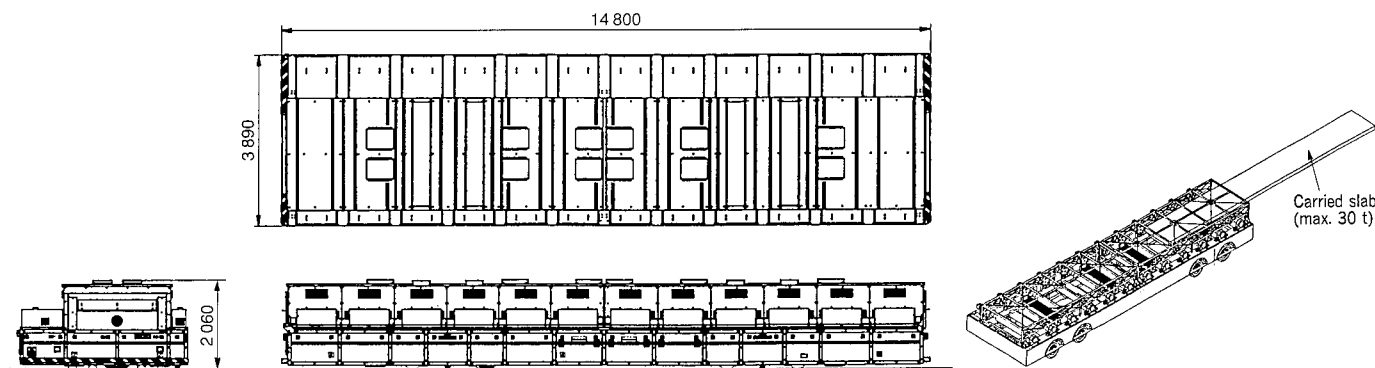


Fig. 2 External appearance of AGV-L

## Air Conditioner of Hong Kong APM

Mitsubishi Heavy Industries (MHI) is a total refrigeration product maker manufacturing a large variety of air conditioning, freezing, cold storage, and refrigeration applied products. However, the company has so far not entered in the field of air conditioner for train.

Recently MHI has successfully developed an air conditioner for Hong Kong APM (Automated People Mover) as described below.

### 1. System Outline

The system for one train (car) is an exclusive cooling system composed of 2 indoor units, 1 outdoor unit and 1 control panel, with 2 independent refrigerant circuits.

The main general elements are given in Table 1, and the outdoor unit on board in Fig. 1.

### 2. Features

#### 2.1 Machine layout

Most commuter trains in Japan use roof-top integrated type air conditioners due to installation facility. However, since Hong Kong APM trains run through tunnels, the train height is limited, so that the outdoor unit is installed under the floor while the indoor units are embedded separately in both ends of the ceiling, and the control panel is installed in

Table 1 Specifications for Air Conditioner of Hong Kong APM (for 1 car)

Items	Specifications
Type	Separate type, exclusively used for cooling
Power source	Main circuit: 3-phase AC 220 V + 10% - 15% Control circuit: Single-phase AC 100 V + 10% - 15% Operating circuit: DC 100 V $\pm$ 10%
Cooling capacity	23.0 kW (See Note)
Circulating air quantity	50 m <sup>3</sup> /min
Ventilation air quantity	12 m <sup>3</sup> /min
Indoor unit	Heat exchanger 245 $\times$ 1450 $\times$ 622 mm $\times$ 2 units
	Air blower Double suction multiblade fan $\times$ 8 pcs Double-shaft motor (output: 0.135 kW) $\times$ 4 pcs
	Refrigerant control Capillary tube
	Weight 61 kgf $\times$ 2 units
Outdoor unit	Compressor Hermetic scroll type 3.45 kW $\times$ 2 units
	Heat Exchanger 760 $\times$ 1 740 $\times$ 514 mm
	Air blower Axial fan $\times$ 2 pcs Single-shaft motor (output: 0.5 kW) $\times$ 2 pc
	Weight 255 kgf
Control panel	Controller Sequencer
	Weight 11 kgf
Air filter	Dust arrest efficiency over 90% (Conforms to EU standard)

Note: The cooling capacity is under the operating conditions given below.

Indoor: Temperature 24°C, Humidity 60%

Outdoor: Temperature 40°C, Humidity 40%

the wall of the cabin.

#### 2.2 Cooling capacity

Taking into consideration the operating environment of high temperature and high humidity, the large number of passengers and the large quantity of ventilating air, the cooling capacity is upgraded by 1.3 times the capacity of an air conditioner for the same class train.

#### 2.3 Power source

Three-power-source system is applied befitting with the train power source: 3-phase AC 220 V for main circuit, single-phase AC 100 V for control circuit, and DC 100 V for operating circuit. The electric equipment is also designed to meet with the requirements for trains such as voltage regulation, momentary blackout, etc.

#### 2.4 Main machines

The main machines such as compressor, heat exchanger, air blower, etc. have their resistance against vibration or shock (impact) improved on the basis of commercial use air conditioner.

#### 2.5 Control and operation

The air conditioner keeps the cabin in optimum condition by means of the control program of the sequencer installed on the control panel on the basis of the data received from temperature sensors and pressure switches.

Since the APM trains use automated operation system, the air conditioner is designed to be operated and monitored from the control room. Further, the control panel is also equipped with operating switch to allow operation of the air conditioner in inspection and maintenance shop, etc.

#### 2.6 Standard

The materials used are selected to conform to the British Standard applied in Hong Kong. The adopted air filter has the dust arrest efficiency over 90% conforming to the EU standard.

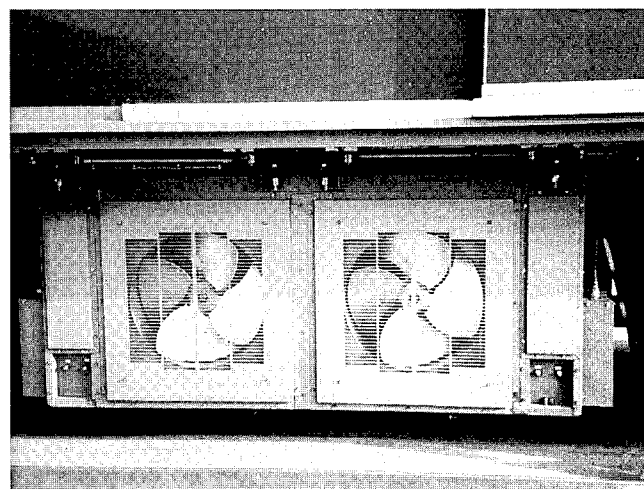


Fig. 1 Outdoor unit

# Introducing

## Mitsubishi Juko Giho

The articles in this edition are selected and translated from the Mitsubishi Juko Giho written in Japanese, Vol.34 No.5 and Vol.34 No.6. The following are remaining technical papers and articles not included.

Vol.34 No.5

### Technical Trend of Large Container Ship

Since we built the first Japanese fully cellular container ship Hakone-maru in 1968, we have delivered many container ships which have incorporated the latest technology every time. Recently we have received many orders of large container ships from major operators who aim at rationalized sea containers transportation in the severe competitions and we now have the largest market share of large container ships in the world. In this paper, we give a brief history of container ships and describe the recent circumstances surrounding the enormous number of orders to build large container ships. We also describe the characteristics of our latest Over-Panamax container ship and also study the possibility of further enlarging the size of container ships.

### Design of Floating Production Storage & Offloading Unit (FPSO)

In the past, large scale fixed production facilities such as fixed platforms and sub-sea pipelines were normally used for offshore oil production. However, offshore activities are increasingly involving marginal fields which has resulted in an increasing demand for Floating Production Storage and Offloading units (FPSO) as relocatable facilities. Accordingly, Mitsubishi Heavy Industries, Ltd. has designed and built the hull part of the world largest class FPSO, the ANASURIA for Shell UK Exploration and Production (Shell Expro) in the UK North Sea and delivered her to Single Buoy Moorings Inc. on January, 1996. This paper introduces the technical features of MHI's ANASURIA.

### New Generation RO/RO Cargo Ship

Mitsubishi Heavy Industries, Ltd. Nagasaki Shipyard & Machinery Works delivered TARONGA, a multi-purpose RO/RO cargo ship, to Wilhelmssen Lines of Norway in December, 1996. TARONGA is one of the world's largest RO/RO cargo ships and fully incorporates Mitsubishi Heavy Industries, Ltd. newest shipbuilding technology. The technical characteristics of TARONGA are described in this paper.

### Structural Responses of Fully Submerged Hydrofoil Catamarans in Seaways

Full-scale measurements of the first Mitsubishi Super-Shuttle 400, named the "Rainbow," is a fully submerged hydrofoil catamaran, were carried out in order to clarify its structural responses and verify its structural integrity. The wave load acting on the fully submerged foil and the stresses at important points were measured. The predicted foil lift obtained from the ship motion and wave load simulation showed good agreement with the results of the full-scale measurement. Moreover the structural integrity of the ship's hull and hydrofoils was proven through the shipboard testing and 6 months of shipboard monitoring. These results will be all fed back into the design and development of future fast ships.

### Development of Design Support System MATES

MATES, an integrated CAD/CAM system for ships, has been in practical use in our shipyards for more than 10 years. MASTES features a hull structure system and an outfitting system which covers from the basic design to production design stages. After continuous improvement based on its extensive usage in actual ship design, MASTES has been developed into an advanced design support system and has now become the backbone of the CIM system in our shipyards. This paper introduces some of its advanced design support functions and its development concept.

### Fairing and Surface Representation of Ship Hull Forms and Numerically Controlled Model Ship Milling System

The research and development of Computer Integrated Manufacturing and Computational Fluid Dynamics are being carried out intently by ship building companies in order to increase the efficiency of design, engineering and production of ships. This technology is based on the precise expression of hull forms by computer software. An efficient line fairing program has been developed and combined with general 3-D CAD software, so that the precise fairing and surface modeling of complicated hull forms can be performed quickly and easily. Also, a simultaneous 5-axis numerically controlled model ship milling system for towing tank tests has been developed by applying the surface model mentioned above.

### New Low-Temperature Steel Plate and Its Application for Multi-Purpose Gas Carrier

In the selection of materials for cargo tanks for multi-purpose gas carriers, special consideration should be paid to the peculiarities of the cargo as well as to the general material properties required for an LPG carrier. A new low temperature steel (LLF 32), which has a yield stress of 315 MPa level in accordance with new specifications, has been developed and put to practical use. This steel plate has been proven to have sufficient toughness at low temperature as a tank material for multi-purpose gas carriers, even if welded with a large heat input, and also to have stress corrosion cracking resistance to liquid ammonia. It is considered that highly safe and reliable tanks for multi-purpose gas carriers can be constructed using application the new LLF 32 low temperature steel.

### Reduction of Propeller Noise by Using Advanced Prediction Method of Cavitation

The reduction of underwater noise is of primary importance when designing oceanographic research ships so as to secure the reliable operation of acoustic instruments. Propeller cavitation is considered to be one of the most harmful sources of underwater noise, thus the design of the propeller for such ships requires great care to prevent cavitation. In this report, we show a design method for low noise level propellers. The occurrence of cavitation is predicted by using the surface panel method and the 3-Component Laser Doppler Velocimeter. As a result, noise levels can be reduced by more than 10 dB for various oceanographic ships.

## Application of Flow Analysis by CFD to Ship Design

An outline of various methods for numerical flow analysis around a ship using CFD (Computational Fluid Dynamics) is described. First, the Rankine source method, a kind of boundary element method, is used to evaluate the effect of the bulbous bow on the wave-making resistance. Next, a finite volume method as the Navier-Stokes solver, is used to evaluate the viscous resistance and self-propulsion factors of three different hull forms. As a result, it is shown that these numerical analysis methods can predict ship resistance and self-propulsion factors very well, and can give us important information for improving the form of ship's hull. It can be said, therefore, that these methods are useful tools for developing superior hull forms.

## Study on Structural Toughness of Ships against Collision and Grounding

Accidental oil spills from crude oil tankers is one of the great concerns of the world from the viewpoints of the preservation of marine environment and the reduction of economic damage. In the wake of the grounding accident in Alaska in 1989, a new international design standard, that newly constructed large tankers should have a double hull construction or its equivalent, came into effect. This paper discusses large-scale experiments and numerical simulations of collisions and groundings, which were carried out to study the failure mechanisms, resistance forces and energy absorption of ship structures. Employing the proposed numerical method, simulations of actual collision and grounding accidents were performed. The studies were conducted under contract with the Association for Structural Improvement of the Shipbuilding Industry (ASIS) of Japan.

## Design of SOFC Materials with Molecular Dynamics Method

Theory-based materials design and analytical methods are now desired for the development of solid oxide fuel cell (SOFC) materials and other functions. The inter-connector design of SOFC requires the control of thermal expansion and the expansion in a reducing atmosphere. The former has been controlled with empirical knowledge, The later have been confirmed by measuring the sample scale in a reducing atmosphere, and there is not enough empirical knowledge for material design. However, several-simulation methods are now under development, and the molecular dynamics method (MD) is one of them. The application of MD has been restricted because the calculation for the materials composed of the limited elements had been reliable about ceramics. Therefore the potential functions for some elements used in MD were developed in this study. The new method enabled thermal expansion and the expansion in reducing

atmosphere in a perovskite type chromite inter-connector to be predicted using MD.

## Proposal of Sea Energy Storage System

The Sea Energy Storage System (SESS) is designed to utilize the inside to outside pressure difference of a tank, called battery tank, sunk at the sea bottom. The system is to be installed 800 m below the surface to take approximately 82 kgf/cm<sup>2</sup> water pressure. The SESS consists of battery tanks and a container which includes pump turbines and generators. The structure of the battery tank is studied as well as manufacturing procedure, to generate 1 000 MW of electric power for 6 continuous hours a day.

## Development of Investment Casting Bifurcate Tubes for Boiler

The bifurcate tubes used as pressure parts in boilers are usually made by plastic deformation, and grinder, or electric discharge, machining. Recently high temperature, high pressure boilers, however, need bifurcate tubes which have more accurate dimensions and thickness which requires many man-hours to achieve. We have established a new technology employing hot isostatic pressing and precision casting which allows the manufacture of complicated parts with net shape. This new technology enables the manufacture of high quality bifurcate tubes at low cost. The high quality bifurcate tubes made by this new method are by no means inferior to conventional ones in material performance, and are far superior in accuracy of dimensions. Their durability in actual boiler tests of over 20 000 hours was verified, and they are now partly coming into practical use.

## Shape Controllability of MC Roll for Strip Rolling

These days, there is a strong demand for a cold strip mill capable of higher degree of shape control such as control of combined buckling which is necessary as cold strip has tended to become thinner and wider. MHI has already developed the Cluster Mill (CR Mill) capable of high shape control especially of thin stainless steel, and now MHI has designed the divided type back-up-roll with sleeve (MC Roll) whose mechanism is much simpler than the CR Mill, and whose shape control is as high as the CR Mill. This report describes the MC Roll shape control mechanism, and its better shape control than other shape control mills. It also demonstrates that the sleeve of the MC Roll has sufficient fatigue strength even under severe loading and deformation using strength analysis.

## Development of Second Yamanashi Linear Maglev

Superconducting magnetic levitation railway which has been studied as the ideal high-speed transportation system is in the certification phase of feasibility and the running test using the first train is progressing to confirm the performances at the test line in Yamanashi prefecture. Mitsubishi Heavy Industries, Ltd. (MHI) has taken part in developing and manufacturing the maglev vehicle. After delivering the leading car which heads for Kofu city and single suspension spring bogie etc, in 1995 as the first maglev train. MHI is developing and manufacturing the leading car which heads for Tokyo and SCM suspended bogie etc, as the second one used for the high-speed passing performances, etc. This report describes the outline of this second maglev train. Features of the leading car of the second maglev train manufactured by MHI are a power supplying car without passenger seat, no cabin seal and lighter weight compared with the first train car. The shape of this leading car is double cusp same as the first one, obtained as the result of optimization using CFD (Computational Fluid Dynamics) technology and the wind tunnel test to reduce aerodynamic drag and noise. Aircraft designing technique is used to satisfy the light weight requirement by optimization of the skin thickness, the number and the space of the frame, stringer. And one body of the fairing and the structure contributes to reduce weight drastically. The double suspension springs bogie achieves light weight with mixing of aluminium rivet and welded frame and good maintainability using the technique of aircraft's equipment installation.

## Development of Rope Driven Suspended Transportation System SKYRAIL

A rope driven suspended transportation system the SKYRAIL has been developed to improve the mobility of short distance transportation systems. At present the construction of the Seno line in the eastern part of Hiroshima city is well under construction, it will be operated in April 1998. This paper mainly reports the configuration of the Seno line, the development of the fundamental technology and the progress of construction, particular mention is made of a rope grip which provides the ability to climb inclines of up to 27% with a capacity of 25 people per car and has obtained special approval from the Ministry of Transport.

## Development of Automatical Driving and Obstacles Detection Vehicle for Shinkansen Track Confirmation

In case of conventional type inspection car of Sinkansen track, the operator checks ahead visually while driving, and the inspection car is operated manually by the driver. As a development of this, a fully automatic operated vehicle has been manufactured which employs a target speed database by which the vehicle speed is automatically controlled. Equipment to monitor the speed and an obstruction detecting safety system, which checks the way ahead with image processing technology inside the vehicle, are also employed. As a result, a fully automatic obstruction detection test has been realized on Shinkansen track at a maximum speed of 60 km/h.

## Design and Verification Technique to Power Supply System for Three-Phase AC Based New Transit Systems

The Waterfront Line of the Tokyo Waterfront New Transit is the world's first automated people mover system, which runs on a long suspension bridge. The new transit system uses a low voltage, three-phase

AC feeding system according to the New Transit System's guideline. We developed a simulator for the electric power feeding system in which the vehicle's position is considered. The simulator is used for the design of the electric distribution system, in order to avoid low voltage at the suspension bridge. This paper describes the distribution line system of the Tokyo Waterfront New Transit Waterfront Line and the electric power simulator used for the design. By using the newly developed simulator, the Yurikamome, Tokyo Waterfront New Transit Waterfront Line, has been in operation safely since October 1995.

## Development of C/C Composites Disk Brake of High-Speed Shinkansen

Train brakes need to absorb more energy as the speed of Shinkansens increases. Carbon/Carbon (C/C) composites have many favorable properties for this brake, such as durability under high temperature, light weight, strength, and toughness, but they have the problem of an unstable friction coefficient. With the cooperation of JR East, we have successfully developed a disk brake unit using a C/C composite whose friction coefficient is stable. We selected the most suitable C/C composites for the brake and improved its properties with a special impregnation method. The brake unit was tested using a real train (JR East STAR 21 high-speed Shinkansen) to verify its performance and stability. The tests showed that good progress towards the practical use of C/C composites disk brake unit had been made.

## Research and Development of Dual Mode Truck (DMT) System

In consideration of the effect on environment and the transport method of the new freight transport system, which does not change the style of the existing freight transportation, we are researching and developing the Dual Mode Truck System which is based on electric vehicles. This paper mainly reports the development of short headway operation 1 to 3 seconds of headway on the dedicated guideways and computer-controlled vehicles merging at relatively high speed and with short headway at Public Works Research Institute, and also reports the vehicle specification, the method of guide apparatus and guide rail and communication system.

## Real-time Traffic Monitoring System Using Image Processing

Accurate traffic information is required to restrict the traffic flow at highway entrances in order to relieve traffic jams and to reduce traffic accidents in city areas. This paper presents a traffic monitoring system which extracts various traffic information, such as the number and speed of passing vehicles and the spatial occupancy of vehicles, from highway images taken by a road-side ITV camera. The system detects vehicle presence in specified lanes using the y-axis projection of horizontal edge of a vehicle image and tracks the vehicle by a template-matching algorithm. Our real-time image processing board is used for the detection and tracking of moving vehicles every 60 msec. Experiments using a 2 hour daytime image shows that the vehicle count error is within 5% and the deviation of vehicle speed is within 10%.

## Status of Road-Vehicle Communication System for ITS

The research and development of ITS is now being performed all over the world. The objective of ITS is to create an intelligent transportation system, and plural application is to be provided. The road-vehicle communication is the most important technology for combining each

application into a whole system. The standardization of ITS is being carried out by ISO and CEN. We supplied our ETC ITS system, to Malaysia and Singapore, achieving exports to overseas markets. Also, we strenuously participated in the R&D and standardization project organized by several Japanese ministries.

### Development of Concrete Armor Unit "Diablock"

The features and basic performance of the newly developed concrete armor unit "Diablock" is described. The  $K_D$  value using Hudson's formula is obtained as 8.0—8.5 from hydraulic model study. The strength of the block is also confirmed by using FEM analysis. Diablock has high stability, low reflectivity, and high dissipativity for waves. We expect that Diablock will widely contribute to the prevention of disasters and environmental protection.

### Development of Intelligent Control of GMAW Process

The recent shortage of skilled welders has become a serious problem. To solve this problem, it is necessary to raise the level of automated welding. For the purpose of taking over the roles of skilled welders, the authors have been investigating an intelligent TIG welding control system. We have now developed and put to practical use an intelligent MAG welding control system, in which the welding phenomena are more active. In this system the state of welding is detected and controlled using a CCD camera, a laser sensor and a microphone. The system has been successfully applied to the welding of boiler drums.

### Development of Molten Metal Level Monitoring System for Electron Beam Heat Vapor Deposition Equipment

In the vacuum evaporating equipment which is used to deposit a high melting point metal on various materials, the metal in the crucible is heated by an electron beam gun. In order to evaporate the metal stably, the surface of the molten metal needs to be controlled to a constant level by feeding the raw material to the crucible. It is necessary for this purpose to detect the level position precisely by any method. We have developed a level monitoring system composed of two X-ray pinhole cameras based on

triangular measurement. The camera detects the X-rays generated by the electron beam irradiation on the metal surface. This system ensures the level position for an accuracy within  $\pm 1\text{mm}$ . The controllability of the vacuum evaporating equipment will be improved by this monitor.

### Development of Liquefaction Process of Plastic Waste in Supercritical Water

A new liquefaction process of plastic waste in supercritical water has been developed, and a pilot plant of 0.5 ton/day capacity has been constructed. We successfully liquefied scrap of plastic materials of electric cable made of crosslinked polyethylene without any coking trouble and obtained the liquefaction yield of more than 80%. The pilot plant tests showed good stability in daily start and stop operation.

### Development of Aeroacoustics Analysis Program for Helicopter Rotor

An analysis system for predicting helicopter rotor aerodynamic noise has been developed. The system consists of a Navier-Stokes solver for near rotor flow field computation and an acoustic wave equation solver for computing the sound pressure propagation to the far field. For aerodynamic validation, the results obtained from Caradonna's test rotor for hovering and the AH-1 G OLS rotor in forward flight are presented. For aeroacoustic validation, the sound pressure history obtained from the UH-1 rotor for hovering and the AH-1 G OLS rotor in forward flight are presented.

### Development of Energy Absorption Type Structural Controlling System

In this study, a semi-active type structural control system was newly developed which is more effective than the usual passive type device and consumes much less power than the usual active device. This system consists of several variable friction dampers controlled by a specially designed LQ controller which decides the optimal friction force so as to reduce the seismic response of a structure for each second. Through the scaled-down model tests and numerical analysis, the performance of this system was confirmed to reduce the structural response to less than a half of that without control. It was also confirmed that this system absorbed much more seismic energy than the usual constant friction damper.

# MITSUBISHI HEAVY INDUSTRIES, LTD.

## HEAD OFFICE

5-1, Marunouchi 2-chome, Chiyoda-ku,  
Tokyo Japan  
Phone: 81-3-3212-3111  
Fax: 81-3-3212-9800  
P.O.Box: Central 10 Tokyo

## Research & Development Centers

### Advanced Technology Research Center

8-1, Sachiura 1-chome, Kanazawa-ku, Yokohama

### Nagasaki Research & Development Center

717-1, Fukahori-machi, 5-chome, Nagasaki

### Takasago Research & Development Center

1-1, Arai-cho, Shinhamma 2-chome, Takasago

### Hiroshima Research & Development Center

6-22, Kan-on-shin-machi, 4-chome, Nishi-ku  
Hiroshima

### Yokohama Research & Development Center

8-1, Sachiura 1-chome, Kanazawa-ku, Yokohama

### Nagoya Research & Development Center

1, Aza Takamichi, Iwatsuka-cho, Nakamura-ku  
Nagoya

## WORKS

Nagasaki Shipyard & Machinery Works  
Kobe Shipyard & Machinery Works  
Shimonoseki Shipyard & Machinery Works  
Yokohama Dockyard & Machinery Works  
Hiroshima Machinery Works  
Takasago Machinery Works  
Sagamihara Machinery Works  
Nagoya Machinery Works  
Mihara Machinery Works  
Nagoya Aerospace Systems Works  
Nagoya Guidance & Propulsion Systems Works  
Kyoto Machinery Works  
Hiroshima Machine Tool Works  
Air-Conditioning & Refrigeration Machinery Works

## MAIN PRODUCTS

### Shipbuilding & Ocean Development

Shipbuilding, Marine engineering, Ship repairing & conversion, Automatic control systems, Marine structures, Ocean development equipment

### Steel Structures & Construction

Steel structures & products, Transportation & parking systems, Recreation, sports & leisure facilities

### Power Systems

Boilers, steam, gas & water turbines, Thermal, geothermal & wind power plants, Co-generation system, Diesel engines, Diesel power plants, Denitrification plants, Marine machinery

### Nuclear Energy Systems

Nuclear power plants, Advanced reactor power plants, Nuclear fuel cycle equipment, Nuclear fuel Machinery

Environmental plants & equipment, Vacuum sealed conveyance system, Pumps, Iron & steel manufacturing machinery, Cement plant & machinery, Toll collection equipment, Transportation systems, Airport systems & equipment, Electronics systems, Compressors, drive turbines, Rubber & tire machinery, Packaging machinery, General machinery, Testing equipment, Food engineering, Oil refinery plants, Chemical plants & equipment, Oil & gas production, Transportation & storage plants, Desalination plants

### Industrial Machinery

Pulp & paper machinery, Corrugating machinery, Sheet-fed offset presses, Commercial web offset presses, Newspaper offset presses, Electronic printing presses, Extrusion machinery, Injection molding machines, Textile machinery, Beverage bottling & canning machinery, Cleaning machinery, Transmission devices, Industrial robots, Machine tools, Precision tools, Engine valves

### Aircraft & Special Vehicle

Aircraft, Aero engines, Space systems, Special vehicles, Missiles, Torpedoes

### General Machinery & Components

Forklift trucks, Heavy cargo carriers, Earthmoving & grading machinery, Tunnel boring machinery, Foundation works & concrete placing equipment, Gasoline engines, diesel engines (industrial/marine use) Turbochargers, Diesel engine generators, Co-generation systems, Leisure related products

### Air-Conditioning & Refrigeration Systems

Air conditioners, Refrigeration machinery & applied products, Air-conditioning & refrigeration plants, Heat utilization system

## OVERSEAS OFFICES

### Mexico Liaison Office

Paseo de la Reforma No.287, 7 Piso  
Col. Cuauhtemoc, Deleg. Cuauhtemoc C.P. 06500  
Mexico D.F., Mexico  
Phone: 52-5-511-4193, 52-5-514-9982

### Beijing Liaison Office

China World Trade Tower 18F, China World Trade Center, No.1 Jianguomenwai Avenue  
Beijing, The People's Republic of China  
Phone: 86-10-6505-4321, 4322, 1221

### Jakarta Liaison Office

26th Floor Jakarta Stock Exchange Bldg. Jl.  
Jenderal Sudirman Kav. 52-53,  
Jakarta 12190, Indonesia  
Phone: 62-21-515-3221, 3223, 3224, 3225

### Taipei Liaison Office

Hung Kuo Bldg., 11th Fl. Sec. -E 167  
Tun Hua North Road  
Taipei, Taiwan  
Phone: 886-2-2719-8155

### Shanghai Liaison Office

Room Nos.354-357, North Building  
Peace Hotel, 20 Nan Jing Road (East)  
Shanghai, The People's Republic of China  
Phone: 86-21-6329-3030

### New Delhi Liaison Office

Dr. Gopal Das Bhawan (1st Floor)  
28 Barakhamba Road  
New Delhi 110001, India  
Phone: 91-11-3354465, 3354467, 3354469

### Moscow Representative

7 Bolshoi Gnezdnikovskiy Per.,  
2nd Floor, Moscow 103009, Russian Federation  
Phone: 7-095-973-2009  
7-095-956-2969, 2970

### Istanbul Representative

Tekfen Sitesi, Birlik Apartmani Daire 3 Ulus,  
Besiktas 80600, Istanbul, Turkey  
Phone: 90-212-263-1923, 2312

### Middle East Representative

P.O. Box 16767, Jebel Ali Free Zone,  
Dubai, U.A.E.  
Phone: 971-4-817001, 816591

### Dalian Representative

20th Floor, Senmao Building  
Zhongshan Rd., Xigang District, Dalian  
The People's Republic of China  
Phone: 86-411-360-9090, 9191, 9292

### Pusan Representative

8th Floor, Dong-Ah Ilbo Bldg.  
53-11, 4ka Chungang-dong, Chung-ku  
Pusan, Republic of Korea  
Phone: 82-51-462-7316, 464-0801

### Bangkok Representative

208 Wireless Road, 10th Floor  
Lumpini Pathumwan, Bangkok 10330  
Thailand  
Phone: 66-2-651-5601, 5602, 5603, 5604  
66-2-651-5202, 5203, 5204

### Ho Chi Minh City Representative

Unit-E, 4th Floor, OSIC Building, No.8  
Nguyen Hue Street, District 1 Ho Chi Minh City  
Socialist Republic of Viet Nam  
Phone: 84-8-8243279, 8243280

## OVERSEAS SUBSIDIARY COMPANIES

### Mitsubishi Heavy Industries America, Inc.

#### (MHIA) Headquarters

630 Fifth Avenue, New York, NY 10111, U.S.A.  
Phone: 1-212-969-9000

### (MHIA) Houston Office

10795 Hammerly, Suite 350  
Houston, TX 77043, U.S.A.  
Phone: 1-713-935-2585, 2586

### (MHIA) Los Angeles Office

660 Newport Center Drive, Suite 1000  
Newport Beach, CA 92660, U.S.A.  
Phone: 1-714-640-4664, 4772, 5451

### (MHIA) Metals Machinery Division

500 Cherrington Parkway, Suite 300  
Coraopolis, PA 15108, U.S.A.  
Phone: 1-412-269-6630

### (MHIA) Tire Machinery Division

600 Cherry Fork Ave.  
Leetonia, OH 44431, U.S.A.  
Phone: 1-330-427-8900

### (MHIA) Turbocharger Division

1250 Greenbriar Drive, Suite E  
Addison, IL 60101-1065, U.S.A.  
Phone: 1-630-268-0780

### Mitsubishi Heavy Industries Europe, Ltd.

#### (MHIE) Head Office

Bow Bells House, Bread Street (Cheapside)  
London EC4M 9BQ, England  
Phone: 44-171-634-5111

#### (MHIE) Munich Branch

Thomas-Wimmer-Ring 9  
D-80539 Munich, Germany  
Phone: 49-89-211079-0, 11, 12, 13

#### (MHIE) Paris Liaison Office

3 Avenue Hoche 75008, Paris, France  
Phone: 33-1-4267-6075, 9720, 9717, 9718

#### (MHIE) Madrid Branch

C/Serrano 27, 4º- Izquierda 28001, Madrid, Spain  
Phone: 34-91-577-1632, 576-7591, 576-9320

#### (MHIE) Praha Liaison Office

Praha City Center, 6th Floor  
Klimentska 46, Praha 1, The Czech Republic  
Phone: 420-2-2185-6080

### MHI Machine Tool U.S.A. Inc.

330 Bill Bryan Boulevard, Hopkinsville  
KY 42240, U.S.A.  
Phone: 1-502-885-2211

### Mitsubishi Caterpillar Forklift America Inc.

2011 W. Sam Houston Pky. N.  
Houston, TX 77043-2421, U.S.A.  
Phone: 1-713-365-1000

### Mitsubishi Heavy Industries Climate Control Inc.

1200 N. Mitsubishi Parkway  
Franklin, IN 46131, U.S.A.  
Phone: 1-317-346-5000

### MHI Equipment Europe B.V.

Damsluisweg 2, 1332 EC, Almere, the Netherlands  
Phone: 31-36-5388331

### Mitsubishi Caterpillar Forklift Europe B.V.

Hefbrugweg 77, 1332 AM, Almere, the Netherlands  
Phone: 31-36-5494400

### CBC Industrias Pesadas S.A.

Rodovia D. Gabriel Paulino Bueno, Couto. km.  
68-Ermida, CEP 13200 Jundiá, Sao Paulo, Brazil  
Phone: 55-11-7395-5500

### MHI-Mahajak Air Conditioners Co., Ltd.

Lat Krabang Industrial Estate, Phase 3  
200 Moo 4, Lamplatiw, Lat Krabang  
Bangkok 10520, Thailand  
Phone: 66-2-326-0401 to 0416

### Mitsubishi Heavy Industries (Thailand) Ltd.

208 Wireless Road, 10th Floor  
Lumpini Pathumwan, Bangkok 10330, Thailand  
Phone: 66-2-651-5601 to 5604, 5203, 5204

### Mitsubishi Heavy Ind., (Hong Kong) Ltd.

Room 2104-7, Hutchison House  
10, Harcourt Road, Hong Kong  
Phone: 852-2525-5262, 5263, 5264

### MHI South East Asia Pte. Ltd.

No.2, Tuas Avenue 20, Singapore 638818  
Republic of Singapore  
Phone: 65-8622202

### Mitsubishi Heavy Industries Philippines, Inc.

9th Floor, The World Center 330 Sen Gil J. Puyat  
Avenue Makati City, Metro Manila Philippines  
Phone: 63-2-867-8367 to 8372

